

---

Electronic Thesis and Dissertation Repository

---

8-17-2015 12:00 AM

# Non-Invasive Determination of Pre-Clinical Markers of Cardiovascular Diseases in Low Birth Weight and Maternal Western Diet Guinea Pig Offspring Exposed to a Postnatal Western Diet

Jacky Chiu, *The University of Western Ontario*

Supervisor: Dr Timothy Regnault, *The University of Western Ontario*

Joint Supervisor: Dr Ting Lee, *The University of Western Ontario*

A thesis submitted in partial fulfillment of the requirements for the Master of Science degree in Physiology and Pharmacology

© Jacky Chiu 2015

Follow this and additional works at: <https://ir.lib.uwo.ca/etd>



Part of the [Cardiovascular Diseases Commons](#), [Female Urogenital Diseases and Pregnancy Complications Commons](#), [Nutritional and Metabolic Diseases Commons](#), and the [Physiology Commons](#)

---

## Recommended Citation

Chiu, Jacky, "Non-Invasive Determination of Pre-Clinical Markers of Cardiovascular Diseases in Low Birth Weight and Maternal Western Diet Guinea Pig Offspring Exposed to a Postnatal Western Diet" (2015). *Electronic Thesis and Dissertation Repository*. 3170.  
<https://ir.lib.uwo.ca/etd/3170>

This Dissertation/Thesis is brought to you for free and open access by Scholarship@Western. It has been accepted for inclusion in Electronic Thesis and Dissertation Repository by an authorized administrator of Scholarship@Western. For more information, please contact [wlsadmin@uwo.ca](mailto:wlsadmin@uwo.ca).

**NON-INVASIVE DETERMINATION OF PRE-CLINICAL MARKERS OF  
CARDIOVASCULAR DISEASES IN LOW BIRTH WEIGHT AND MATERNAL  
WESTERN DIET GUINEA PIG OFFSPRING EXPOSED TO A POSTNATAL  
WESTERN DIET**

(Thesis format: Integrated Article)

by

Jacky Chiu

Graduate Program in Physiology and Pharmacology

A thesis submitted in partial fulfillment  
of the requirements for the degree of  
Masters of Science

The School of Graduate and Postdoctoral Studies  
The University of Western Ontario  
London, Ontario, Canada

© Jacky Chiu 2015

## **Abstract**

Low birth weight (LBW), and maternal Western Diet (WD) consumption have both been independently implicated to increase the risk of developing cardiovascular diseases (CVDs) in later life. These fetal programmed risks are also believed to exacerbate the effects of a postnatal WD pattern, therefore resulting in the development of pre-clinical markers of CVDs, such as insulin resistance (IR), coronary circulation disruptions. This thesis aimed to elucidate the roles of sub-optimal *in utero* growth through placental insufficiency, or chronic maternal WD consumption, and postnatal WD consumption on the long-term programming of CVDs in a guinea pig model. Early pre-clinical markers of CVD development including reduced coronary flow, left ventricular hypertrophy, and fibrosis were observed in the young LBW offspring. Postnatal consumption of WD was itself strongly associated with the early development of cardiac IR. Collectively these findings suggests that prenatal insults combined with a postnatal dietary insult, can lead to an increased risk of developing CVDs.

## **Keywords**

Intrauterine Growth Restriction, Placental Insufficiency, Low Birth Weight, Fetal Programming, Western Diet, Heart, Cardiovascular Disease, Insulin Resistance, Coronary Blood Flow, Computed Tomography, Positron Emission Tomography, Fibrosis, Ventricular Hypertrophy

## **Statement of Co-Authorship**

Timothy RH Regnault, Ting Y Lee, and Jacky Chiu designed the experiments.

Jennifer Hadway, Jacky Chiu, Ousseynou Sarr, and Kristyn Dunlop assisted with Computed Tomography and Positron Emission Tomography. Ting Y Lee, and Aaron So assisted in the DCE-CT model. Ting Y Lee, and Adam Blais assisted with PET model and in-house program

Timothy RH Regnault, Ousseynou Sarr, Megan Cedrone, Kristyn Dunlop, and Jacky Chiu also assisted in animal handling, and histology slide preparation. Kristina Wiggers and Andrew Bondoc assisted in histology analysis techniques.

Joyce Liu, Alexandra Blake, and Kristina Wiggers assisted with data input and processing.

Jacky Chiu was responsible for data analysis, interpretation, and manuscript preparation.

## Acknowledgments

First of all, I would like to thank Dr. Timothy Regnault. This thesis, and all my accomplishments in the past six years would not have been possible without your guidance, and support. When I first started working in the lab I was just a kid with no purpose, and now with your support and encouragement I am finally getting my MSc. I've been through ups and downs, and each time you had my back. Only you had the patience to deal with my laziness. I will never forget the lab parties, and the taste of guinea pig diets. I will certainly miss working with you. I would also like to thank Dr. Ting Lee for showing me all the wonders of non-invasive imaging. Even with your busy schedule, you always offered me help. I will have to admit, with no experience in medical biophysics, it was very challenging to make sense of this project, but you always provided me with support, and endured my bad jokes. I would also like to thank my advisory committee, Dr. Dean Betts, Dr. Lisa Hoffman, Dr. Maria Drangova, and Dr. Morris Karmazyn for their support throughout my masters.

It's been six years since I stepped foot in the DDT lab. I would like to thank everyone in the DDT lab that I've met. A special thanks to Dr. Lin Zhao, my mentor, for his support in the lab. You've always took time to help me with my project, and expanding my knowledge and interest in science. I've enjoyed all the discussions about life that we had, and I will certainly miss it. Thank you to Dr. Hardy, I still think about that night, and the mess I made on your carpet every day. Thanks Ousseynou for stealing my bike, but it was fun working with you, I know you will miss having someone to argue with in the future. I would also like to thank Jennifer Hadway, Brad Matuszewski, Dr. Aaron So, and Adam Blais for all the help with the animals and imaging. It wouldn't be possible without you guys.

Lastly I would like to thank all my friends and family for their support. Thanks to all my buddies back in Toronto, without you guys, this thesis would have been done a year ago. Thank you to Jason Wong, and Mandy Leung, you guys have been awesome roommates, sorry for all the late night gaming. Thanks to Peter Vo, Katherine Lee and Noelle Ma, I won't be here without your support, and encouragement. Thank you to Megan Cedrone, Joo-wan Kim, Ian Tobias, Laura Rodgers, Michael Wong, and Kristyn Dunlop, you guys made my Masters experience interesting. I know you guys will miss me and all the Viet Thai lunch runs. Also thanks to Alex Elias, I enjoyed our time together in Italy, just remember to go on instinct rather than a map next time when you are in Italy. In typical Jacky Chiu fashion, as I am writing this, the deadline for submission approaches, and I would like to thank everyone in the DDT lab, and all my friends that I've missed. Six years is a long time, and I enjoyed working with each and every one of you, I wish you guys all the best in the future.

Finally, this work would not have been possible without the financial support of the Canadian Institute of Health and Research, the Children's Health Research Institute, Obstetrics and Gynecology Graduate Scholarship, and Ontario Graduate Scholarship. Thank you

# Table of Contents

<b>Abstract</b> .....	ii
<b>Statement of Co-Authorship</b> .....	iii
<b>Acknowledgments</b> .....	iv
<b>Table of Contents</b> .....	vi
<b>List of Tables</b> .....	x
<b>List of Figures</b> .....	xi
<b>List of Appendices</b> .....	xii
<b>List of Abbreviations</b> .....	xiii
<b>Dedication</b> .....	xv
<b>Chapter 1</b> .....	1
<b>1 Literature Review</b> .....	1
1.1 Cardiovascular Diseases.....	2
1.1.1 Cardiomyopathy.....	3
1.1.2 Cardiac Hypertrophy.....	4
1.1.3 Preclinical Metabolic Markers of CVD Development.....	5
1.1.4 Coronary Blood Flow as Markers of Cardiomyopathy Development.....	8
1.1.5 Cardiac Remodeling Consequences.....	9
1.2 Developmental Origins of Health and Disease.....	11
1.2.1 Intrauterine Growth Restriction and Low Birth Weight.....	11
1.2.2 Placental Insufficiency.....	13
1.2.3 Fetal Programming and Catchup Growth.....	14
1.2.4 Fetal Programming of CVDs.....	17
1.3 Adverse Postnatal Diets.....	19
1.3.1 Cardiovascular Dysfunction and WD.....	19

1.4	Methods for Studying Cardiac Blood Flow and Metabolism .....	23
1.4.1	Doppler Ultrasound.....	23
1.4.2	Echocardiography .....	24
1.4.3	Positron Emission Tomography.....	24
1.4.4	Dynamic Contrast Enhanced Computed Tomography .....	26
1.5	Research Goals.....	29
1.6	References.....	30
<b>Chapter 2</b>	.....	<b>46</b>
<b>2</b>	<b>The Impact of an Adverse In Utero Environment Resulting in Low Birth Weight, and a Postnatal Wester Diet on Early Development of Cardiovascular Diseases in Guinea Pigs .....</b>	<b>46</b>
2.1	Introduction.....	47
2.2	Methods.....	50
2.2.1	Animals.....	50
2.2.2	Imaging .....	53
2.2.3	Dynamic Contrast Enhanced Computed Tomography .....	53
2.2.4	Position Emission Tomography .....	54
2.2.5	Tissue Collection .....	56
2.2.6	Quantitative Real-Time PCR .....	56
2.2.7	Western Blot .....	57
2.2.8	Histological Analysis .....	58
2.2.9	Statistical Analysis.....	59
2.3	Results.....	60
2.3.1	Birthweight and Development .....	60
2.3.2	LBW Resulted in Reduction in Basal Coronary Blood Flow in Young Adulthood .....	63
2.3.3	WD Consumption Reduced Basal Glucose Uptake by Adulthood.....	66



2.3.4	Cardiac Remodeling and Collagen Content Were Increased in LBW Offspring .....	68
2.3.5	Expressions of Collagen Increased in LBW Females .....	68
2.3.6	WD Feeding is Associated with a Reduction in AKT Activation .....	69
2.4	Discussion .....	75
2.5	References .....	82
<b>Chapter 3</b>	.....	<b>91</b>
<b>3</b>	<b>The Impact of an Adverse Maternal Diet Prior to and During Pregnancy Upon Young Guinea Pigs Fed a Postnatal Western Diet on the Early Development of Cardiovascular Diseases.</b> .....	<b>91</b>
3.1	Introduction .....	92
3.2	Methods .....	95
3.2.1	Animal Model .....	95
3.2.2	Imaging .....	95
3.2.3	Dynamic Contrast Enhanced Computed Tomography (DCE-CT) .....	96
3.2.4	Positron Emission Tomography .....	97
3.2.5	Tissue Collection .....	98
3.2.6	Quantitative Real-Time PCR .....	99
3.2.7	Western Blot .....	100
3.2.8	Statistical Analysis .....	101
3.3	Results .....	102
3.3.1	Maternal WD Did Not Result in LBW, or Rapid Catch-Up Growth.....	102
3.3.2	Basal and Reserve Coronary Blood Flow Not Affected by Maternal or Postnatal WD Consumption.....	105
3.3.3	Postnatal WD Consumption Resulting in Reduced Glucose Uptake.....	108
3.4	Discussion .....	112
3.5	References .....	119
<b>Chapter 4</b>	.....	<b>126</b>

<b>4 Discussion</b> .....	126
4.1 Summary.....	127
4.2 Speculations.....	131
4.3 Potential Limitations and Future Improvements.....	134
4.4 Conclusions.....	137
4.5 References.....	139
<b>Appendices</b> .....	146
<b>Curriculum Vitae</b> .....	157

## **List of Tables**

Table 2.1 Diet Composition .....	52
Table 2.2 Baseline Physiological Parameters during Scanning Procedures. ....	64
Table 2.3 Relative mRNA Expression of Fibrotic Genes .....	72

## List of Figures

Figure 1.1 Prenatal and Postnatal Factors That May Contribute to the Development of Cardiovascular Diseases in Adult Life .....	22
Figure 2.1 Characteristics at Birth. ....	61
Figure 2.2 Putdown Characteristics .....	62
Figure 2.3 Basal Coronary Blood Flow Determined by DCE-CT .....	65
Figure 2.4 Cardiac Glucose Uptake Determined by PET .....	67
Figure 2.5 Cross-Sectional Area of Cardiomyocytes .....	70
Figure 2.6 Collagen Content in the Left Ventricle .....	71
Figure 2.7 Type 1 Collagen mRNA Expression .....	73
Figure 2.8 AKT Expression in the Left Ventricle at Putdown .....	74
Figure 3.1 Birth Characteristics .....	103
Figure 3.2 Post-Weaning Growth Characteristics. ....	104
Figure 3.3 Basal Coronary Blood Flow at 110 and 210 Days. ....	106
Figure 3.4 Coronary Reserve .....	107
Figure 3.5 Glucose Uptake Determined by PET .....	109
Figure 3.6 Protein Expression of pAKT (T308) at Putdown. ....	110
Figure 3.7 Protein Expression of pIRS (S307) and pAKT (S473) at Putdown .....	111

## List of Appendices

Appendix A. Primer sequences of selected target genes utilized in real-time PCR. ....	147
Appendix B. Ethics Approval.....	148
Appendix C. ANOVA Table for Figure 2.3 Basal Coronary Blood Flow Determined by DCE-CT. ....	149
Appendix D. ANOVA Table for Figure 2.4 Cardiac Glucose Uptake by PET .....	150
Appendix E. ANOVA Table for Figure 2.5 Cross-Sectional Area of Cardiomyocytes .....	151
Appendix F. ANOVA Table for Figure 2.6 Collagen Content in the Left Ventricle .....	152
Appendix G. ANOVA Table for Figure 2.7 Type 1 Collagen mRNA Expression .....	153
Appendix H. ANOVA Table for Figure 2.8 AKT Expression in the Left Ventricle at Putdown. ....	154
Appendix I. ANOVA Table for Figure 3.5 A. Glucose Uptake Determined by PET .....	155
Appendix J. ANOVA Table for Figure 3.6 Protein Expression of pAKT (T308) at Putdown. .....	156

## List of Abbreviations

$\alpha$ SMA – Alpha Smooth Muscle Actin

AKT – Protein Kinase B

ATP – Adenosine Triphosphate

BMI – Body Mass Index

CD – Control Diet

CVD – Cardiovascular Disease

DAG - Diacylglycerol

DCE-CT – Dynamic Contrast Enhanced Computed Tomography

DIP – Dipyridamole

FDG – Flurodeoxyglucose ( $^{18}\text{F}$ )

GLUT – Glucose Transporter

HFD – High Fat Diet

IR – Insulin Resistance

IRS – Insulin Receptor Substrate

IUGR – Intrauterine Growth Restriction

LBW – Low Birth Weight

MC – Maternal Control Diet

MMP1 – Matrix Metalloproteinase

MW – Maternal Western Diet

NCD – Non-Communicable Diseases

PET – Positron Emission Tomography

PGC-1 $\alpha$  – Peroxisome Proliferator- Activated Receptor-Gamma Co-activator 1-Alpha

PI – Placental Insufficiency

PI3-K – Phosphoinositide 3- Kinase

PPAR $\alpha$  – Peroxisome Proliferator-Activated Receptor Alpha

TGF- $\beta$  - Transforming Growth Factor Beta

qPCR – Quantitative Real-Time Polymerase Chain Reaction

ROI – Region of Interest

ROS – Reactive Oxygen Species

SEM – Standard Error of the Mean

SUV – Standardized Uptake Value

TTDE – Transthoracic Doppler Echocardiography

WD – Western Diet

## **Dedication**

For my Mom, and Dad..... and all the guinea pigs!!



# Chapter 1

## 1 Literature Review

## 1.1 Cardiovascular Diseases

The burdens of chronic non-communicable diseases (NCDs) are becoming more apparent in today's society. According to the World Health Organization, NCDs are responsible for approximately nine million of all premature deaths before the age of 60. In particular, low and middle income countries are especially susceptible to NCDs, where they make up 90% of all NCD related premature deaths. Of the many types of NCDs, cardiovascular disease (CVD) distinguishes itself ahead of cancers, respiratory diseases and diabetes as the leading cause of NCD related deaths. In 2008 alone, approximately 17.3 million people worldwide died from CVDs, with a mortality rate of 17%<sup>1,2</sup>. Unfortunately, this figure is expected to rise in the future, with an estimated growth to 24% of all mortalities<sup>1,2</sup>.

These alarming trends can be attributed to the increasing prevalence of risk factors for CVDs in both developing and developed countries. These risk factors include tobacco use, physical inactivity, obesity, and dietary choices such as the consumption of foods high in sugars and/or saturated fatty acids<sup>3-5</sup>. In addition, prenatal complications and the associated low birth weight (LBW) are also recognized by the United Nations as factors which predispose an individual to the development of heart diseases and obesity in adulthood<sup>6</sup>. Collectively these risk factors contribute to the development of different types of CVDs, including coronary artery disease, congenital heart diseases, hypertension, and cardiomyopathy. In particular, cardiomyopathy, with its asymptomatic nature, and ties to both prenatal and postnatal risk factors, presents a substantial risk to our society, and is therefore an important area of focus<sup>7,8</sup>.

### *1.1.1 Cardiomyopathy*

Cardiomyopathy is defined as the disease of the myocardium associated with mechanical or electrical dysfunction, leading to cardiovascular death and progressive heart failure<sup>8,9</sup>. In a 2010 study by the American Heart Association, cardiomyopathy affects approximately 2.6% of the US population with a mortality rate of 56.3%, costing the health care system approximately \$39.2 billion<sup>10</sup>. Patients with cardiomyopathy experience shortness of breath, fatigue, and chest pain; however, many remain asymptomatic<sup>7,8</sup>.

Cardiomyopathy can be categorized into two major groups: primary or secondary. Primary cardiomyopathies are solely confined to the heart, while secondary cardiomyopathies result from conditions which affect other parts of the body such as Gaucher disease and diabetes<sup>11</sup>. A common type of primary cardiomyopathy is hypertrophic cardiomyopathy, where the enlargement of cardiomyocytes results in the asymmetric thickening of the left ventricle, increase in left ventricular stiffness, and ischemia<sup>9,12</sup>. The etiology of hypertrophic cardiomyopathy is familial or genetic, but can also develop over time from chronic high blood pressure<sup>9,12</sup>. Clinically, hypertrophic cardiomyopathy is characterized by a hypertrophied myocardium and an un-dilated left ventricular chamber. In comparison, another type of the disease is dilated cardiomyopathy, where the enlargement of cardiomyocytes results in the stretching and thinning of the left ventricle and a dilated ventricular chamber<sup>13</sup>. Dilated cardiomyopathy is non-ischemic in nature, and although categorized as a primary type of the disease, it is idiopathic, with probable causes such as infections, genetic factors, diabetes, and heart attack<sup>7,9</sup>. While both hypertrophic and dilated cardiomyopathy have different causes and pathophysiology, they

do, however, share a common feature, which is cardiomyocyte enlargement. This process, otherwise known as cardiac hypertrophy, is an important risk factor in myocardial infarction, sudden death, and nearly all forms of heart failure including cardiomyopathy<sup>14</sup>.

### 1.1.2 Cardiac Hypertrophy

The heart is composed of cardiomyocytes (muscle cells) and non-myocytes such as fibroblasts and endothelial cells<sup>15</sup>. As a post-mitotic organ, cardiomyocyte proliferation normally occurs *in utero*. Shortly after birth, cardiomyocytes lose the ability to proliferate, and as a result, postnatal cardiac growth is dependent on cardiomyocyte enlargement and the proliferation of non-myocytes<sup>16,17</sup>. Often, in response to chronic increases in functional load, ventricular wall stress, and load which the blood is ejected against, intrinsic mechanosensing mechanisms which signals the enlargement of heart mass are activated. This cardiomyocyte enlargement is defined as cardiac hypertrophy, and is a major component of cardiac remodelling<sup>18-20</sup>.

Hypertrophic growth can be classified as concentric or eccentric depending on the change in cardiomyocyte shape. In concentric hypertrophy, the increase in cardiac myocyte width in response to pressure overload results in the thickening of the ventricular wall and minor reductions in chamber volume. In comparison, eccentric growth is the increase in cardiomyocyte length in response to volume overload, which results in increased chamber volume with decreased or unaltered wall thickness<sup>21,22</sup>. Cardiac hypertrophy can be further classified as either physiological or pathological hypertrophy. Physiological hypertrophy

is exercise induced, with normal cardiac morphology, and is typically reversible<sup>23</sup>. In contrast, pathological growth occurs as a result of increased load in a disease setting such as myocardial infarction, coronary artery disease, and cardiomyopathy<sup>14</sup>. Depending on the nature of the disease, such as pressure or volume overload, pathological hypertrophy can occur under concentric or eccentric growth promoting conditions. In addition to increased heart and cardiomyocyte size, pathological hypertrophy is also accompanied by cardiomyocyte death, and fibrosis<sup>14,24,25</sup>. More worryingly, over 50% of all hypertrophy-related deaths in adults are sudden, with minimal or no prior symptoms<sup>26</sup>. Given the high prevalence of hypertrophy related cardiac dysfunctions, and the sudden nature of hypertrophy-related deaths<sup>27,28</sup>, it is important to examine possible markers of CVD development for diagnostic and intervention purposes.

### *1.1.3 Preclinical Metabolic Markers of CVD Development*

The main source of energy generation in the heart is from fatty acid oxidation (~70% of ATP production), while glucose metabolism accounts for approximately 30% of ATP production. In order to maintain a steady supply of energy, the heart is also capable of switching between energy sources in order to adapt to different workloads, or fuel molecules<sup>29</sup>. Interestingly, in the early stages of pathological hypertrophy, a decrease in fatty oxidation and increase in glucose metabolism is observed<sup>30-32</sup>. This switch towards glucose metabolism often occurs during the early stages of CVDs, and mirrors the metabolic patterns of a fetal or newborn heart<sup>33</sup>. However, like the fetal heart, glucose

transport is mainly handled by the insulin independent glucose transporter 1 (GLUT1) rather than the insulin dependent GLUT4. This results in a reduction in GLUT4/GLUT1 ratio, and insulin dependent glucose uptake<sup>34,35</sup>. While this mechanism is initially protective against further disease progression (e.g. increasing blood pressure, and reducing coronary blood flow). However, ATP production falls as glucose uptake and metabolism is progressively reduced with the emergence of insulin resistance (IR), a key pre-clinical marker associated with developing CVD<sup>36-38</sup>.

A canine model of advanced dilated cardiomyopathy demonstrated that myocardial IR and increases in fatty acid concentration occurred in parallel with CVD disease progression<sup>39</sup>. Additionally, in severe cases of cardiomyopathy, ATP levels are decreased along with the impairment of cardiac insulin signaling pathways<sup>39</sup>. It can be inferred that IR is associated with decreased ATP stores during a period of crucial dependence on glucose uptake and utilization<sup>39</sup>. Other studies have also suggested that the development of cardiac IR is in fact a protective mechanism against heart failure, particularly in the presence of a high-saturated fat diet<sup>40</sup>. For example, insulin resistant rats with mild to moderate heart failure that were fed a high fat diet exhibited decreased glucose utilization, but preserved contractile function<sup>40</sup>. The reduction in glucose metabolism was likely compensated by increased fatty acid oxidation<sup>41</sup>, and that the insulin resistant animals were therefore forced to use fatty acid oxidation as a means for energy production. This in turn would direct fatty acids to productive pathways such as  $\beta$ -oxidation and triglyceride synthesis, which therefore reduce the formation of lipotoxic intermediates such as diacylglycerol (DAG) and ceramides to preserve cardiac function<sup>40,42</sup>. Nonetheless, the implications of cardiac IR are still poorly defined. However, it is apparent that its

development, along with alterations in glucose uptake is often in concert with CVDs such as cardiomyopathy.

Under normal circumstances, cardiac glucose uptake is mediated by insulin dependent glucose transporters GLUT4 and insulin independent GLUT1, which accounts for approximately 60% and 40% of all glucose uptake in the heart respectively<sup>43</sup>. Both transporters are widely distributed in fetal tissues. However, while GLUT1 is membrane bound and insulin independent, GLUT4 activity requires its translocation to the membrane, a process mediated by the insulin signaling pathway<sup>44</sup>. Interestingly, although GLUT1 activity is classically non-insulin dependent, recent evidence shows that insulin may play a minor role in GLUT1 translocation during diabetic stages<sup>45</sup>. In inducing GLUT4 transporter proteins to the cell membrane, insulin first binds to insulin receptor on the cell surface, which leads to the phosphorylation of insulin receptor, tyrosine phosphorylation of insulin receptor substrate (IRS), the activation PI3-kinase, and phosphorylation of AKT (protein kinase B) at Threonine 308 and Serine 473. Activated AKT and PI 3-kinase is then involved in promoting the translocation of GLUT4 from intracellular storage to the plasma membrane<sup>46</sup>. This signaling pathway, particularly Phosphoinositide 3- Kinase (PI3-K) activation, is necessary for insulin stimulated glucose uptake. However, during states of IR when the action of insulin is impaired, there appears to be a decrease in insulin associated stimulation of IRS and PI3-kinase, and activation of AKT. This ultimately results in a decrease of GLUT4 translocation, and a reduction in glucose uptake and metabolism<sup>47</sup>. Taken together, given that this state of myocardial IR typically precedes the onset of severe CVDs, early detection of changes in myocardial insulin sensitivity and glucose uptake may be an effective early predictor CVD<sup>48</sup>.

#### *1.1.4 Coronary Blood Flow as Markers of Cardiomyopathy Development*

With the increasing severity of myocardial IR and CVD development, comes progressive injury to the coronary circulation<sup>37</sup>. For example, in the previously mentioned canine model of advanced dilated cardiomyopathy, progressive hemodynamic impairment in coronary blood flow also occurred in parallel with myocardial IR and increasing severity of cardiovascular complications<sup>39</sup>. Symptoms of coronary vascular dysfunction are often found in patients with cardiomyopathy. A substantial body of evidence also suggests that reductions in coronary blood flow is a key marker in the development of cardiomyopathy<sup>49,50</sup>. For instance, coronary blood flow, as determined by Positron Emission Tomography (PET), was particularly blunted in patients later identified with severe heart failure or death<sup>51</sup>. Similarly, patients with dilated cardiomyopathy also displayed reduced coronary blood flow in conjunction with cardiac enlargement<sup>52</sup>. It is clear from these studies that impairments in coronary flow underlie the development of many CVDs. Furthermore, an Italian study of patients with various degrees of left ventricular dysfunction suggests that coronary blood flow reduction is a stronger predictor of risk of death and development of heart failure than other common clinical prognoses such as echocardiography<sup>53</sup>. The effects of IR on coronary circulation remains to be elucidated. However it is clear that progressively worsening coronary circulation function occurs with increasing severity of IR. A possible underlying factor may be the abnormal insulin mediated, nitric oxide dependent vasodilation during IR<sup>54</sup>. Nevertheless, it is



evident that coronary blood flow is a reliable predictor of systolic dysfunction and developing heart failure associated with cardiac remodeling processes.

### *1.1.5 Cardiac Remodeling Consequences*

Pathological hypertrophy is characterized in the later disease stages by cardiomyocyte enlargement, and the onset of fibrosis, resulting in the thickening and stiffening of the ventricular wall<sup>52</sup>. These cardiac remodeling processes are considered a crucial component leading to systolic dysfunction, and impediment of contractility. Furthermore, there are compelling evidence which suggests that the reduction in resting coronary flow may be associated with the expansion of extra-cellular space and ventricular dilation<sup>52</sup>. Specifically, the onset of fibrosis from an excessive expression of collagen is associated with diminished capillary density and myocardial ischemia<sup>55</sup>. Myocardial capillaries are known to be the primary determinant of coronary microvascular flow. Reductions in capillary density may result in higher capillary resistance, which requires arteriole and vein vasodilatation to maintain blood flow<sup>56</sup>. This has been observed in patients with dilated cardiomyopathy where, despite the appearance of normal coronary arteries, reduction in myocardial capillary density was strongly associated with reduced coronary blood flow and heart failure<sup>57</sup>. In addition, the accumulation of collagen in the cardiac interstitium (interstitial fibrosis) in cases of heart failure may also lead to a decrease in capillary density, subjecting cardiac myocytes to a state of hypoxia<sup>58</sup>.

The development of CVDs such as cardiomyopathy are characterized by cardiac remodeling processes such as hypertrophy and fibrosis, as well as alterations in cardiac glucose metabolism and insulin sensitivity. As these factors accumulate, they lead to the development of systolic dysfunction, heart failure, and ultimately, death. Given the clear metabolic and functional consequences of CVDs such as cardiomyopathy, early detection of these markers prior to the onset of severe disease phenotypes is crucial for interventional therapies. Traditionally, risk factors for the development of CVDs are primarily postnatal. However, emerging evidence suggests that the origin of these chronic adult diseases may be as early as during the *in utero* period<sup>59</sup>. Therefore, a key question in this thesis is whether prenatal insults, combined with the traditional postnatal factors for CVDs, can lead to the early development of CVDs.

## 1.2 Developmental Origins of Health and Disease

### 1.2.1 *Intrauterine Growth Restriction and Low Birth Weight*

According to the World Health Organization, the worldwide prevalence of low birth weight babies (LBW; <2500g) is at approximately 15.5%<sup>60</sup>. Specifically, the Canada-wide occurrence of LBW is lower at 5.9%. LBW infants are often a consequence of sub-optimal *in utero* environments, such as in cases of intrauterine growth restriction (IUGR). Clinically, growth restriction can be defined as birth weight falling below the 10<sup>th</sup> percentile for a specific sex of gestational age<sup>60</sup>. This inability of the fetus to reach its expected growth potential may impart significant risks in perinatal morbidity and mortality<sup>61,62</sup>. Interestingly, studies have demonstrated that offspring beyond the arbitrary birthweight cut-off in the clinical IUGR categorization can also be exposed to an adverse *in utero* environment, and display the same complications in adulthood<sup>63</sup>. This is exemplified by reports of offspring above the clinical birthweight cut-off displaying markers of poor *in utero* growth, such as thinness at birth, and pattern of rapid postnatal catch-up growth<sup>64</sup>. Therefore, a potentially larger number of adversely grown offspring may be at risk for later life complications such CVDs than what the traditional measures suggest. Given the increasing risk of developing metabolic diseases in later life, and the potentially higher cost of treating later life disease as opposed to early intervention programs, it is imperative that we understand the etiology, and underlying mechanisms of growth restriction and fetal programming<sup>59,65</sup>.

A reliable diagnosis of IUGR infants is crucial to understanding the effects of growth restriction on the development of complications in later life. Traditionally, the use of Ponderal index, the ratio of weight/(height<sup>3</sup>), is an excellent assessment of neonatal growth retardation, and is positively correlated with fetal nutritional status at term<sup>66,67</sup>. Furthermore, IUGR can be classified under two distinct patterns of growth abnormality: symmetrical, or asymmetrical, therefore, careful attention to body and growth relationships are essential in understanding the *in utero* growth regime<sup>68</sup>. Symmetrical IUGR, which is the proportionate decrease of fetal abdomen and head growth, results in a normal Ponderal index. It is generally associated with early fetal insults during the first or second trimester<sup>69,70</sup>. Asymmetrical IUGR in comparison, refers to the disproportionate decrease in fetal abdomen and head growth, known as the “brain sparing” effect, and is the most common form of IUGR (~70%). This is attributed to the ability of the fetus to adapt, and redistribute its cardiac output to essential circulations such as cerebral, and coronary circulation in response to insults during the last trimester<sup>71,72</sup>.

The causes of IUGR are multifactorial and can be summarized into three major scenarios: inadequate maternal supply of oxygen and nutrients, inability of fetus to fully utilize the supply of oxygen and nutrients, and abnormal placental function<sup>71</sup>. Maternal complications such as hypertension, diabetes, and under-nutrition accounts for approximately 25-30% of IUGR cases<sup>73</sup>. For example, maternal hypoxia in conditions such as pulmonary diseases and hypertension are often associated with growth restricted fetuses<sup>74,75</sup>. To a lesser extent, fetal disorders, including genetic diseases, and congenital malformations are also associated with the development of IUGR<sup>76</sup>. According to the Metropolitan Atlanta Congenital Defects Program, approximately 38% of chromosomally

abnormal infants displayed signs of IUGR<sup>77</sup>. Lastly, because fetal growth and development is largely dependent on oxygen delivery. It can therefore be inferred that normal placental development is integral for the transport of oxygen and nutrient to the fetus, and maintaining a healthy pregnancy. Furthermore, smaller placentas, and reduced placenta to fetal weight ratio are associated with growth restricted infants<sup>78</sup>. A common complication which plagues the prevalence of growth retardation is placental insufficiency.

### 1.2.2 *Placental Insufficiency*

Placental insufficiency (PI) is the inability of the placenta to provide the required transport of oxygen and nutrients to fully support the developing fetus. PI is known to be responsible for the majority of IUGR cases, and a critical component is fetal hypoxia<sup>79,80</sup>. Although the mechanisms underlining the development of PI are idiopathic, these idiopathic pregnancies and fetal hypoxia occur due to natural placental development failures<sup>81,82</sup>. Normally, as gestation advances, the growing vascular network and decrease in vascular resistance, results in the increase in both uterine and umbilical blood flow<sup>83,84</sup>. However, as PI develops, vascular growth is impaired, and vascular resistance in umbilical and uterine arteries increases, resulting in a 2.5 fold reduction in absolute blood flow<sup>85-87</sup>. Studies have also postulated that abnormal fetal trophoblast invasion of maternal decidua is associated with an impaired transformation of spiral arteries into low resistance vessels, thus reducing utero-placental blood flow<sup>88</sup>. It is thus evident that when the placenta fails to supply the fetus with adequate oxygen and nutrients, fetal growth will fall from its genetic trajectory and result in growth restriction<sup>89</sup>

### 1.2.3 *Fetal Programming and Catchup Growth*

The theory of fetal programming suggests that insults during gestation may impair the growth of the fetus, and can lead to the development of chronic diseases in later life<sup>59</sup>. The association between growth *in utero* and adult disease development was first developed by Forsdahl in the 1970s. Using official statistical data in Norway, Forsdahl reported that poor environments in childhood and adolescence followed by periods of prosperity was correlated with the risk of coronary heart disease<sup>90</sup>. Moving forward to the 1980s, Barker and colleagues also reported a strong correlation between LBW and later life development of coronary heart diseases in England and Wales<sup>91</sup>. In addition, using the official Hertfordshire medical records from 1911-1930, Barker also reported that LBW was associated with the development of IR at a mature age of 64<sup>92</sup>. These studies eventually spawned the Forsdahl-Barker hypothesis, then later, the Developmental Origins of Health and Disease hypothesis, which recognized that development of chronic metabolic diseases in later life are a result of programming mechanisms during critical periods of *in utero* life.

Further support for the idea that the prenatal period represents a critical period in later life disease development is highlighted by the study of the Dutch hunger winter at the height of the Second World War. As a result of the German occupation and blockade, civilians in the Netherlands experienced a famine during the winter of 1944. Individuals born during this period with maternal caloric restrictions displayed a 300 gram decrease in average birth weight, and in later life, an impaired glucose tolerance compared to those born prior to the incident<sup>93,94</sup>.

In response to inadequate *in utero* environments, the fetus may be programmed for a nutritionally poor postnatal environment<sup>95,96</sup>. However in setting this phenotype, a mismatch of postnatal environment can also predispose the individual to later life development of chronic diseases. This can be highlighted by examining the events of the Leningrad siege during the Second World War. These studies demonstrated that the glucose tolerance of individuals born during the siege (exposed to the famine) were not different from the individuals born after the siege<sup>97</sup>. This observation may seem at odds with previous example of the Dutch hunger winter, however this discrepancy can be explained by a major difference between the two events. While the Dutch hunger winter lasted for 6 months, the Leningrad siege lasted for 28 months. Victims from the Leningrad siege were therefore born into the famine and experienced a low nutrient diet longer than those of the Dutch hunger winter<sup>98</sup>. Thus, it can be inferred that unlike their counterparts in Leningrad, infants of the Dutch hunger experienced a mismatched postnatal environment of high nutrient intake, which resulted in the programmed IR in adulthood. These studies also highlights the postnatal period as another critical period in the development of diseases in later life. Therefore warranting our attention to the concept of “catch-up growth”.

A postnatal “catch-up growth” describes the accelerated postnatal growth profile which compensates for restricted growth during prenatal life, and is usually associated with asymmetrical growth restriction<sup>69</sup>. However many studies have associated this accelerated growth trajectory with the development of diseases in adulthood. For example, similar to the original Barker studies, a longitudinal study in Finland demonstrated that women born of LBW and experienced rapid postnatal growth were associated with the development of coronary heart disease in later life<sup>99</sup>. In another study, this “catch-up growth” in LBW

children was also strongly associated with an impaired glucose tolerance at seven years of age<sup>100</sup>. Alarming, this accelerated period of growth resulting from sub-optimal *in utero* environments, is highly correlated with CVD development. A Finnish study reported that the highest death rates from coronary heart disease were from children who were thin at birth, but had caught up to average body weight by childhood<sup>101</sup>. These studies provide strong evidence for the role of “catch-up growth” in exacerbating growth restricted individuals and programming of diseases in later life. Interestingly, the current arbitrary birth weight cut-off in IUGR categorization cannot account for the possibility that newborns above the 10<sup>th</sup> percentile can also be exposed to an adverse *in utero* environment<sup>63</sup>. The inappropriate growth patterns associated with insufficient *in utero* environments can still be present despite not being reflected in birth weight outcomes. In support, a study reported that accelerated growth during the first 4 months of post-natal life is associated with childhood obesity, and is also independent of birth weight<sup>64</sup>. Therefore inferring that the accelerated growth pattern maybe a more crucial factor behind the adverse health outcomes than birth weight alone. In support, risk of chronic disease development have also been demonstrated to occur independent of birth weight<sup>102,103</sup>. This highlights the possibility that the risk of disease development is not solely caused by a drop in birthweight, but by a combination of *in utero* induced stress factors, and an accelerated growth pattern. As a result, it is important to further examine the underlying processes behind fetal programming of CVD development in later life and the contributions of a postnatal catch up growth.



#### 1.2.4 *Fetal Programming of CVDs*

Barker and colleagues initially demonstrated that mortality from heart diseases are strongly associated with fetal programming, both animal and human studies continued to support Barker's original work and add further understanding to the *in utero* programmed mechanisms underlying development of diseases in later life<sup>104-106</sup>.

Mechanisms such as *in utero* hypoxia have been known to alter heart development, and suppress cardiac contractility<sup>107,108</sup>. Specifically, *in utero* insults are also associated with the development of cardiac hypertrophy, and cardiac remodeling. For example, the expression of pro-fibrotic genes, with discrete structural abnormalities such as deposition of collagen in the heart at adolescence have been found in rats born of hypoxic IUGR<sup>109</sup>. Additionally, rats born from a hypoxic pregnancy also displayed left ventricular enlargement at 12 months of age with strong indication of left ventricular dysfunction and pulmonary hypertension<sup>110</sup>. Collectively, these studies suggests that IUGR individuals may be predisposed to the development of CVDs in later life through these progressive cardiac remodeling situations.

The programming of CVD such as cardiomyopathy may stem from placental insufficiencies given that the placenta regulates flow of oxygen and necessary nutrients for the fetus' development. Amounting evidence have linked later life cardiovascular problems early markers such as disturbed endothelial function, and persistent alterations in cardiac metabolisms<sup>111,112</sup>. These manifestations can be traced back to the *in utero* environment. For example, impedance to placental blood flow, a characteristic of PI, often results in the

increase in placental bed resistance<sup>113,114</sup>. In order to overcome the mechanical force required to eject against a high resistance vascular bed, abnormal fetal heart growth typically occurs as adaptation. During post-natal life, this is associated with an increased ventricular load, which can contribute to the development of cardiac hypertrophy<sup>113,114</sup>. Interestingly, heart weights are not always altered in the placental restricted offspring, however there is certainly a higher proportion of mononucleated cardiomyocytes as demonstrated in a sheep model<sup>115</sup>. Furthermore, cardiomyocyte size relative to heart size is increased in the placental insufficient offspring. Normally, cardiomyocytes undergo binucleation during late gestation. However due to environmental factors such as placental restriction, this process – an indicator of heart maturation – is delayed<sup>116,117</sup>. As a result, chronic placental restriction results in delayed binucleation during development, and larger but fewer cardiomyocytes at term<sup>115</sup>. These adaptations to chronic placental restriction are risk factors for the development of cardiac hypertrophy in adulthood, and can have long term consequences in later life. These studies altogether indicate the importance of fetal programming as a predictor of cardiovascular complications in later life. In summary, it is clear that *in utero* environments play a crucial role in later life disease development through inappropriate growth adaptations. Furthermore, these adaptations, when challenged by additional insults such as an unhealthy dietary pattern, can further increase the susceptibility to CVD development in the offspring.

### 1.3 Adverse Postnatal Diets

As previously mentioned in the fetal programming discussion, another critical period in determining development of chronic diseases is the postnatal period. Specifically, a mismatch between prenatal and postnatal environment can lead to the development of metabolic complications in later life, as demonstrated by the Dutch hunger winter<sup>93</sup>. An increasing concern in our modern society is believed to affect this said critical postnatal growth period. This concern is known as the “Western Diet” (WD), which is characterized by high saturated fats, and high sugar contents<sup>118,119</sup>. According to the World Health Organization, the consumption of this energy-dense diet combined with the lack of physical activity are the fundamental causes of obesity. Recent estimates of world-wide obesity rates is at 10%, with more than 40 million children categorized as overweight or obese<sup>120</sup>. As American corporations expand their fast food empire into developing countries, rates of obesity has also risen approximately 30%<sup>120</sup>. It therefore draws to our attention, how the mismatch between restricted *in utero* environments and an energy dense postnatal diet may affect health in adulthood

#### 1.3.1 *Cardiovascular Dysfunction and WD*

The most concerning aspect of the consumption of a WD and increased Body Mass Index (BMI) is the risk of developing CVDs in adulthood<sup>120</sup>. In an eight year study, men aged 40-75 years whom, according to a questionnaire, declared a frequent consumption of WD had a higher risk of developing cardiovascular diseases compared to men who

primarily consumed a prudent diet<sup>121</sup>. A more recent study using logistic regression demonstrated that, after adjusting for coronary risk factors, women whom consumes processed meats, and sugars have a higher relative risk for heart diseases<sup>119</sup>. These epidemiological studies demonstrates that unhealthy dietary patterns such as the WD closely predicts the risk of CVDs later in life. Several animal studies also attempted to investigate the underlying mechanisms of this association. For example, a recent study demonstrated that rats fed with a high fat diet were associated with mild reduction in ejection fraction, increased left ventricular mass and IR<sup>122</sup>. As previously discussed, a state of IR in the heart is strongly associated with cardiac remodeling and heart failure<sup>123</sup>. However, this insulin resistant state can be attributed to the consumption of diet high in fats such as the WD. In response, to the high levels of fatty acids, cardiomyocytes increase its expression of CD36 transporter for fatty acid uptake, and reduce GLUT4 mediated glucose uptake<sup>124,125</sup>. Maladaptation in the saturated fatty acid oxidation often leads to the increase in its by-product: reactive oxygen species (ROS), and the accumulation of lipid intermediates such as diacylglycerol (DAG), and ceramide<sup>126</sup>. In turn, ROS and DAG are associated with the inhibition of serine phosphorylation of IRS-1 in the insulin signaling pathway. In addition, ceramide is also associated with the inhibition of AKT<sup>127</sup>. As a result, increased saturated fatty acids, and lipid intermediates can impair the heart's ability to uptake glucose, resulting in IR. Furthermore, ROS is also associated with cardiac hypertrophy, where it has been shown to activate mitogen-activated protein kinases, and matrix metalloproteinase (MMP) involved in extracellular matrix remodeling and fibrosis<sup>128,129</sup>.

Despite its importance to cardiac metabolism, the consequences of the change towards fatty acid oxidation is not completely understood. Take for example a study in 2006 which examined the effects of high fat diets on the development of left ventricular remodeling in response to hypertension. Compared to a low fat diet, rats fed on a high fat diet (60% of total energy) did not demonstrate increases in left ventricular mass, myocyte cross-sectional area<sup>130</sup>. This suggests that a switch towards increased fatty acid oxidation can improve heart failure outcomes of hypertensive, and high fat diet fed rats. However, other studies have suggested that this may be due to the differential effects of saturated and unsaturated fatty acid content. Specifically, rats fed on saturated fatty acids demonstrated increased cardiomyocyte apoptosis compared to rats fed on unsaturated fatty acids, possibly due to an association with increased ceramide content<sup>131</sup>. In addition, another study demonstrated that rats developed contractile dysfunction when fed a WD (which contains a higher carbohydrate content), but not when fed a strictly high-fat diet<sup>118</sup>. This difference may be attributed to the fatty acid oxidation maladaptation, and the induction of fatty acid responsive genes associated with WD feeding. Considering the evidences presented, fatty acid oxidation surely plays an important and dynamic role in the development of heart failure. It is also evident that prolonged WD feeding is indeed associated with development of heart failure and cardiac remodeling due to maladapted fatty acid oxidation. With a significant portion of our population already predisposed to later life CVD development from *in utero* origins, the consumption of such unhealthy dietary patterns may exacerbate the existing consequences. Particularly, it can result in an earlier expression of the disease phenotype, and thus warrants our attention to new reliable diagnosis techniques in order to provide earlier intervention.

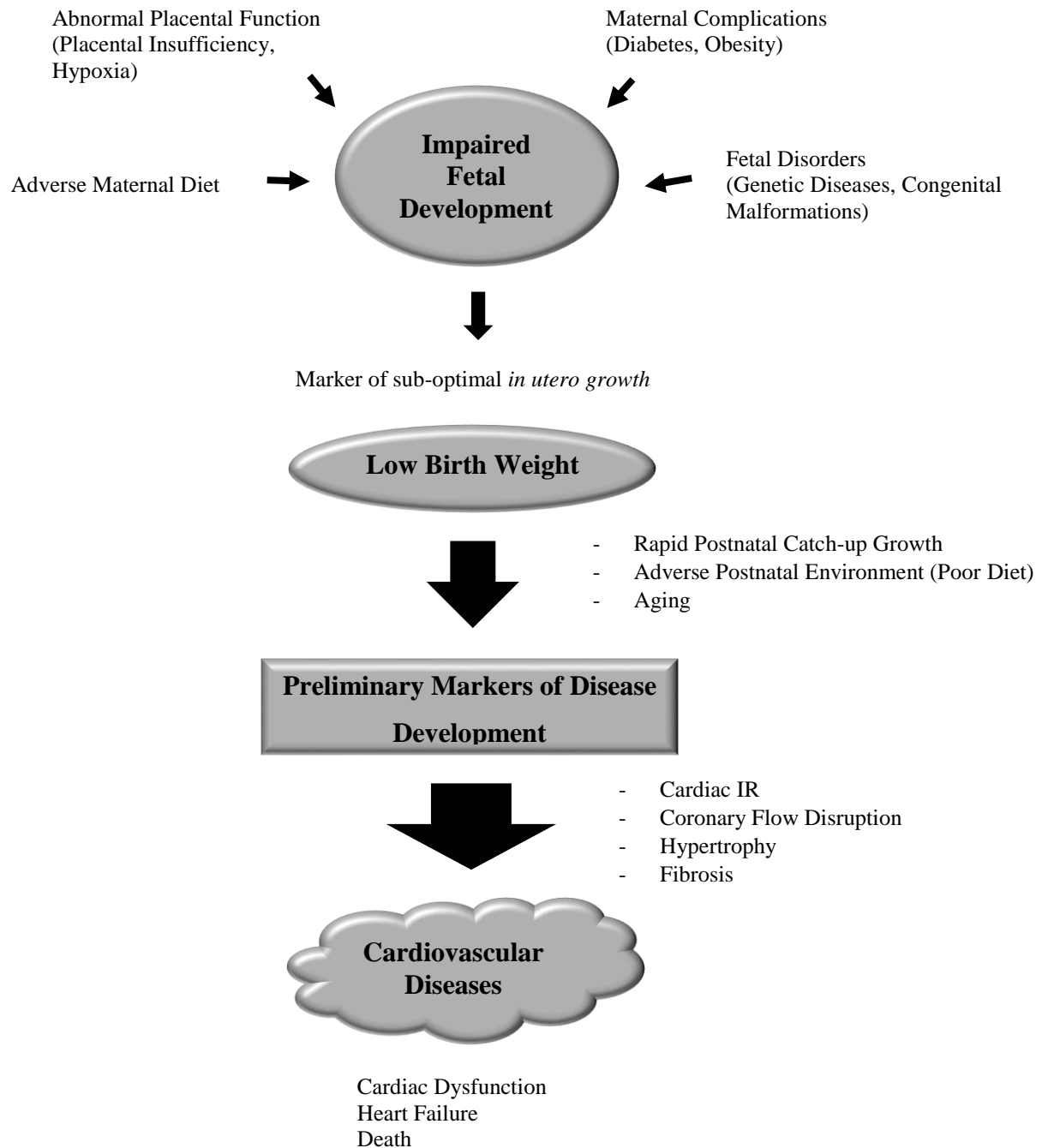


**Figure 1.1 Prenatal and Postnatal Factors That May Contribute to the Development of Cardiovascular Diseases in Adult Life.** In utero insults such as PI, or poor maternal diet induces an unfavorable intrauterine environment, resulting in intrauterine growth restriction, and a low birth weight outcome. This predisposes the offspring to a period of rapid catch-up growth, associated with development of many adult diseases. This can be further aggravated by a postnatal insult from WD consumption. By adulthood, this may lead to the emergence of markers of CVDs such as IR, and disruptions in coronary blood flow. Eventually, these factors contribute to the development of a severe CVD.

## 1.4 Methods for Studying Cardiac Blood Flow and Metabolism

### 1.4.1 *Doppler Ultrasound*

Although currently there are no clinical technique available which allows the direct visualization of the coronary microcirculation, techniques which measures coronary blood flow are commonly used to assess the function of microvasculature. Several of these techniques utilizes the Doppler principle which allows the measurement of instantaneous changes in coronary blood flow. One such example is the Doppler catheter technique. Introduced in the 1970s by Hartley and Cole, it utilizes a piezoelectric crystal tipped catheter placed at the coronary ostium<sup>132,133</sup>. In addition, the introduction of the Doppler-tipped guide wires, the 90s also saw the use of intracoronary flow measurement as an accepted approach in coronary blood flow measurements<sup>134</sup>. This method utilizes a thin flexible steerable guide wire with an ultrasound transducer tip which is placed in the left circumflex coronary artery. It offers improvement over the thicker Doppler catheters which are prone to alteration of velocity profile and obstruction of vessel<sup>135</sup>. Both of the Doppler techniques have already been established as useful techniques, however they require invasive catheterization, which may limit its usefulness as a clinical assessment of CVD development. In addition, although the use of Doppler catheters or wire are determined to be safe, severe complications such as bradycardia and coronary spasms can occur<sup>134</sup>. As a result, a safer, and equally reliable non-invasive technique in coronary flow, and perfusion measurements should be explored.

#### 1.4.2 *Echocardiography*

Echocardiography is performed by placing an ultrasound transducer on the chest wall of the subject, which creates two-dimensional images of the heart<sup>136</sup>. It can provide detailed information such as ventricular wall thickness, and the size and shape of the heart. In addition, it is also capable of calculating ejection fraction, cardiac output and diastolic function by estimating the changes of ventricle size during diastole and systole<sup>137</sup>. As a result, the use of echocardiography is common amongst physicians for the diagnosis of cardiomyopathies and hypertrophy. Additionally advancements in ultrasound technology also allows the measurement of coronary flow using the Transthoracic Doppler Echocardiography (TTDE) technique. Specifically, the TTDE utilizes pulsed wave Doppler echocardiography and color Doppler flow mapping for the measurement of flow at the left anterior descending coronary artery<sup>136,138</sup>. The advantageous of echocardiography is that it provides a non-invasive assessment of various heart functions with no known risks or side effects. However results from echocardiography may be very operator dependent, and thus lack specificity<sup>139</sup>. More importantly, the measurement of heart functions such as cardiac output are end point measurements, and not early diagnostic targets prior to the onset of diseases.

#### 1.4.3 *Positron Emission Tomography*



Positron Emission Tomography (PET) is a highly sensitive modality which provides localization of radioactively labeled tracer concentrations through the detection of gamma rays resulting from positron annihilation<sup>140</sup>. These tracers can provide important hemodynamic and metabolic information. In patients with hypertrophic cardiomyopathy, coronary blood flow reserve measured with <sup>15</sup>O-labelled water and <sup>13</sup>N-labelled ammonia has been shown to be decreased<sup>49,141</sup>. Similarly, patients with dilated cardiomyopathy also demonstrated an abnormal coronary reserve measured by <sup>15</sup>O-labelled water<sup>142</sup>.

Measurement of perfusion parameters are also typically performed in conjunction with cardiac metabolism imaging. Measurement of cardiac metabolic rate is typically achieved by <sup>18</sup>F-2-fluoro-2-deoxy-d-glucose (<sup>18</sup>F -FDG) tracer. [<sup>18</sup>F] FDG is a glucose analog which is taken up by tissues such as the heart, muscle, and liver. However, [<sup>18</sup>F] FDG cannot be metabolized due to the hydroxyl group at 2' position substituted with a radioactive isotope <sup>18</sup>F, As a result, the measured activity of [<sup>18</sup>F] FDG is indicative of glucose uptake, and degree of glycolysis<sup>143</sup>. The use of [<sup>18</sup>F] FDG as indicators of tissue insulin sensitivity is common in clinical practice. For example a study with [<sup>18</sup>F] FDG PET clearly demonstrated that insulin sensitivity was highly associated with increased glucose uptake in the liver<sup>144,145</sup>. Furthermore, [<sup>18</sup>F] FDG PET can also be used to determine myocardial viability, using the criteria of low perfusion and low metabolism<sup>145,146</sup>. In summary, PET offers a well-established, and non-invasive method for the measurement of hemodynamic and metabolic parameters in the target organ. However, PET requires the injection of radioactive tracers, and exposure to ionizing radiation. Nonetheless, PET is an important imaging modality in research due to its ability to detect problems prior to actual onset of diseases.

#### 1.4.4 *Dynamic Contrast Enhanced Computed Tomography*

Developed in the 1970s, Dynamic Contrast Enhanced Computed Tomography (DCE-CT) aims to provide a non-invasive solution to the study of hemodynamics in tissue<sup>147</sup>. However due to limitations in spatial and temporal resolution during its infancy, the widespread use of DCE-CT failed to gain traction. Fortunately, over the next couple of decades, significant advancements in CT technology have addressed these limitations and propelled DCE-CT to be a competitive imaging modality with wide clinical acceptance. For example, development of slip-ring technology has dramatically improved temporal resolutions. In addition, advancements in detector technology has allowed the imaging of whole organs in a single study. As a result, DCE-CT has become an excellent diagnostic tool in the study of vascular changes, and coronary circulation associated with CVDs<sup>148-150</sup>. In comparison to the previously mentioned modalities, DCE-CT provides a more complete evaluation of tissue hemodynamics with its capability to measure perfusion, blood volume, mean transit time, and capillary permeability surface area product in a single study<sup>151</sup>. In comparison to MRI, DCE-CT may appear disadvantaged due to the use of ionizing radiation. However, the gadolinium-based contrast agent used in contrast-enhanced MR lacks a linear relationship between signal intensity and concentration. In contrast, DCE-CT provides a linear relationship between iodine contrast concentration and X-ray attenuation<sup>152</sup>.

Several studies in cardiac imaging have given solid validation to the use of DCE-CT as a reliable diagnostic tool. One such study, recruited patients with coronary artery disease with varying degree of stenosis as classified from catheter-based angiograms.

DCE-CT with dipyridamole infusion as performed, and analyzed to calculate myocardial blood flow, and blood volume. The results demonstrated that blood flow is significantly lower in stenosed patients, and that DCE-CT appeared to be a useful predictor of functionally significant coronary stenosis<sup>150</sup>. In another evaluation of the use of CT perfusion, it demonstrated a high sensitivity and specificity in diagnosis of chest pain from coronary stenosis<sup>149</sup>.

In DCE-CT imaging, X-ray iodinated contrast agent is injected in peripheral vein, while the CT scanner image the passage of contrast through the myocardium. Two assumptions must be made in perfusion calculations: first is the uniform distribution of iodinated contrast through the vascular system. Second, is that the increase in attenuation in tissue is proportional to the concentration of contrast agent<sup>153</sup>. Typically, CT scanner scans the region of interest continuously for a prolonged acquisition period which captures the slow leakage of contrast from blood vessels into interstitial space. The algorithm used in DCE-CT is based on the approximation of the Johnson-Wilson model which explains the bidirectional exchange of contrast between the capillaries and the interstitium. This adiabatic approximation assumes that changes in tracer concentration are slower in parenchymal tissue compared to that in capillaries<sup>154</sup>. With the algorithm it is then possible to calculate blood flow and display the values in rainbow colored functional maps.

DCE-CT is an excellent imaging modality for the study of hemodynamical changes. It is non-invasive and widely available in hospitals, with rapid scan times. More importantly, it can image soft tissues, bone, and blood vessels with excellent temporal and spatial resolution. However, a major drawback of DCE-CT is the exposure to carcinogenic ionizing radiation. In addition, the injection of contrast agents which may impair renal

functions. Nonetheless, the use of DCE-CT may potentially provide a means to monitor for the onset and progression of diseases such as CVDs.

## 1.5 Research Goals

The objective of this thesis was to investigate the combined effects of *in utero* insults from placental insufficiency, or high energy diets during pregnancy, combined with an adverse postnatal diets on the development of CVDs in early adulthood. In addition, this project aimed to assess the use of DCE-CT and PET in the study of CVDs in a guinea pig model. In this regard, the two primary goals of the thesis were as follows:

- 1) Investigate the effects of placental insufficiency induced low birth weight and postnatal Western diet on the development of CVD in a guinea pig model with DCE-CT and PET imaging.
- 2) Examine the effects of high energy maternal diet and postnatal Western diet on the development of CVD in a guinea model with DCE-CT and PET imaging.

## 1.6 References

1. A Global Brief on Hypertension World Health Day 2013. (2013).
2. *Noncommunicable Diseases. World Health Organization.* (2013).
3. Bridget B. Kelly (Institute of Medicine). *Promoting Cardiovascular Health in the Developing World:: A Critical Challenge to Achieve Global Health.* (National Academies Press, 2010).
4. Howard, B. V. Sugar and Cardiovascular Disease: A Statement for Healthcare Professionals From the Committee on Nutrition of the Council on Nutrition, Physical Activity, and Metabolism of the American Heart Association. *Circulation* **106**, 523–527 (2002).
5. Hooper, L. *et al.* Reduced or modified dietary fat for preventing cardiovascular disease. *Cochrane database Syst. Rev.* CD002137 (2011). doi:10.1002/14651858.CD002137.pub2
6. *Political Declaration of the High-level Meeting of the General Assembly on the Prevention and Control of Non-communicable Diseases.* (2012).
7. Dec, G. & Fuster, V. Idiopathic dilated cardiomyopathy. *N. Engl. J. Med.* **331**, 1564–1575 (1994).
8. Maron, B. J. *et al.* Contemporary definitions and classification of the cardiomyopathies: an American Heart Association Scientific Statement from the Council on Clinical Cardiology, Heart Failure and Transplantation Committee; Quality of Care and Outcomes Research and Functio. *Circulation* **113**, 1807–16 (2006).
9. Kasper, D. *Harrison's Principles of Internal Medicine.* (McGraw-Hill, 2005).

10. Lloyd-Jones, D. *et al.* Heart disease and stroke statistics--2010 update: a report from the American Heart Association. *Circulation* **121**, e46–e215 (2010).
11. McCartan, C., Mason, R., Jayasinghe, S. R. & Griffiths, L. R. Cardiomyopathy classification: ongoing debate in the genomics era. *Biochem. Res. Int.* **2012**, 796926 (2012).
12. Maron, B. J. Hypertrophic Cardiomyopathy. *JAMA* **287**, 1308–1320 (2002).
13. Roberts, W. C., Siegel, R. J. & McManus, B. M. Idiopathic dilated Cardiomyopathy: Analysis of 152 necropsy patients. *Am. J. Cardiol.* **60**, 1340–1355 (1987).
14. Levy, D. & Garrison, R. Prognostic implications of echocardiographically determined left ventricular mass in the Framingham Heart Study. *N. Engl. J. Med.* **322**, 1561–1566 (1990).
15. Zak, R. Growth of the Heart in Health and Disease. *New York Raven Press* 1–24, 131–185, 381–420 (1984).
16. Chien, K., Knowlton, K., Zhu, H. & Chien, S. Regulation of cardiac gene expression during myocardial growth and hypertrophy: molecular studies of an adaptive physiologic response. *FASEB J* **5**, 3037–3046 (1991).
17. Karsner, H. T., Saphir, O. & Todd, T. W. The State of the Cardiac Muscle in Hypertrophy and Atrophy. *Am. J. Pathol.* **1**, 351–372.1 (1925).
18. Sopontammarak, S. *et al.* Mitogen-activated protein kinases (p38 and c-Jun NH<sub>2</sub>-terminal kinase) are differentially regulated during cardiac volume and pressure overload hypertrophy. *Cell Biochem. Biophys.* **43**, 61–76 (2005).
19. Knöll, R., Hoshijima, M. & Chien, K. Cardiac mechanotransduction and implications for heart disease. *J. Mol. Med. (Berl)*. **81**, 750–6 (2003).

20. Hoshijima, M. Mechanical stress-strain sensors embedded in cardiac cytoskeleton: Z disk, titin, and associated structures. *Am. J. Physiol. Heart Circ. Physiol.* **290**, H1313–25 (2006).
21. Grossman, W., Jones, D. & McLaurin, L. P. Wall stress and patterns of hypertrophy in the human left ventricle. *J. Clin. Invest.* **56**, 56–64 (1975).
22. Pluim, B. M., Zwinderman, A. H., van der Laarse, A. & van der Wall, E. E. The Athlete's Heart: A Meta-Analysis of Cardiac Structure and Function. *Circulation* **101**, 336–344 (2000).
23. Maron, B. J., Gohman, T. E. & Aeppli, D. Prevalence of sudden cardiac death during competitive sports activities in Minnesota High School athletes. *J. Am. Coll. Cardiol.* **32**, 1881–1884 (1998).
24. Weber, K., Brilla, C. & Janicki, J. Myocardial fibrosis: functional significance and regulatory factors. *Cardiovasc. ...* **27**, 341–348 (1993).
25. Cohn, J. N. *et al.* Report of the National Heart, Lung, and Blood Institute Special Emphasis Panel on Heart Failure Research. *Circulation* **95**, 766–770 (1997).
26. Maron, B. J. *et al.* Epidemiology of hypertrophic cardiomyopathy-related death: revisited in a large non-referral-based patient population. *Circulation* **102**, 858–64 (2000).
27. Frenneaux, M. P. Assessing the risk of sudden cardiac death in a patient with hypertrophic cardiomyopathy. *Heart* **90**, 570–5 (2004).
28. Maron, B. J. *et al.* Epidemiology of hypertrophic cardiomyopathy-related death: revisited in a large non-referral-based patient population. *Circulation* **102**, 858–64 (2000).
29. Vusse, G. Van der & Glatz, J. Fatty acid homeostasis in the normoxic and ischemic heart. *Physiol. Rev.* **72**, (1992).



30. Allard, F. *et al.* Contribution of oxidative metabolism to ATP production in hypertrophied and glycolysis hearts. *Am. J. Physiol.* **267**, H742–H750 (1994).
31. Christe, M. E. & Rodgers, R. L. Altered glucose and fatty acid oxidation in hearts of the spontaneously hypertensive rat. *J. Mol. Cell. Cardiol.* **26**, 1371–5 (1994).
32. Dávila-Román, V. G. *et al.* Altered myocardial fatty acid and glucose metabolism in idiopathic dilated cardiomyopathy. *J. Am. Coll. Cardiol.* **40**, 271–277 (2002).
33. Paternostro, G. Insulin resistance in patients with cardiac hypertrophy. *Cardiovasc. Res.* **42**, 246–253 (1999).
34. Wang, C. & Hu, S. M. Developmental regulation in the expression of rat heart glucose transporters. *Biochem. Biophys. Res. Commun.* **177**, 1095–100 (1991).
35. Santalucía, T. *et al.* Developmental regulation of GLUT-1 (erythroid/Hep G2) and GLUT-4 (muscle/fat) glucose transporter expression in rat heart, skeletal muscle, and brown adipose tissue. *Endocrinology* **130**, 837–46 (1992).
36. Neubauer, S. The Failing Heart — An Engine Out of Fuel. *N. Engl. J. Med.* **356**, 1140–1151 (2007).
37. Prior, J. O. *et al.* Coronary circulatory dysfunction in insulin resistance, impaired glucose tolerance, and type 2 diabetes mellitus. *Circulation* **111**, 2291–8 (2005).
38. Rutter, M. K. Impact of Glucose Intolerance and Insulin Resistance on Cardiac Structure and Function: Sex-Related Differences in the Framingham Heart Study. *Circulation* **107**, 448–454 (2003).
39. Nikolaidis, L. The development of myocardial insulin resistance in conscious dogs with advanced dilated cardiomyopathy. *Cardiovasc. Res.* **61**, 297–306 (2004).
40. Christopher, B. a *et al.* Myocardial insulin resistance induced by high fat feeding in heart failure is associated with preserved contractile function. *Am. J. Physiol. Heart Circ. Physiol.* **299**, H1917–27 (2010).

41. Randle, P. J., Garland, P. B., Hales, C. N. & Newsholme, E. A. The Glucose Fatty-Acid Cycle its role in insulin sensitivity and the metabolic disturbances of diabetes mellitus. *Lancet* **281**, 785–789 (1963).
42. Wende, A. R. & Abel, E. D. Lipotoxicity in the heart. *Biochim. Biophys. Acta* **1801**, 311–9 (2010).
43. Fischer, Y. *et al.* Insulin-induced Recruitment of Glucose Transporter 4 (GLUT4) and GLUT1 in Isolated Rat Cardiac Myocytes: Evidence of the existence of different intracellular GLUT4 vesicle populations. *J. Biol. Chem.* **272**, 7085–7092 (1997).
44. Bell, G. I. *et al.* Molecular biology of mammalian glucose transporters. *Diabetes Care* **13**, 198–208 (1990).
45. Fischer, Y., Thomas, J., Rösen, P. & Kammermeier, H. Action of metformin on glucose transport and glucose transporter GLUT1 and GLUT4 in heart muscle cells from healthy and diabetic rats. *Endocrinology* **136**, 412–20 (1995).
46. Lizcano, J. M. & Alessi, D. R. The insulin signalling pathway. *Curr. Biol.* **12**, R236–8 (2002).
47. Pessin, J. E. & Saltiel, A. R. Signaling pathways in insulin action: molecular targets of insulin resistance. *J. Clin. Invest.* **106**, 165–9 (2000).
48. McFarlane, S. I., Banerji, M. & Sowers, J. R. Insulin resistance and cardiovascular disease. *J. Clin. Endocrinol. Metab.* **86**, 713–8 (2001).
49. Camici, P. *et al.* Coronary vasodilation is impaired in both hypertrophied and nonhypertrophied myocardium of patients with hypertrophic cardiomyopathy: a study with nitrogen-13 ammonia and positron emission tomography. *J. Am. Coll. Cardiol.* **17**, 879–86 (1991).
50. Kawada, N. *et al.* Hypertrophic cardiomyopathy: MR measurement of coronary blood flow and vasodilator flow reserve in patients and healthy subjects. *Radiology* **211**, 129–35 (1999).

51. Olivotto, I. *et al.* Relevance of coronary microvascular flow impairment to long-term remodeling and systolic dysfunction in hypertrophic cardiomyopathy. *J. Am. Coll. Cardiol.* **47**, 1043–8 (2006).
52. Jerosch-Herold, M. *et al.* Cardiac magnetic resonance imaging of myocardial contrast uptake and blood flow in patients affected with idiopathic or familial dilated cardiomyopathy. *Am. J. Physiol. Heart Circ. Physiol.* **295**, H1234–H1242 (2008).
53. Neglia, D. Prognostic Role of Myocardial Blood Flow Impairment in Idiopathic Left Ventricular Dysfunction. *Circulation* **105**, 186–193 (2002).
54. Prior, J. O. *et al.* Coronary circulatory dysfunction in insulin resistance, impaired glucose tolerance, and type 2 diabetes mellitus. *Circulation* **111**, 2291–8 (2005).
55. Gunasinghe, S. K., & Spinale, F. G. Myocardial basis for heart failure. In D. L. Mann (Ed.). *Role Card. Interstitium Hear. Fail.* 57–70 (2004).
56. Kaul, S. & Jayaweera, A. R. Myocardial capillaries and coronary flow reserve. *J. Am. Coll. Cardiol.* **52**, 1399–401 (2008).
57. Tsagalou, E. P. *et al.* Depressed coronary flow reserve is associated with decreased myocardial capillary density in patients with heart failure due to idiopathic dilated cardiomyopathy. *J. Am. Coll. Cardiol.* **52**, 1391–8 (2008).
58. Sabbah, H. N., Sharov, V. G., Lesch, M. & Goldstein, S. Progression of heart failure: A role for interstitial fibrosis. *Mol. Cell. Biochem.* **147**, 29–34 (1995).
59. Barker, D. J. Intrauterine programming of adult disease. *Mol. Med. Today* **1**, 418–23 (1995).
60. Manning, F. Intrauterine growth retardation. *Fetal Med. Princ. Pract.* **317**, (1995).
61. Scifres, C. M. & Nelson, D. M. Intrauterine growth restriction, human placental development and trophoblast cell death. *J. Physiol.* **587**, 3453–8 (2009).

62. Williams RL, Creasy RK, Cunningham GC, H. W. & Norris FD, T. M. Fetal Growth and Perinatal Viability in California. *Obstet. Gynecol.* **59**, 624–32 (1982).
63. Saintonge, J. & Côté, R. Intrauterine growth retardation and diabetic pregnancy: two types of fetal malnutrition. *Am. J. Obstet. Gynecol.* **146**, 194–8 (1983).
64. Stettler, N., Zemel, B. S., Kumanyika, S. & Stallings, V. A. Infant Weight Gain and Childhood Overweight Status in a Multicenter, Cohort Study. *Pediatrics* **109**, 194–199 (2002).
65. Eriksson, J., Forsen, T., Tuomilehto, J., Osmond, C. & Barker, D. Fetal and Childhood Growth and Hypertension in Adult Life. *Hypertension* **36**, 790–794 (2000).
66. Brandt, I., Sticker, E. J. & Lentze, M. J. Catch-up growth of head circumference of very low birth weight, small for gestational age preterm infants and mental development to adulthood. *J. Pediatr.* **142**, 463–8 (2003).
67. Fay, R. A., Dey, P. L., Saadie, C. M. J., Buhl, J. A. & Gebiski, V. J. Ponderal Index: A Better Definition of the ‘At Risk’ Group With Intrauterine Growth Problems than Birth-weight for Gestational Age in Term Infants. *Aust. New Zeal. J. Obstet. Gynaecol.* **31**, 17–19 (1991).
68. Pollack, R. N., & Divon, M. Y. Intrauterine Growth Retardation: Definition, Classification, and Etiology. *Clin. Obstet. Gynecol.* **35**, 99–107 (1992).
69. Wollmann, H. A. Intrauterine Growth Restriction: Definition and Etiology. *Horm. Res. Paediatr.* **49**, 1–6 (1998).
70. Al Riyami, N. *et al.* Utility of head/abdomen circumference ratio in the evaluation of severe early-onset intrauterine growth restriction. *J. Obstet. Gynaecol. Can.* **33**, 715–9 (2011).
71. Brodsky, D. & Christou, H. Care Medicine Current Concepts in Intrauterine Growth Restriction. (2004). doi:10.1177/0885066604269663

72. Lin, C.-C., Su, S.-J. & River, L. P. Comparison of associated high-risk factors and perinatal outcome between symmetric and asymmetric fetal intrauterine growth retardation. *Am. J. Obstet. Gynecol.* **164**, 1535–1542 (1991).
73. Lin, C. & Santolaya-forgas, J. Current concepts of fetal growth restriction: Part I. Causes, classification, and pathophysiology. **7844**, 1044–1055 (1997).
74. Van Geijn, H. P., Kaylor, W. M., Nicola, K. R. & Zuspan, F. P. Induction of severe intrauterine growth retardation in the Sprague-Dawley rat. *Am. J. Obstet. Gynecol.* **137**, 43–7 (1980).
75. Resnik, R. Intrauterine growth restriction. *Obstet. Gynecol.* **99**, 490–6 (2002).
76. Snijders, R. J. M., Sherrod, C., Gosden, C. M. & Nicolaides, K. H. Fetal growth retardation: Associated malformations and chromosomal abnormalities. *Am. J. Obstet. Gynecol.* **168**, 547–555 (1993).
77. Brenner, W. E., Edelman, D. A. & Hendricks, C. H. A standard of fetal growth for the United States of America. *Am. J. Obstet. Gynecol.* **126**, 555–64 (1976).
78. Heinonen, S., Taipale, P. & Saarikoski, S. Weights of placentae from small-for-gestational age infants revisited. *Placenta* **22**, 399–404 (2001).
79. Baschat, A. A. & Hecher, K. Fetal growth restriction due to placental disease. *Semin. Perinatol.* **28**, 67–80 (2004).
80. Salafia, C. M., Pezzullo, J. C., Ghidini, A., Lopèz-Zeno, J. A. & Whittington, S. S. Clinical correlations of patterns of placental pathology in preterm pre-eclampsia. *Placenta* **19**, 67–72 (1998).
81. Lim, K. H. *et al.* Human cytotrophoblast differentiation/invasion is abnormal in pre-eclampsia. *Am. J. Pathol.* **151**, 1809–18 (1997).

82. Kingdom, J., Huppertz, B., Seaward, G. & Kaufmann, P. Development of the placental villous tree and its consequences for fetal growth. *Eur. J. Obstet. Gynecol. Reprod. Biol.* **92**, 35–43 (2000).
83. Sutton, M. S. *et al.* Changes in placental blood flow in the normal human fetus with gestational age. *Pediatr. Res.* **28**, 383–7 (1990).
84. Rudolph, a. M. Distribution and regulation of blood flow in the fetal and neonatal lamb. *Circ. Res.* **57**, 811–821 (1985).
85. Galan, H. L. *et al.* Fetal hypertension and abnormal Doppler velocimetry in an ovine model of intrauterine growth restriction. *Am. J. Obstet. Gynecol.* **192**, 272–9 (2005).
86. Ferrazzi, E. *et al.* Umbilical vein blood flow in growth-restricted fetuses. *Ultrasound Obstet. Gynecol.* **16**, 432–8 (2000).
87. Konje, J. C., Howarth, E. S., Kaufmann, P. & Taylor, D. J. Longitudinal quantification of uterine artery blood volume flow changes during gestation in pregnancies complicated by intrauterine growth restriction. *BJOG An Int. J. Obstet. Gynaecol.* **110**, 301–305 (2003).
88. Pijnenborg, R., Bland, J. M., Robertson, W. B. & Brosens, I. Uteroplacental arterial changes related to interstitial trophoblast migration in early human pregnancy. *Placenta* **4**, 397–413 (1983).
89. Anthony, R. V, Scheaffer, a N., Wright, C. D. & Regnault, T. R. H. Ruminant models of prenatal growth restriction. *Reprod. Suppl.* **61**, 183–94 (2003).
90. Forsdahl, A. Are poor living conditions in childhood and adolescence an important risk factor for arteriosclerotic heart disease? *J. Epidemiol. Community Heal.* **31**, 91–95 (1977).
91. Barker, D. Infant mortality, childhood nutrition, and ischaemic heart disease in England and Wales. *Lancet* **327**, 1077–1081 (1986).

92. Hales, C. N. *et al.* Fetal and infant growth and impaired glucose tolerance at age 64. *BMJ* **303**, 1019–22 (1991).
93. Stein, Z. & Susser, M. The Dutch famine, 1944-1945, and the reproductive process. I. Effects on six indices at birth. *Pediatr. Res.* **9**, 70–6 (1975).
94. Ravelli, A. *et al.* Glucose tolerance in adults after prenatal exposure to famine. *Lancet* **351**, 173–177 (1998).
95. Desai, M. & Hales, C. Role of fetal and infant growth in programming metabolism in later life. *Biol. Rev. Camb. Philos. Soc.* **72**, 329–348 (1997).
96. Bateson, P. *et al.* Developmental plasticity and human health. *Nature* **430**, 419–21 (2004).
97. Stanner, S. A. *et al.* Does malnutrition in utero determine diabetes and coronary heart disease in adulthood? Results from the Leningrad siege study, a cross sectional study. *BMJ* **315**, 1342–1348 (1997).
98. Yudkin, J. S. & Stanner, S. Prenatal exposure to famine and health in later life. *Lancet* **351**, 1361–2 (1998).
99. Forsen, T., Eriksson, J. G., Tuomilehto, J., Osmond, C. & Barker, D. J. P. Growth in utero and during childhood among women who develop coronary heart disease: longitudinal study. *BMJ* **319**, 1403–1407 (1999).
100. Crowther, N. J., Cameron, N., Trusler, J. & Gray, I. P. Association between poor glucose tolerance and rapid post natal weight gain in seven-year-old children. *Diabetologia* **41**, 1163–7 (1998).
101. Eriksson, J. G. *et al.* Catch-up growth in childhood and death from coronary heart disease: longitudinal study. *BMJ* **318**, 427–431 (1999).

102. Thamotharan, M. *et al.* Transgenerational inheritance of the insulin-resistant phenotype in embryo-transferred intrauterine growth-restricted adult female rat offspring. *Am. J. Physiol. Endocrinol. Metab.* **292**, E1270–9 (2007).
103. Kuzawa, C. W. & Adair, L. S. Lipid profiles in adolescent Filipinos: relation to birth weight and maternal energy status during pregnancy. *Am J Clin Nutr* **77**, 960–966 (2003).
104. Rueda-Clausen, C. F., Morton, J. S. & Davidge, S. T. Effects of hypoxia-induced intrauterine growth restriction on cardiopulmonary structure and function during adulthood. *Cardiovasc. Res.* **81**, 713–22 (2009).
105. Jaquet, D., Gaboriau, A., Czernichow, P. & Levy-Marchal, C. Insulin resistance early in adulthood in subjects born with intrauterine growth retardation. *J. Clin. Endocrinol. Metab.* **85**, 1401–6 (2000).
106. Curhan, G. C. *et al.* Birth Weight and Adult Hypertension, Diabetes Mellitus, and Obesity in US Men. *Circulation* **94**, 3246–3250 (1996).
107. Browne, V. A., Stiffel, V. M., Pearce, W. J., Longo, L. D. & Gilbert, R. D. Cardiac beta-adrenergic receptor function in fetal sheep exposed to long-term high-altitude hypoxemia. *Am. J. Physiol.* **273**, R2022–31 (1997).
108. Xiao, D., Ducsay, C. A. & Zhang, L. Chronic Hypoxia and Developmental Regulation of Cytochrome C Expression in Rats. *J. Soc. Gynecol. Investig.* **7**, 279–283 (2000).
109. Menendez-castro, C. *et al.* Early and Late Postnatal Myocardial and Vascular Changes in a Protein Restriction Rat Model of Intrauterine Growth Restriction. **6**, (2011).
110. Rueda-Clausen, C. F., Morton, J. S. & Davidge, S. T. Effects of hypoxia-induced intrauterine growth restriction on cardiopulmonary structure and function during adulthood. *Cardiovasc. Res.* **81**, 713–22 (2009).



111. Mazzuca, M. Q., Wlodek, M. E., Dragomir, N. M., Parkington, H. C. & Tare, M. Uteroplacental insufficiency programs regional vascular dysfunction and alters arterial stiffness in female offspring. *J. Physiol.* **588**, 1997–2010 (2010).
112. Rueda-Clausen, C. F., Morton, J. S., Lopaschuk, G. D. & Davidge, S. T. Long-term effects of intrauterine growth restriction on cardiac metabolism and susceptibility to ischaemia/reperfusion. *Cardiovasc. Res.* **90**, 285–94 (2011).
113. Kiserud, T., Ebbing, C., Kessler, J. & Rasmussen, S. Fetal cardiac output, distribution to the placenta and impact of placental compromise. *Ultrasound Obstet. Gynecol.* **28**, 126–36 (2006).
114. Cooper, G. Cardiocyte adaptation to chronically altered load. *Annu. Rev. Physiol.* **49**, 501–518 (1987).
115. Morrison, J. L. *et al.* Restriction of placental function alters heart development in the sheep fetus. *Am. J. Physiol. Regul. Integr. Comp. Physiol.* **293**, R306–13 (2007).
116. Louey, S., Jonker, S. S., Giraud, G. D. & Thornburg, K. L. Placental insufficiency decreases cell cycle activity and terminal maturation in fetal sheep cardiomyocytes. *J. Physiol.* **580**, 639–48 (2007).
117. Clubb, F. J. & Bishop, S. P. Formation of binucleated myocardial cells in the neonatal rat. An index for growth hypertrophy. *Lab. Invest.* **50**, 571–7 (1984).
118. Wilson, C. R., Tran, M. K., Salazar, K. L., Young, M. E. & Taegtmeier, H. Western diet, but not high fat diet, causes derangements of fatty acid metabolism and contractile dysfunction in the heart of Wistar rats. *Biochem. J.* **406**, 457–67 (2007).
119. Fung, T. T., Willett, W. C., Stampfer, M. J., Manson, J. E. & Hu, F. B. Dietary patterns and the risk of coronary heart disease in women. *Arch. Intern. Med.* **161**, 1857–62 (2014).
120. WHO | *Obesity and overweight*. (World Health Organization, 2014). at <<http://www.who.int/mediacentre/factsheets/fs311/en/>>

121. Hu, F. B. *et al.* Prospective study of major dietary patterns and risk of coronary heart disease in men. *Am. J. Clin. Nutr.* **72**, 912–21 (2000).
122. Nagarajan, V. *et al.* Cardiac function and lipid distribution in rats fed a high-fat diet: in vivo magnetic resonance imaging and spectroscopy. *Am. J. Physiol. Heart Circ. Physiol.* **304**, H1495–504 (2013).
123. Coort, S. L. M., Bonen, A., van der Vusse, G. J., Glatz, J. F. C. & Luiken, J. J. F. P. Cardiac substrate uptake and metabolism in obesity and type-2 diabetes: role of sarcolemmal substrate transporters. *Mol. Cell. Biochem.* **299**, 5–18 (2007).
124. Glatz, J. F. C., Luiken, J. J. F. P. & Bonen, A. Membrane fatty acid transporters as regulators of lipid metabolism: implications for metabolic disease. *Physiol. Rev.* **90**, 367–417 (2010).
125. Schenk, S., Saberi, M. & Olefsky, J. M. Insulin sensitivity: modulation by nutrients and inflammation. *J. Clin. Invest.* **118**, 2992–3002 (2008).
126. Yu, C. *et al.* Mechanism by which fatty acids inhibit insulin activation of insulin receptor substrate-1 (IRS-1)-associated phosphatidylinositol 3-kinase activity in muscle. *J. Biol. Chem.* **277**, 50230–6 (2002).
127. Suzanne, S., De Wald, D. & Summers, S. Ceramide dissociates 3'-phosphoinositide production from pleckstrin homology domain translocation. *Biochem. J.* **354**, 359–368 (2001).
128. Kandasamy, A. D., Chow, A. K., Ali, M. A. M. & Schulz, R. Matrix metalloproteinase-2 and myocardial oxidative stress injury: beyond the matrix. *Cardiovasc. Res.* **85**, 413–23 (2010).
129. Molkenin, J. D. Calcineurin-NFAT signaling regulates the cardiac hypertrophic response in coordination with the MAPKs. *Cardiovasc. Res.* **63**, 467–75 (2004).

130. Okere, I. C. *et al.* Low carbohydrate/high-fat diet attenuates cardiac hypertrophy, remodeling, and altered gene expression in hypertension. *Hypertension* **48**, 1116–23 (2006).
131. Okere, I. C. *et al.* Differential effects of saturated and unsaturated fatty acid diets on cardiomyocyte apoptosis, adipose distribution, and serum leptin. *Am. J. Physiol. Heart Circ. Physiol.* **291**, H38–44 (2006).
132. Wilson, R. F. *et al.* Transluminal, subselective measurement of coronary artery blood flow velocity and vasodilator reserve in man. *Circulation* **72**, 82–92 (1985).
133. Cole, J. S. & Hartley, C. J. The pulsed Doppler coronary artery catheter preliminary report of a new technique for measuring rapid changes in coronary artery flow velocity in man. *Circulation* **56**, 18–25 (1977).
134. Qian, J. *et al.* Safety of intracoronary Doppler flow measurement. *Am. Heart J.* **140**, 502–10 (2000).
135. Doucette, J. W. *et al.* Validation of a Doppler guide wire for intravascular measurement of coronary artery flow velocity. *Circulation* **85**, 1899–1911 (1992).
136. Hozumi, T. *et al.* Noninvasive Assessment of Significant Left Anterior Descending Coronary Artery Stenosis by Coronary Flow Velocity Reserve With Transthoracic Color Doppler Echocardiography. *Circulation* **97**, 1557–1562 (1998).
137. Liebson, P. R. & Savage, D. D. Echocardiography in Hypertension: A Review. *Echocardiography* **4**, 215–249 (1987).
138. Dimitrow, P. Transthoracic Doppler echocardiography - noninvasive diagnostic window for coronary flow reserve assessment. *Cardiovasc. Ultrasound* **1**, 4 (2003).
139. Chew, M. S. Haemodynamic Monitoring Using Echocardiography in the Critically Ill: A Review. *Cardiol. Res. Pract.* **2012**, doi:10.1155/2012/139537 (2012).

140. Kaufmann, P. A. & Camici, P. G. Myocardial Blood Flow Measurement by PET: Technical Aspects and Clinical Applications. *J. Nucl. Med.* **46**, 75–88 (2005).
141. Choudhury, L. *et al.* Transmural myocardial blood flow distribution in hypertrophic cardiomyopathy and effect of treatment. *Basic Res. Cardiol.* **94**, 49–59 (1999).
142. Stolen, K. Q. *et al.* Myocardial perfusion reserve and peripheral endothelial function in patients with idiopathic dilated cardiomyopathy. *Am. J. Cardiol.* **93**, 64–68 (2004).
143. Som, P. *et al.* A fluorinated glucose analog, 2-fluoro-2-deoxy-D-glucose (F-18): nontoxic tracer for rapid tumor detection. *J. Nucl. Med.* **21**, 670–5 (1980).
144. Iozzo, P. *et al.* Insulin Stimulates Liver Glucose Uptake in Humans: An 18F-FDG PET Study. *J. Nucl. Med.* **44**, 682–689 (2003).
145. Iozzo, P. *et al.* Independent Association of Type 2 Diabetes and Coronary Artery Disease With Myocardial Insulin Resistance. *Diabetes* **51**, 3020–3024 (2002).
146. Hoh, C. K. Clinical use of FDG PET. *Nucl. Med. Biol.* **34**, 737–42 (2007).
147. Axel, L. Cerebral blood flow determination by rapid-sequence computed tomography: theoretical analysis. *Radiology* **137**, 679–86 (1980).
148. So, A. & Lee, T.-Y. Quantitative myocardial CT perfusion: a pictorial review and the current state of technology development. *J. Cardiovasc. Comput. Tomogr.* **5**, 467–81 (2011).
149. Feuchtner, G. M. *et al.* Evaluation of myocardial CT perfusion in patients presenting with acute chest pain to the emergency department: comparison with SPECT-myocardial perfusion imaging. *Heart* **98**, 1510–7 (2012).
150. So, A. *et al.* Non-invasive assessment of functionally relevant coronary artery stenoses with quantitative CT perfusion: preliminary clinical experiences. *Eur. Radiol.* **22**, 39–50 (2012).

151. Lee, T.-Y., Purdie, T. G. & Stewart, E. CT imaging of angiogenesis. *Q. J. Nucl. Med.* **47**, 171–87 (2003).
152. Miles, K. A. *et al.* Application of CT in the investigation of angiogenesis in oncology. *Acad. Radiol.* **7**, 840–850 (2000).
153. Lee, T.-Y. Functional CT: physiological models. *Trends Biotechnol.* **20**, S3–S10 (2002).
154. St Lawrence, K. S. & Lee, T. Y. An adiabatic approximation to the tissue homogeneity model for water exchange in the brain: I. Theoretical derivation. *J. Cereb. Blood Flow Metab.* **18**, 1365–77 (1998).

## Chapter 2

- 2 The Impact of an Adverse In Utero Environment Resulting in Low Birth Weight, and a Postnatal Western Diet on Early Development of Cardiovascular Diseases in Guinea Pigs**

## 2.1 Introduction

Cardiovascular Diseases (CVDs) are the leading causes of mortality world-wide, accounting for more than 17 million deaths in 2008 alone<sup>1</sup>. Characterized by cardiac remodeling and metabolic dysfunction processes, notable types of CVDs such as cardiomyopathy are typically associated with cardiac failure<sup>2-6</sup>. Traditionally, risk factors for CVD development are mostly attributed to life-style choices such as tobacco use, physical inactivity, or unhealthy dietary patterns<sup>7,8</sup>. Indeed, diets such as the increasingly prevalent Western Diet (WD), with its high levels of processed carbohydrates and saturated fatty acids, is strongly associated with an increasing risk of CVD development<sup>9,10</sup>. Interestingly, amounting evidence now also highlights the importance of intrauterine environment as a risk factor for developing chronic diseases in later life, particularly in cases of intrauterine growth restriction (IUGR)<sup>11</sup>.

IUGR is defined as the inability of the fetus to reach its expected growth potential, often resulting in low birth weight (LBW)<sup>12</sup>. A common cause of IUGR is placental insufficiency (PI), where the placenta fails to provide optimal oxygen and nutrient supply to the fetus<sup>13,14</sup>. Clinically, IUGR is categorized as birthweight falling below the 10<sup>th</sup> percentile<sup>12</sup>. However, this categorization method based on an arbitrary birthweight under-represents newborns which lie outside the cut-off but are still exposed to the same sub-optimal *in utero* environment<sup>15</sup>. For example, the development of severe adult diseases from *in utero* insults have been shown to occur independent of birthweight changes<sup>16</sup>. It is more likely that programming for disease development stems from a combination of *in utero* induced stress factors and an irregular developmental profile such as accelerated

catch-up growth in early postnatal life<sup>17,18</sup>. Of additional concern are evidence which highlight that *in utero* programmed changes can further sensitize and accelerate the development of CVDs from postnatal insults<sup>19</sup>. Amidst the increasing prevalence of WD, infants born from adverse *in utero* environments may become more susceptible to the enhanced deleterious effects of a growth restricted development profile. However our understanding of the relationship between prenatal and postnatal insults on offspring disease development has yet to be thoroughly investigated.

Part of this investigation is to understand the developmental progressions of CVDs prior to the onset of more severe consequences. Disease progression in the myocardium is often in concert with impairments in coronary blood flow, and metabolic alterations such as increased fatty acid oxidation, and cardiac insulin resistance (IR)<sup>6,20-23</sup>. Collectively, these are pre-clinical hallmarks of early CVD progression, and can be valuable markers for diagnosis. With the advancements in non-invasive imaging modalities commonly used in cancer diagnoses, these applications are now beginning to expand to the field of cardiovascular diagnoses. For example, new developments in Dynamic Contrast Enhanced Computed Tomography (DCE-CT) allows accessible, and non-invasive assessment of coronary flow and perfusion in the coronary microvasculature<sup>24,25</sup>. Additionally, Positron Emission Tomography (PET) has been extensively used to measure tissue specific glucose uptake, an indicator of IR<sup>26</sup>. These imaging modalities can prove to be valuable resources in identifying at risk individuals, monitoring disease progression, and potentially setting the stage for the development of more preventative therapies.



Understanding the relationship between the prevalence of CVDs and its risk factors is crucial in efforts to minimize harmful societal impact. The purpose of this study was to utilize DCE-CT and PET imaging supported by traditional molecular techniques to examine the developmental profile associated with early CVD development in a guinea pig model of *in utero* growth restriction and postnatal dietary insult. We postulated that offspring born of LBW– a marker of inadequate *in utero* growth – would exhibit pre-clinical markers of cardiac dysfunction, including disruptions in basal coronary flow, and cardiac glucose metabolism by early adulthood. Additionally, we postulated that the combination of LBW and a postnatal WD would result in an accelerated advancement of these CVD development parameters

## 2.2 Methods

### 2.2.1 Animals

Pregnant Dunkin-Hartly guinea pigs (Charles River Laboratories, Wilmington, MA) were fed *ad libitum* guinea pig chow (LabDiet diet 5025: 27% protein, 13% fat, 60% carbohydrates), and housed in individual cages ( $20 \pm 2^\circ\text{C}$ , and 30-40% humidity) with a 12 hour/light dark cycle. Uterine artery ablation (UAA) procedure was selected to impair placental function, fetal growth, and induce markers of CVD<sup>27,28</sup>. Briefly, all pregnant guinea pigs at mid gestation (~32 days) were placed in an anesthetic chamber (4-5% isoflurane with 2 L/min O<sub>2</sub>, and maintained at 2-3% isoflurane with 1 L/min O<sub>2</sub>) and immediately after induction, a subcutaneous injection of Robinul (0.01 mg/kg glycopyrrolate; Sandoz Canada, Montreal, QC) was administered. A midline incision was made below the umbilicus to expose the mesometrium of one horn of the uterus, where every second arterial vessel branch was cauterized using an Aaron 2250 electro-surgical generator (Bovie Medical, Clearwater, FL). Following surgery, a subcutaneous injection of Temgesic (0.025 mg/kg buprenorphine; Schering-Plough, Kenilworth, NJ) was administered. Sows delivered naturally, and within 12 hours, birth weights and crown rump of each pup were recorded. At the end of the pupping period, guinea pig pups were defined as normal birth weight (NBW) if their birth weights were between 25<sup>th</sup> to 75<sup>th</sup> percentiles, and LBW if below the 25<sup>th</sup> percentile. Based on this criteria, and in accordance with previous UAA and maternal feed restriction guinea pig models, NBW pups were determined to be greater than 90g, while LBW pups were determined to be below 85g<sup>29-</sup>

<sup>31</sup>. All pups were weighed daily from birth until 15 days of age, where pups were weaned and randomly assigned onto either a control diet (CD) (TD: 110240, Harlan Laboratories, Madison WI), or a WD (TD: 110239, Harlan Laboratories, Madison WI). Both CD and WD contained 21% protein (% of total kcal). However, these diets differed in carbohydrates and fat, wherein CD contained 60% carbohydrates [distribution (% by weight): 35% corn starch, 10% sucrose], and 18.4% fats, while WD contained 33% carbohydrates [distribution (% by weight): 19% sucrose, 6.5% fructose] and 45% fats. In addition, composition of fats also differed, wherein CD consisted of 2.8% saturated fatty acids (SFA), 4.4% monounsaturated fatty acids (MUFA), and 11.2% polyunsaturated fatty acids (PUFA), while WD consisted of 31.7% SFA, 11.8% MUFA, 1.8% PUFA [distribution (% of total kcal)] (Table 2.1). In total, CD contained 3.4 kcal/g while WD contained 4.2 kcal/g energy. Guinea pigs were housed in individual cages at 20°C and 30-40% humidity with 12 hour light-dark cycle. Food intake was recorded daily and body weights were recorded twice weekly until putdown at young adulthood (150 days). The resulting division in groups for the study was NBW/CD, NBW/WD, LBW/CD, and LBW/WD, which was further divided by sex.

**Table 2.1 Diet Composition**

<i>Diet Component</i>	<i>Control Diet (CD)</i>	<i>Western Diet (WD)</i>
<b><i>Total Protein (%kcal)</i></b>	22	21
<b><i>Total Fat (%kcal)</i></b>	18	46
Saturated Fatty Acids	15	70
Polyunsaturated Fatty Acids	61	4
Monounsaturated Fatty Acids	24	26
<b><i>Total Carbohydrate (%kcal)</i></b>	60	33
Sucrose	11	22
Fructose	-	7.6
<b><i>Cholesterol (%kcal)</i></b>	-	0.25
<b><i>Density (kcal/g)</i></b>	3.4	4.2

### 2.2.2 *Imaging*

Guinea pigs underwent DCE-CT and PET imaging at 50 and 110 days of life. The scan time point of 110 days or early adulthood was selected based on a previous study, which investigated IUGR/LBW associated changes in whole body glucose tolerance and reported alterations in offspring glucose tolerance at 101 days<sup>32</sup>. The earlier time point of 50 days was selected to investigate possible developmental changes prior to young adulthood an active post weaning growth phase, as previous studies using the UAA model have demonstrated increased cardiac and renal fibrosis at 60 days of age<sup>28</sup>. Prior to scanning, baseline glucose levels were measured using a Bayer Contour glucometer (Bayer Diabetes, Mississauga, ON). In addition, during scanning, heart rate, respiration rate and arterial O<sub>2</sub> saturation were monitored and recorded using MouseOx pulse oximeter for small animals (Starr Life Science Corp, Oakmont PA).

### 2.2.3 *Dynamic Contrast Enhanced Computed Tomography*

DCE-CT scans were performed using a clinical GE multi-slice CT scanner (Discovery VCT, GE Healthcare, Waukesha, Wis). Guinea pigs were anaesthetized in an anesthetic chamber (4-5% isoflurane with 2 L/min O<sub>2</sub>), before transferred to a tight fitting nose cone to maintain anesthesia with 2-3% isoflurane at a flow rate of 1 L/min. Once anesthesia was stably established (absence of response to pain stimuli), guinea pigs were positioned in the center of the CT scanner. A scout localization scan was performed to find the slice locations of the heart. A two phase dynamic scan of the heart at the determined

slice locations was conducted following an injection of 1mL/kg of iodinated contrast (Omnipaque 200mgI/mL) via a pedal vein catheter at 8 mL/min. In the first phase of the dynamic scan, images were acquired continuously at every second for 14.6 seconds at a tube rotation speed of one revolution per second, voltage of 120 kV and current of 180 mA. This was followed by the second phase where images were acquired every 15 seconds for 200 seconds using the same scan parameters (tube voltage, current, and rotation speed) as the first phase. The dynamic images were reconstructed with the GE Healthcare proprietary detail filter with a slice thickness of 1.25mm. The reconstructed images were transferred to an image processing workstation (Advantage Windows 4; GE Healthcare, Waukesha Wis). Using CT Perfusion 5 program (GE Healthcare, Waukesha, Wis), an arterial input curve of contrast medium concentration was generated with a region of interest (ROI) placed in the left ventricle chamber of a slice which showed the maximum size of the chamber. Following which, another ROI was outlined around the contour of the heart in the first image of the dynamic series of the same slice. Subsequent images which did not conform to this heart outline were removed from the study as they were mis-registered with the first image from either breathing or cardiac motion of the animal. Blood flow maps of the chosen slice were generated with the CT Perfusion 5 software (GE Healthcare, Waukesha, Wis.). Myocardial blood flow was calculated as the mean pixel value in a ROI placed in the inferior wall of the left ventricle where it is least affected by either respiratory or cardiac motion.

#### 2.2.4 *Position Emission Tomography*

Guinea pigs were first anaesthetized in an air-tight box with 4-5% isoflurane at 2L/min, and injected with ~25kBq/kg (0.2-0.3mL) of [<sup>18</sup>F]- fluoro-deoxy-glucose ([<sup>18</sup>F] FDG) via the pedal vein. Animals were then recovered, returned to their cage, and placed in a lead brick shield. Approximately 40 minutes later, they were again anaesthetized with 4-5% isoflurane as before, and placed on the bed of a micro-PET scanner (GE eXplore Vista DR, GE Healthcare, Waukesha, Wis). Anesthesia was maintained with a nose cone through which 2.5-3% isoflurane was flowing at the rate of 1L/min, and a 20 minute emission scan of the heart region was then acquired.

After correction for scatter and random coincidences, the scan was reconstructed into sixty 0.78mm thick slices. The reconstructed images were analyzed using an in-house MATLAB program (MathWorks Inc., MA, USA). For each slice in which the left ventricle was visible for analysis, two ROIs were drawn: one outlining the epicardial surface, and the other one the endocardial surface of the left ventricle. The difference in the total counts was divided by the difference in volume of the ROIs to arrive at the average count in the myocardium. This average was converted to activity (Bq) using a sensitivity calibration factor determined from routine quality assurance of the scanner. The image derived activities from all LV slices were averaged together to calculate myocardial activity. Standardized Uptake Value (SUV) in the left ventricular myocardium was calculated as:

$$SUV = \frac{\textit{Myocardial Activity}}{\textit{Injected Activity/Body Weight}} \quad (1)$$

### 2.2.5 *Tissue Collection*

Following a recovery period after the 110 day scan, at postnatal day  $143 \pm 1.9$ , animals were sacrificed by CO<sub>2</sub> inhalation following an overnight fast<sup>33</sup>. The heart was removed, trimmed of connective tissue, weighed, and carefully separated into left or right ventricles. A coronal cross section above the apex of the left ventricle of approximately 3mm thick was placed in 4% paraformaldehyde for histological analyses<sup>34</sup>. The remainder of the left ventricle was frozen in liquid nitrogen for RNA and protein analysis.

### 2.2.6 *Quantitative Real-Time PCR*

Flash frozen left ventricular tissues were homogenized in Trizol® (Invitrogen Life Technologies Co., Burlington, ON), followed by 200 µL of chloroform for each tissue sample. The mixed solution was centrifuged at 12,000g for 15 minutes at 4°C. The resulting aqueous phase was transferred to new RNase-free tubes, and 500 µL of isopropyl alcohol was added. The new solution was centrifuged at 12,000g for 10 minutes at 4°C to obtain RNA precipitate. Following three 75% ethanol washes at 7500g for 5 minutes, the RNA pellet was reconstituted in RNAase free diethylpyrocarbonate water. Yield and quality (A260/A280 ration) of RNA was determined with NanoDrop 2000 UV-Vis Spectrophotometer (Thermo Scientific, Waltham MA, US). Isolated RNA (4µg) were reverse transcribed into complementary DNA with M-MLV Reverse Transcriptase (Invitrogen Life Technologies Co., Burlington ON). Real-time qPCR was performed for each sample in duplicate and was completed using a Bio-Rad CFX384 real time PCR



detector (Bio-Rad Laboratories Mississauga, ON) at a denaturing temperature of 95°C, annealing temperature of 59.5°C, and elongation temperature of 72°C for 39 cycles. Data are presented as a fold change in expression compared to NBW/CD exposed animals. The  $2^{-\Delta CT}$  method with  $\beta$ -Actin as housekeeping gene was used for analysis<sup>35</sup>. Primer sets are listed in Appendix A.

### 2.2.7 *Western Blot*

Flash frozen left ventricular tissues were pulverized and homogenized in RIPA lysis buffer (50 mM Tris-HCl, NP-40 1%, Na-deoxycholate 0.25%, 1mM EDTA, 150 mM NaCl, 50 mM NAF, 1mM NaV, 25 mM  $\beta$ -glycerophosphate, pH 7.4) with protease and phosphatase inhibitor. Homogenates were centrifuged at 10,000g for 15 minutes at 4°C. Supernatants were transferred to fresh tubes and used as protein preparations, which were quantified with DCTM Protein Assay Kit (Bio-Rad Laboratories, Mississauga, ON). Loading samples of 30  $\mu$ g protein were then separated by size on 6% Bis-Tris gels, and transferred on to nitrocellulose membranes for an overnight block with 5% bovine serum albumin at 4°C. Blots were then probed with AKT-1 (Cell Signaling® #4691, 1:1000), pAKT Serine 473 (Cell Signaling® #9271, 1:1000), pAKT Threonine 308 (Cell Signaling® #9275, 1:1000), and monoclonal horseradish peroxidase-conjugated  $\beta$ -actin Sigma-Aldrich #A3854, 1:50000) diluted in 5% bovine serum albumin in Tris-buffered saline/Tween 20 (0.01%) for 1 hour at room temperature. Blots were then probed with horseradish peroxidase conjugated goat anti-rabbit IgG (Cell Signaling® #7074, 1:1000) secondary antibody diluted in 5% bovine serum albumin in Tris-buffered saline/Tween 20

(0.01%) for 1 hour at room temperature. Immunoreactive bands were detected using Luminata Forte Western HRP Substrate chemi-luminescence (EMD Millipore, Darmstadt, Germany), and imaged with VersaDoc Imaging System (Bio-Rad Laboratories Mississauga, ON). Densitometry values (arbitrary units) were determined using the ImageLab software (Bio-Rad Laboratories, Mississauga, ON), and the abundance of proteins were expressed relative to  $\beta$ -Actin.

### 2.2.8 *Histological Analysis*

Immediately following putdown, coronal cross-sections of the guinea pig left ventricles were collected in 4% paraformaldehyde, embedded in paraffin, and then sliced in 5 $\mu$ m sections. Paraffin-embedded sections were stained with hematoxylin and eosin (H&E) or Masson's trichrome for histological analysis of hypertrophy, inflammation and fibrosis. Eight non-overlapping colored images of the H&E stained slides were obtained at 200x magnification using Leica DMI 6000B microscope (Leica Microsystems, Wetzlar, Germany). Utilizing Leica MMAF software (v1.40, Leica Microsystems, Wetzlar, Germany), cardiomyocytes with visible nuclei was outlined in each of the eight non-overlapping images. The cardiomyocyte cross sectional area were calculated in square micrometers, and averaged between the non-overlapping images as per previous studies on cardiac hypertrophy<sup>36</sup>. Similarly, eight non-overlapping colored images of the Masson's trichrome stained sections were obtained at 100x magnification. Again, utilizing the Leica MMAF program, areas of the blue stained collagen fields were measured and divided by the total area of the field, omitting the voids<sup>36,37</sup>. The collagen fractions of each section

were then expressed as the mean percentage of collagen. Analysis of the histological sections were performed under blinded conditions.

### 2.2.9 *Statistical Analysis*

Statistical Analysis was performed with SPSS software (SPSS v22.0, Chicago, IL, USA). A mixed model ANOVA analysis was used to determine significant differences ( $p < 0.05$ ) from sex, age, birth weight, and postnatal diet. If significant differences or interactions were determined, student t-tests were used for post-hoc analyses of differences between groups.

## 2.3 Results

### 2.3.1 *Birthweight and Development*

Clinically, determination of growth restriction is arbitrary assigned based on measurement of birth weight (<10<sup>th</sup> percentile)<sup>38</sup>. Similarly, this study categorized LBW, a proxy for growth restriction, as offspring whose birthweight fell below the 25<sup>th</sup> percentile of mean birth weights. As a result, pups which were categorized as LBW were 29% lighter at birth compared to those which were categorized as NBW, independent of sex (Figure 2.1,  $p < 0.05$ ). In addition, at birth these LBW offspring displayed a lower Weight/Length ratio, a measure of leanness (Figure 2.1,  $p < 0.05$ ), which have been previously observed in other models of IUGR<sup>32</sup>. By putdown at  $143 \pm 1.9$  days, these LBW offspring displayed similar body weights to that of the NBW group, however, females demonstrated a diet induced reduction in bodyweight (Figure 2.2,  $p < 0.05$ ). Moreover, heart weight relative to body weight was not significantly altered between groups (Figure 2.2).

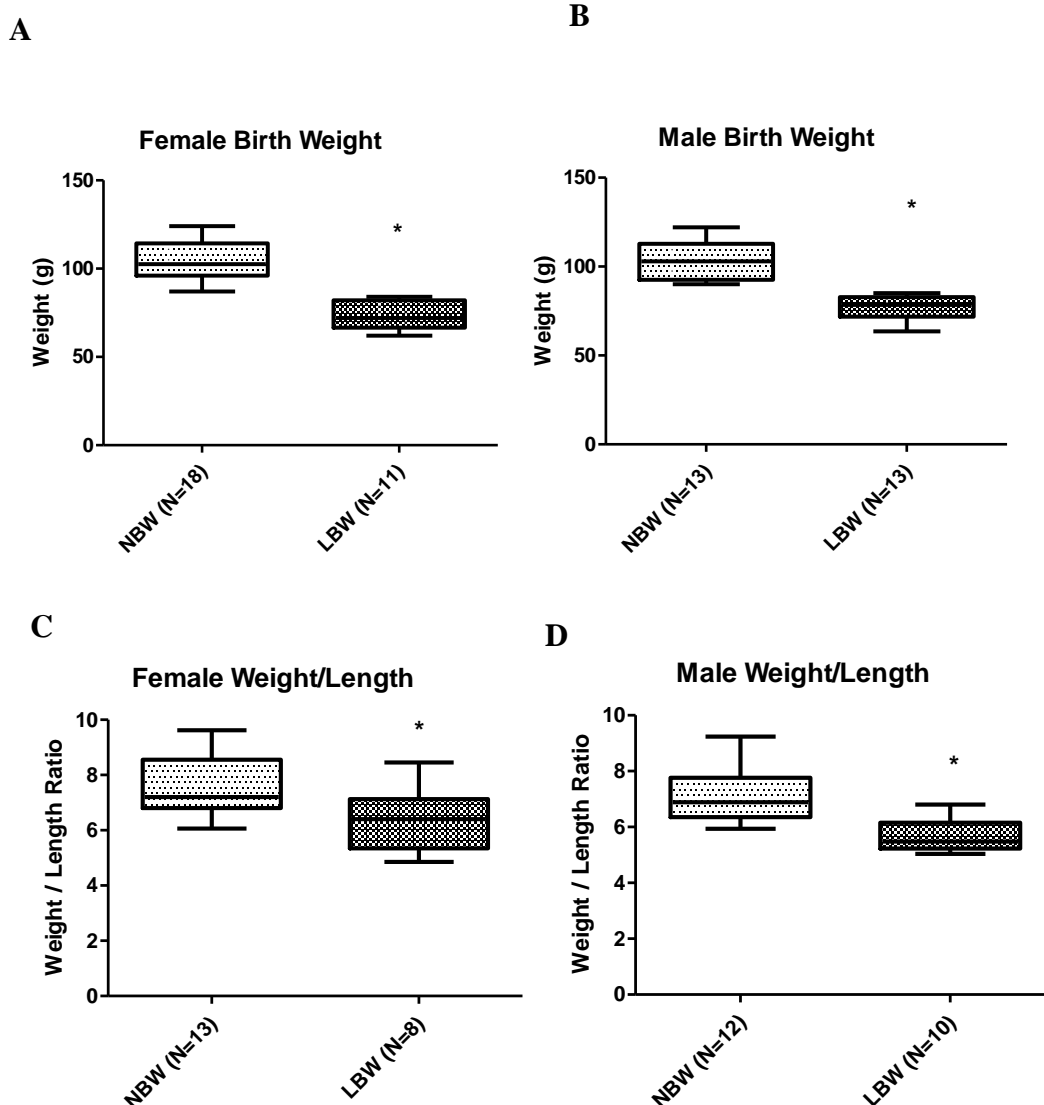


**Figure 2.1 Characteristics at Birth.** Pups were categorized as LBW group based on a pre-established cut-off determined as below the 25<sup>th</sup> percentile of average birth weights. Birth weight of **A**) female, **B**) male guinea pig pups were recorded. N=18 (NBW), N=11 (LBW) in females, and N=13 (NBW), N=13 (LBW) in males. In addition, ratio of birth weight over crown rump length of **C**) female, and **D**) male guinea pig pups was determined. N=13 (NBW), N=8 (LBW) in females, and N=12 (NBW), N=10 (LBW) in males. \* $p < 0.05$ . Box represents Mean and SEM, while whiskers represents Max and Min values. Statistical significance was determined by student's t-test.

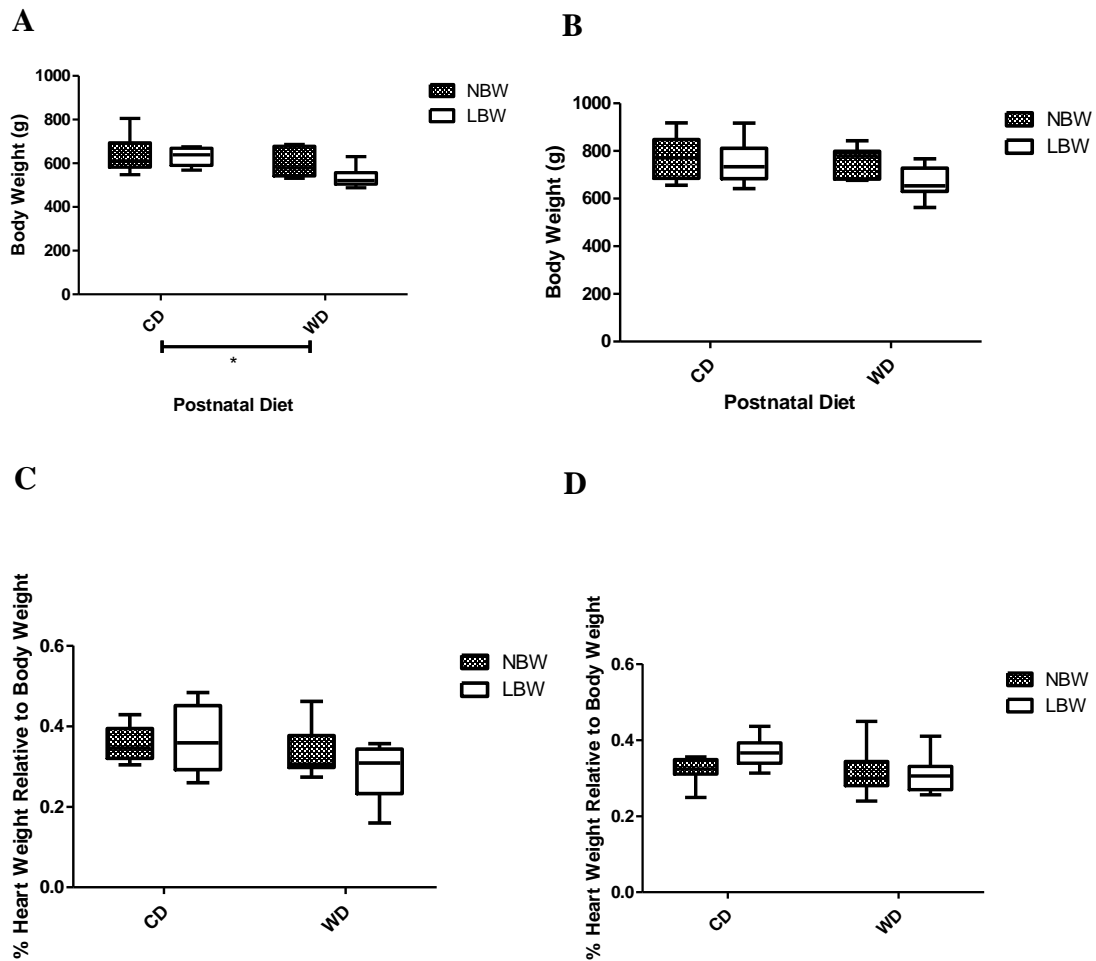


**Figure 2.2 Putdown Characteristics.** Bodyweights of **A)** female and **B)** male guinea pigs. Percent ratio of heart weight relative to body weight at of **C)** female and **D)** males at day  $143 \pm 1.9$ .  $N=8$  (NBW/CD),  $10$  (NBW/WD),  $5$  (LBW/CD),  $6$  (LBW/WD) for females.  $N=6$  (NBW/CD),  $7$  (NBW/WD),  $6$  (LBW/CD),  $7$  (LBW/WD) for males.  $*p<0.05$ . Box represents Mean and SEM, while whiskers represents Max and Min values. Statistical analysis performed by two-way ANOVA.

### 2.3.2 *LBW Resulted in Reduction in Basal Coronary Blood Flow in Young Adulthood*

Following a 2 hour fast, and just prior to DCE-CT and PET scanning, animals from all four treatment groups, displayed a similar glucose level of  $9.1 \pm 0.4$  mmol/L. During scanning, the animals maintained an average heart rate of  $205 \pm 24$  bmp, and an average oxygen saturation above 98%. No significant deviations in these physical parameters were observed during the 40 minute scan period (Table 2.2).

Coronary vascular dysfunction often occurs with the increasing severity of cardiac hypertrophy, and cardiomyopathy<sup>20,39,40</sup>. More importantly, alterations in coronary flow and microvasculature precedes heart failure, and is known to be a strong predictor of hypertrophic cardiomyopathy<sup>41</sup>. Using DCE-CT, basal coronary flow in the inferior wall of the left ventricle was determined at 50 and 110 days. A significant birthweight and age interaction was observed, where coronary flow of LBW guinea pigs was reduced by 17% compared to NBW as they reach adulthood (Figure 2.3,  $p < 0.05$ ). In comparison, NBW animals demonstrated a 10% increase in coronary blood flow as they reach adulthood.

**Table 2.2 Baseline Physiological Parameters during Scanning Procedures.** Average baseline readings of glucose, heart rate, and oxygen saturation during CT and PET scanning at (A) 50 days, and (B) 110 days. Data presented as mean  $\pm$  standard error. N=12 (NBW/CD), 14 (NBW/WD), 7 (LBW/CD), 6 (LBW/WD) for females. N=9 (NBW/CD), 9 (NBW/WD), 5 (LBW/CD), 3 (LBW/WD) for males. Statistical significance examined by two-way ANOVA.

<b>Sex</b>	<b>BW</b>	<b>Diet</b>	<b>Glucose</b>	<b>Heart Rate (bpm)</b>	<b>O2 Saturation (%)</b>
<u>Female</u>	NBW	CD	9.33 $\pm$ 1.05	243.6 $\pm$ 9.7	98.4 $\pm$ 0.9
		WD	9.85 $\pm$ 0.91	232.9 $\pm$ 7.9	97.7 $\pm$ 0.7
	LBW	CD	8.02 $\pm$ 1.29	250.1 $\pm$ 9.7	97.6 $\pm$ 0.9
		WD	8.45 $\pm$ 1.82	234.7 $\pm$ 13.7	97.6 $\pm$ 1.2
<u>Male</u>	NBW	CD	10.56 $\pm$ 0.86	228.9 $\pm$ 9.0	98.4 $\pm$ 0.8
		WD	8.80 $\pm$ 0.97	261.0 $\pm$ 9.7	96.9 $\pm$ 0.9
	LBW	CD	10.64 $\pm$ 1.15	220.9 $\pm$ 9.0	97.7 $\pm$ 0.8
		WD	8.40 $\pm$ 1.29	235.5 $\pm$ 10.6	96.8 $\pm$ 0.9
<b>Significance</b>			ns	ns	ns

<b>Sex</b>	<b>BW</b>	<b>Diet</b>	<b>Glucose</b>	<b>Heart Rate (bpm)</b>	<b>O2 Saturation (%)</b>
Female	NBW	CD	8.83 $\pm$ 0.92	223.6 $\pm$ 10.7	96.1 $\pm$ 1.2
		WD	8.35 $\pm$ 0.58	217.9 $\pm$ 6.8	98.0 $\pm$ 0.7
	LBW	CD	9.97 $\pm$ 0.70	235.1 $\pm$ 8.1	97.6 $\pm$ 0.9
		WD	8.73 $\pm$ 0.92	207.4 $\pm$ 10.7	97.8 $\pm$ 1.2
Male	NBW	CD	9.12 $\pm$ 0.53	228.2 $\pm$ 6.2	99.0 $\pm$ 0.7
		WD	8.25 $\pm$ 0.75	224.3 $\pm$ 8.8	99.2 $\pm$ 1.0
	LBW	CD	9.80 $\pm$ 0.83	234.1 $\pm$ 9.6	98.4 $\pm$ 1.0
		WD	8.65 $\pm$ 0.92	223.6 $\pm$ 9.6	97.6 $\pm$ 1.0
<b>Significance</b>			ns	ns	ns



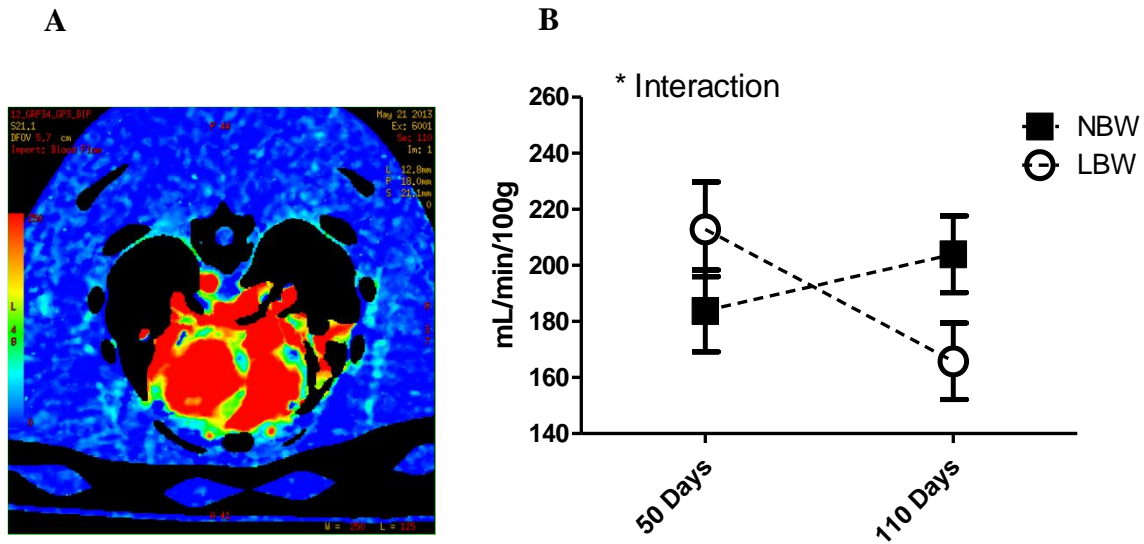


**Figure 2.3 Basal Coronary Blood Flow Determined by DCE-CT.** **A)** Color coded blood flow maps were calculated from DCE-CT, where cool colors represent areas of low blood flow, while warm colors represent areas of high blood flow. **B)** Mean coronary blood flow in the inferior wall of left ventricle at 50 and 110 days of post-natal life determined by CT Perfusion software (GE Healthcare, Waukesha, Wis). \* $p < 0.05$  Interaction.  $N = 27$  and  $30$  for 50 day old guinea pigs of NBW and LBW respectively, and  $N = 18$  and  $22$  for 110 day old guinea pigs of NBW and LBW respectively. A repeated measures three-way ANOVA was used to determine statistical significance. ANOVA table presented in Appendix C.

### 2.3.3 *WD Consumption Reduced Basal Glucose Uptake by Adulthood*

In the development phase of many CVDs, the cardiac metabolic profile is often altered, resulting in a state of IR<sup>42,43</sup>. Specifically, a switch in favor of fatty acid oxidation was believed to be a protective mechanism against heart failure<sup>44</sup>. As a result, changes in glucose metabolism, a proxy for determining IR, is a useful pre-clinical marker for diseases such as hypertrophic cardiomyopathy.

Determination of basal cardiac glucose uptake at 50 and 110 days was completed using [<sup>18</sup>F] FDG -PET. Where, chronic postnatal WD consumption resulted in a 21% reduction in glucose uptake compared to CD groups at both time points (Figure 2.4,  $p < 0.05$ ). No alterations in glucose uptake were influenced by birthweight.

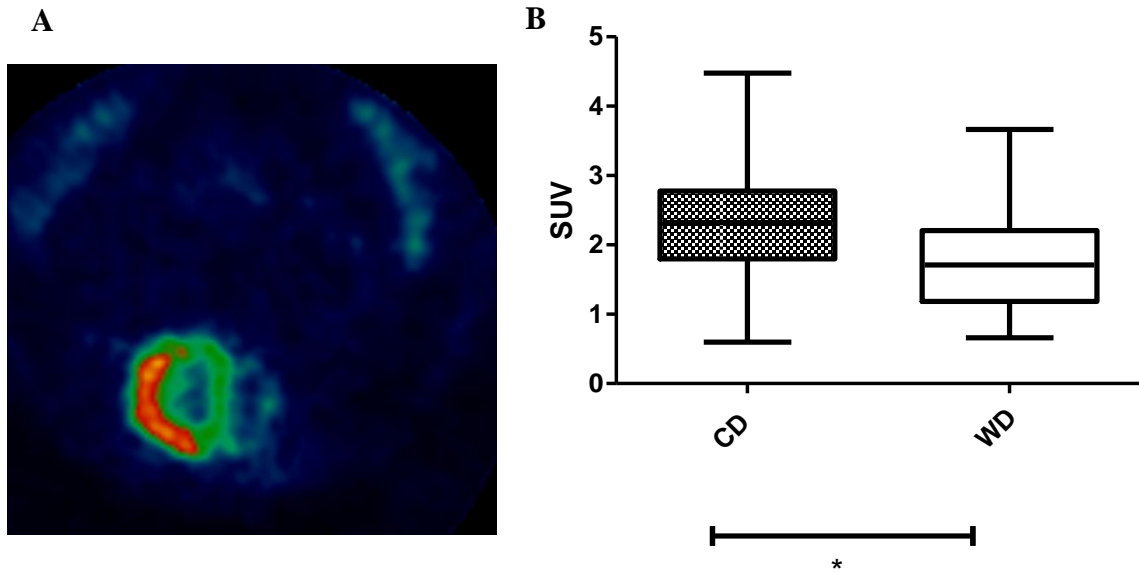


**Figure 2.4 Cardiac Glucose Uptake Determined by PET.** **A)** Color coded image of F-18 fluorodeoxyglucose ( $[^{18}\text{F}]$  FDG) uptake determined by PET, where areas of warm colors describe the intensity of  $[^{18}\text{F}]$  FDG uptake. Standardized uptake value (SUV), a semi-quantitative index of  $[^{18}\text{F}]$  FDG uptake, and insulin sensitivity, was determined in the left ventricle by defining a region of interest around the left ventricle. **B)** SUV of CD and WD animals at both 50 and 110 day time points.  $N = 27$  for CD fed animals and  $N=22$  for WD fed animals.  $*p<0.05$ . Box represents Mean and SEM, while whiskers represents Max and Min values. A repeated measures three-way ANOVA was used to determine statistical significance. ANOVA table presented in Appendix D.

#### 2.3.4 *Cardiac Remodeling and Collagen Content Were Increased in LBW Offspring*

Inadequate cardiac development, which is likely the result of adverse *in utero* environments, combined with an accelerated growth profile may trigger the hypertrophic growth of cardiomyocytes and proliferation of non-myocytes such as fibroblasts, therefore setting the stage for pathological hypertrophy<sup>45,46</sup>. These cardiac remodeling processes are crucial components in the eventual development of systolic dysfunction, and are strongly associated with alterations in coronary circulation<sup>40</sup>. Following putdown, cross-sections of left ventricles were analyzed for histological markers of hypertrophy and fibrosis. Heart sections from LBW offspring displayed a 20% increase in cardiomyocyte cross-sectional area compared to NBW offspring (Figure 2.5,  $p < 0.05$ ), indicative of a hypertrophic growth phenotype.

#### 2.3.5 *Expressions of Collagen Increased in LBW Females*

Enlargements in cardiomyocytes can be attributed to both classifications of cardiac hypertrophy, which is physiological or pathological. However, pathological hypertrophy differs in that it is characterized by fibrosis, particularly an excessive expression of collagen<sup>47,48</sup>. In the LBW, and NBW/WD sections, a 1.9 fold increase in collagen composition compared to NBW/CD sections was recorded, therefore highly suggestive of a pathological hypertrophy phenotype (Figure 2.6,  $p < 0.05$ ).

Additionally, the mRNA expression of pro-fibrotic genes as  $\alpha$  smooth muscle actin ( $\alpha$ -SMA), Type 1 and 3 collagen, matrix metalloproteinase-1 (MMP1) and transforming growth factor  $\beta$  (TGF- $\beta$ ) was determined (Table 2.3). These genes are known to play important roles in the tissue fibrosis pathway<sup>49</sup>. A significant sex and birth weight interaction for type 1 collagen mRNA was observed, where female LBW animals demonstrated a significantly higher expression than NBW females (Figure 2.7,  $p < 0.05$ ). The expression of the other targets,  $\alpha$ -SMA, type 3 collagen, MMP1, and TGF- $\beta$  were consistent across sex, BW, and diet.

#### 2.3.6 *WD Feeding is Associated with a Reduction in AKT Activation*

One of the main markers of CVD development is cardiac IR, an observation reported in conjunction with WD consumption<sup>50,51</sup>. Specifically, the disruption of kinases in the insulin stimulated glucose uptake pathway, such as insulin receptor substrate (IRS), and Protein Kinase B (AKT), is an important marker behind tissue specific IR<sup>44,52,53</sup>. Other reports in skeletal muscle also reported reductions in AKT activation, specifically Threonine 308 (T308) and Serine 473 (S473), was strongly associated with growth restriction<sup>54-56</sup>. In the current study, despite no alterations in pIRS protein expression, pAKT (T308) to total AKT-1 was significantly reduced in female WD fed guinea pigs (Figure 2.8,  $p < 0.05$ ), whereas males appeared to be unaffected by diet. Furthermore, birthweight appeared to not confer any adverse impact in both sexes.

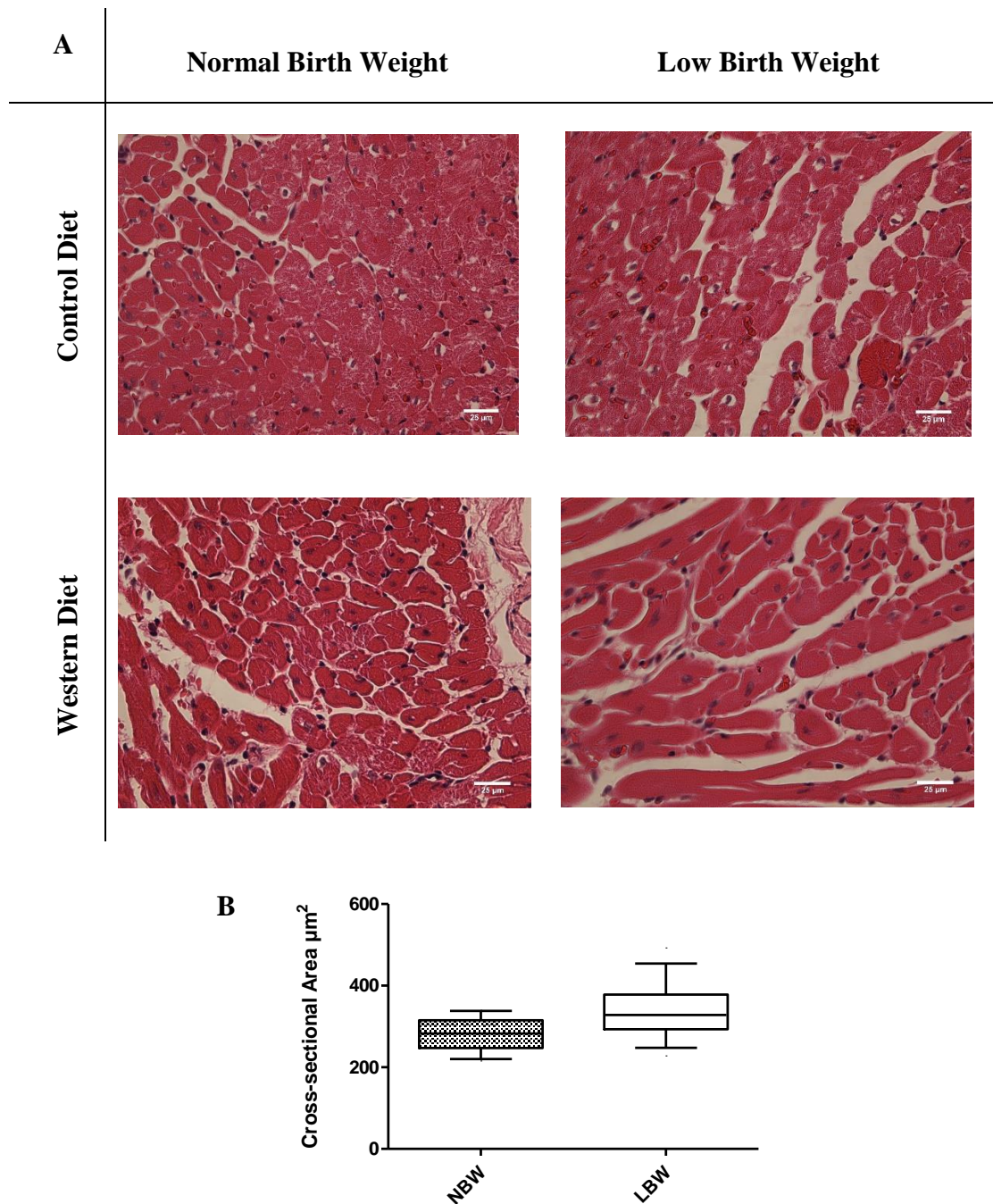


**Figure 2.5 Cross-Sectional Area of Cardiomyocytes.** **A)** Hematoxylin and Eosin stained cross-sectional histological sections of left ventricles at putdown. Average cross-sectional area ( $\mu\text{m}^2$ ) of cardiomyocytes in the left ventricle was determined between multiple representative slides. White scale bar in representative images indicate  $25 \mu\text{m}$  length. **B)** Cardiomyocyte cross-sectional area between NBW and LBW animals.  $*p < 0.05$ .  $N=15$  for NBW and  $N=13$  for LBW animals. Box represents Mean and SEM, while whiskers represents Max and Min values. Statistical significance was determined by a two-way ANOVA. ANOVA table presented in Appendix E.

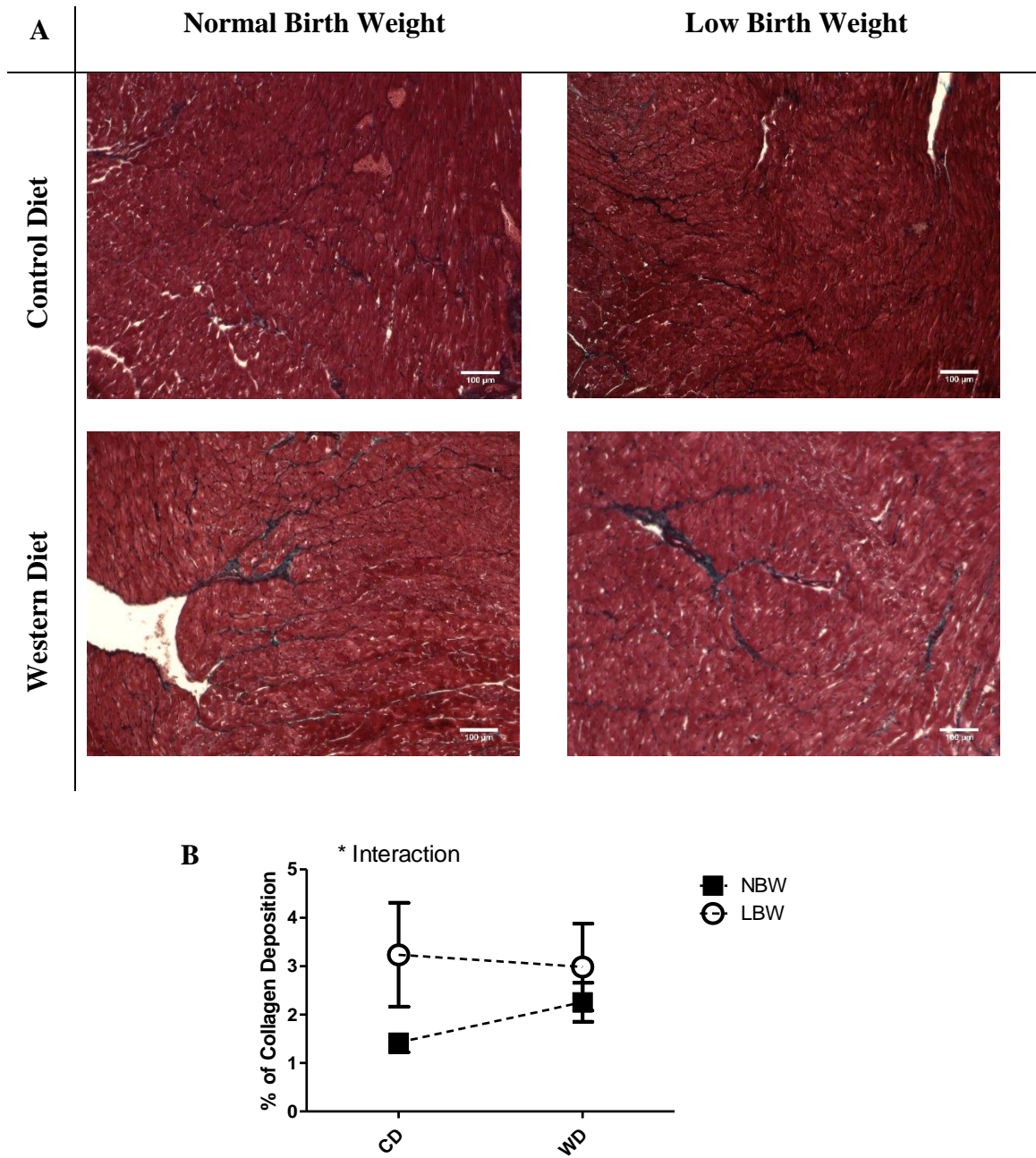


**Figure 2.6 Collagen Content in the Left Ventricle** **A)** Trichrome stained histological sections of left ventricle. Average area ( $\mu\text{m}^2$ ) of blue shaded collagen deposition was determined as an indicator of fibrotic growth. White scale bar in representative images indicate 100  $\mu\text{m}$  length. **B)** % of Collagen deposition. \* $p < 0.05$  Interaction.  $N=8$  for both CD and WD fed NBW guinea pigs, and  $N=4$  and  $6$  for CD and WD fed LBW guinea pigs, respectively. Data presented as Mean  $\pm$  SEM. Statistical differences determined by two-way ANOVA. ANOVA table presented in Appendix F.

**Table 2.3 Relative mRNA Expression of Fibrotic Genes.** Relative mRNA expression of  $\alpha$ SMA, Type 3 collagen, MMP-1, and TGF $\beta$  to Female NBW-CD group. No significant differences were observed in the mRNA expression of these genes. N= 4 for NBW/CD, NBW/WD, LBW/CD and LBW/WD in each sex. Statistical analysis completed by two-way ANOVA.

<b>Sex</b>	<b>BW</b>	<b>Diet</b>	<b><math>\alpha</math>SMA</b>	<b>Type 3 Collagen</b>	<b>MMP-1</b>	<b>TGF<math>\beta</math></b>
<u>Female</u>	NBW	CD	1	1	1	1
		WD	1.07	1.13	0.98	0.66
	LBW	CD	1.12	1.49	0.8	0.87
		WD	0.78	1.19	0.77	0.85
<u>Male</u>	NBW	CD	0.71	0.99	0.89	0.66
		WD	0.36	1.62	0.91	1.05
	LBW	CD	0.43	1.33	1.13	1.02
		WD	0.79	1.19	1.18	1.32



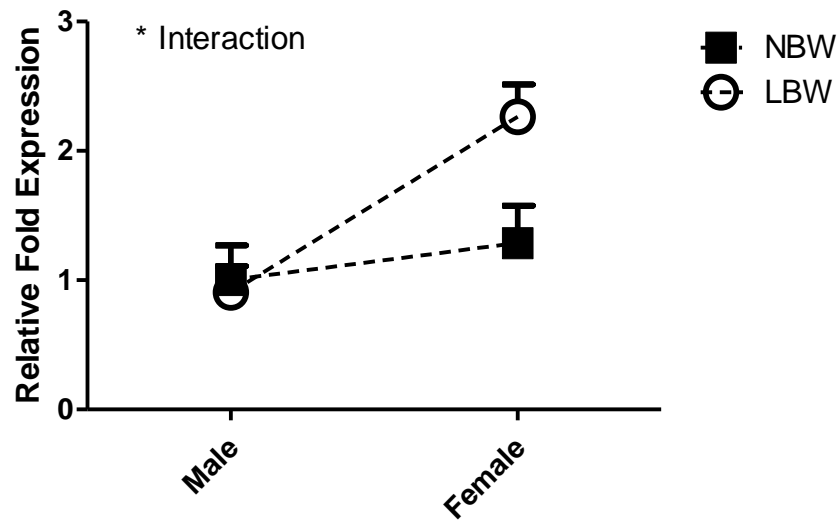


**Figure 2.7 Type 1 Collagen mRNA Expression.** Relative mRNA expression of Type 1 Collagen in the left ventricle at  $140 \pm 1.9$  day putdown. \* $p < 0.05$  Interaction.  $N = 4$  for NBW/CD, NBW/WD, LBW/CD and LBW/WD in each sex. Data presented as Mean  $\pm$  SEM. Statistical significance determined by two-way ANOVA. ANOVA table presented in Appendix G.

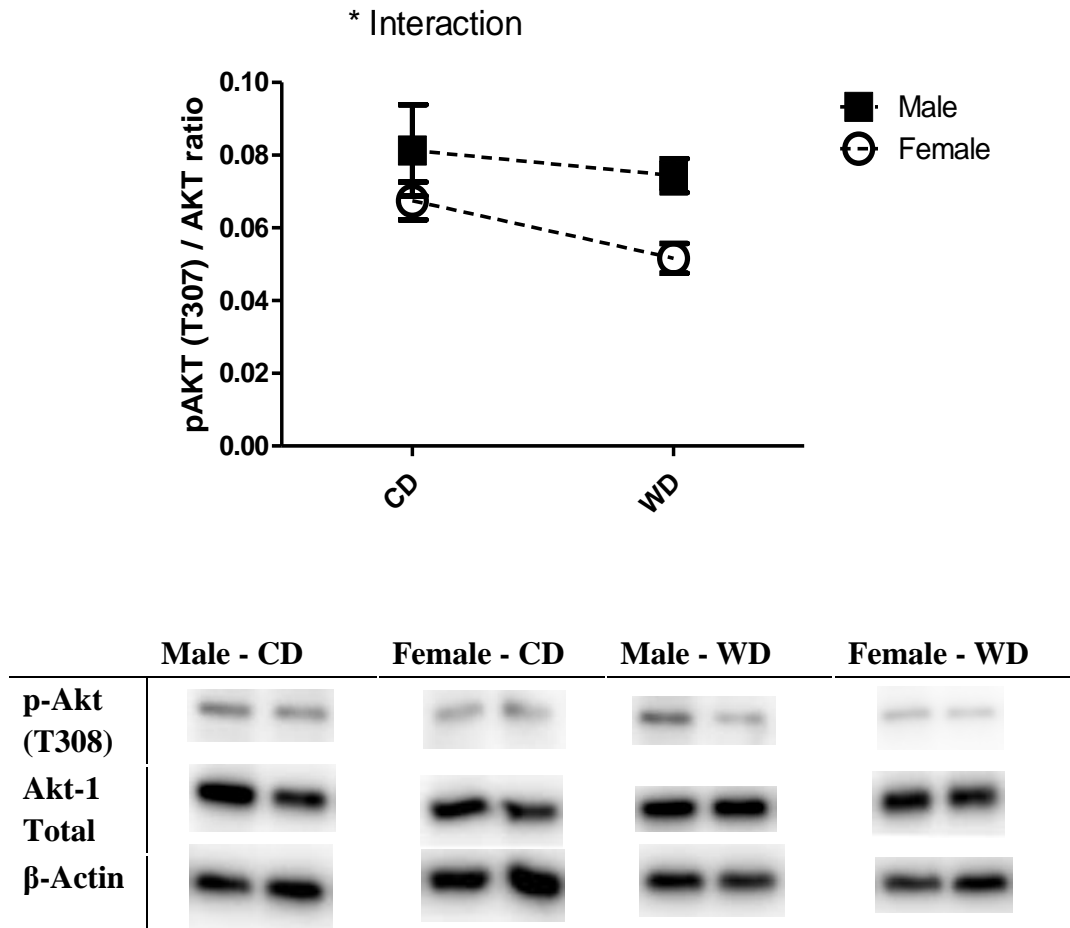


**Figure 2.8 AKT Expression in the Left Ventricle at Putdown.** Expression of pAKT (T308) relative to total AKT-1 protein in the left ventricle at  $140 \pm 1.9$  days of age. \* $p < 0.05$  Interaction.  $N = 4$  for NBW/CD, NBW/WD, LBW/CD, and LBW/WD in both males and females. Data presented as Mean  $\pm$  SEM. Statistical significance determined by two-way ANOVA. ANOVA table presented in Appendix H,

## 2.4 Discussion

Adverse *in utero* environments such as PI are known risk factors for the development of heart diseases in later life. Abnormal cardiac development processes which result from growth restricted pregnancies are believed to underlie the development of myocardial complications in later life<sup>34</sup>. Similarly, postnatal WD consumption is also known to result in CVD development, including the onset of cardiac IR, and eventually, cardiac dysfunction<sup>9,57</sup>. It can be inferred from these individual findings that the predisposition of CVDs from *in utero* factors can further increase an individual's susceptibility to a secondary postnatal insult such as WD consumption. This study intended to elucidate the independent and combined effects of LBW and WD on early markers of impaired cardiac function in a guinea pig model. The principle findings of this study were that 1) an adverse *in utero* environment resulting in LBW was associated with reduction in resting coronary blood flow and the onset of pathological hypertrophy, and 2) postnatal WD consumption resulted in reduced cardiac glucose uptake. Together, these findings in early adulthood demonstrated that following an adverse *in utero* environment and a poor postnatal diet, key pre-clinical markers of CVDs are present. Given that these early markers are associated with severe cardiac dysfunction in later life, the current experiment highlights an early stage of disease development that may serve as a platform from which to undertake early intervention therapies.

The guinea pig was selected as an animal model in this study due to its similarities to humans with respect to *in utero* developmental programming. Unlike other rodents, guinea pigs are prenatal organ developers, where pups are mature at birth<sup>58,59</sup>. For this

reason, the guinea pig fetus is particularly vulnerable to influences in placental function such as the UAA procedure, PI (where reduction in oxygen and nutrient delivery typically results in growth restriction), and LBW<sup>13,60–62</sup>. As a result, not only are the birth weights of LBW categorized offspring reduced, but body composition is also altered, as evident by the reduction in weight/length ratio<sup>32,62</sup>. An *in utero* insult such as UAA likely impacts genetically determined growth differentially. Yet, during post-natal life, a reversal of this delayed growth trajectory was observed in LBW offspring, where, by young adulthood, LBW body weights were similar to the NBW group. This pattern of rapid catch-up growth is a known consequence of asymmetrical growth restriction<sup>63,64</sup>. More importantly, this accelerated growth trajectory during the critical postnatal developmental periods have been implicated in metabolic and endothelial impairments, as well as the development of chronic diseases such as adulthood diabetes and CVDs<sup>29,65,66</sup>.

CVDs such as cardiomyopathy are often accompanied by the development of cardiac hypertrophy. This hypertrophic phenotype is an important marker of deteriorating cardiac health, and eventually, heart failure<sup>4,67</sup>. Interestingly, during critical periods of cardiac disease progression, disturbances in coronary flow can also occur. For example, up to a 16% reduction in basal coronary blood flow have been observed in patients with hypertrophic cardiomyopathy<sup>20,21</sup>. Therefore, we regarded these parameters as essential clues in recognizing early changes to cardiac health, and valuable predictors of systolic dysfunction and cardiomyopathy<sup>47</sup>. Utilizing DCE-CT, we observed that LBW offspring had a 17% reduction in basal coronary flow compared to the NBW group at 110 days of age. This reduction in coronary flow may reflect disturbances in myocardial capillaries, and microvasculature, which are the main determinants of coronary blood flow. It has been

previously reported that during pathological hypertrophy, capillary density in the left ventricle is greatly reduced<sup>47</sup>. This led us to speculate that LBW may be a major risk factor for CVD development in adulthood via hypertrophic and fibrotic processes. Indeed, by putdown, histological analyses revealed that the average cardiomyocyte size in LBW animals were significantly increased compared to NBW animals. Furthermore, LBW animals also displayed a higher percentage of collagen composition independent of sex, and an increased mRNA expression of type 1 collagen in females. The enlargement in cardiomyocytes and the abundance of collagen are hallmarks of a pathological hypertrophy phenotype, and supports our speculation that reductions in coronary flow determined by DCE-CT maybe a reflection of its development.

This apparent prenatal programming of cardiac remodeling may have emerged from the hindered development of cardiomyocytes *in utero*. A reduction in cardiomyocyte numbers has been identified as a major consequence of an insufficient *in utero* environment, and since proliferation of cardiomyocytes halts in the postnatal period, the demand for postnatal cardiac growth is therefore fulfilled by hypertrophic growth<sup>68,69</sup>. Furthermore, remodeling of the developing heart may be driven by increased vascular bed resistance in LBW offspring *in utero*, resulting in an increased mechanical force for ejection<sup>70,71</sup>. This chronic increase in ventricular load has been shown to trigger cardiac remodeling processes that underlie the development of pathological hypertrophy early in adolescence<sup>71,72</sup>. Together, these underlying factors can be further aggravated by the increasing demand for growth in a rapid post-natal growth profile, and as a result, rapid development of CVD may occur. Growth restricted pregnancies have been documented to result in increased ventricular diameter, intima-media thickness, and altered ventricular

shape in children, all indications of an early hypertrophic phenotype<sup>73</sup>. Altogether, these results suggests that an adverse *in utero* environment characterized by insufficient supply of oxygen and nutrition to meet the adequate growth potential during pregnancy, combined with the postnatal pressures of catch-up growth underlies the development of pathological hypertrophy. This *in utero* programmed alteration in cardiac physiology may very well be responsible for the vulnerability of LBW offspring to CVD development in later life.

Diets such as the WD during postnatal life can also have major consequences in cardiac health. Long term consumption of a WD is associated with diabetes, hypertension, and heart failure<sup>9,57</sup>. While these gross abnormalities develop over the course of adulthood, tissue specific alterations in metabolism develop prior to whole body expression of the disease states. For example, cardiac IR has been shown to occur prior to that of whole body IR and more importantly, prior to cardiovascular dysfunction<sup>6,44,50</sup>. Interestingly, we have seen that both LBW and postnatal high fat/sugar diet exposure are required to unmask the consequential effects on glucose homeostasis, and insulin signaling<sup>19</sup>. Therefore, we suspect that WD consumption and cardiac IR can exacerbate the consequences of prenatal programming of CVDs. Despite normal whole body glucose tolerance (K. Dunlop, per comms), cardiac PET scan demonstrated that WD consumption was associated with a reduction in basal glucose uptake in the left ventricle, independent of BW. Additionally, postnatal WD feeding was associated with a reduction in AKT-1 T308 phosphorylation, with a higher magnitude of reduction in females, despite no changes in AKT-1 S473 phosphorylation. Activation of AKT is an important step in the insulin mediated glucose uptake pathway, and is normally represented by phosphorylation at both S473 and T308<sup>74</sup>. However, reports have suggested that the activity of AKT is more closely correlated with

T308 phosphorylation, and that concurrent inhibition at both sites is not required for depression in insulin signaling<sup>75-77</sup>. This suggests the possibility that glucose transport and uptake in the left ventricle may have been suppressed by WD consumption via the inhibition of T308 phosphorylation of AKT-1. Together, these findings suggests that WD plays a prominent role in the onset of cardiac IR through disruptions in the insulin signaling pathway. Interestingly, we suspect that the onset of cardiac IR is an early protective mechanism against cardiac dysfunction. This same idea was also advocated by a study which demonstrated preserved cardiac functions in insulin resistant high-fat diet fed rats<sup>44</sup>. However, with time, a more advanced stage of the disease can unfold, where fatty acid oxidation – the primary energy source in cardiac metabolism – is disrupted, and may lead to severe cardiovascular dysfunction<sup>78,79</sup>. In further support, high-fat diet studies have also demonstrated that fatty acid oxidation was increased in an early non-hypertrophied myocardium, but maladapted in a hypertrophied myocardium<sup>10,80</sup>. Based on these reports, the diet dependent depression in basal glucose uptake observed in this study suggests that these animals are in an early stage of CVD progression, with the potential for more severe cardiovascular related consequences in later life.

Interestingly, WD fed NBW animals also demonstrated high amounts of collagen in the left ventricle, similar to the levels measured in LBW animals. This is likely the result of excessive accumulation of ROS from saturated fatty acids present in the WD, which is linked to extracellular matrix remodeling and fibrosis<sup>79,78</sup>. However, since LBW and WD consumption individually resulted in similar levels of collagen content, this implied that the combination of LBW and WD did not result in an additive relationship at the age studied. Similarly, our group's previous study also discovered that endothelial dependent

relaxation was blunted in LBW offspring, but again not affected by the secondary insult from WD<sup>29</sup>. However, other studies have proposed that IUGR could enhance the harmful metabolic responses to a high fat diet through IR and adipocyte dysfunctions<sup>81</sup>. Perhaps the *in utero* enhancements of diet induced CVD development processes requires a longer manifestation period. Thus, further studies on long term impact should be conducted. Nonetheless, it is clear that the consequences from WD consumption may not be manifested as rapidly as *in utero* insults, and may also occur in a different manner. For example, hypertrophic growth and fibrosis in LBW offspring may have arisen from chronic increases in vascular bed resistance *in utero* combined with pressures from rapid postnatal growth. Meanwhile, consumption of WD is associated with cardiac IR, with multiple proposed underlying mechanisms, including adipocyte dysfunction, inflammation, and release of fatty acid metabolites<sup>19,82,83</sup>. Despite the disassociation between LBW and WD effects in our study, other reports have demonstrated that growth restricted fetuses are linked to the development of IR in adulthood. Specifically, during growth restriction, the limited supply of glucose can lead to the shutdown of the Insulin like Growth Factor (IGF) system<sup>84</sup>. However during postnatal life, the abundance in nutrients, and demand for catch-up growth results in excessive increases in insulin production, and activation of IGF system and insulin-like actions, which ultimately, results in adult IR<sup>85</sup>. Therefore, given that LBW and WD insults share similar cardiovascular consequences, we expect that with age, these common consequences of LBW and postnatal WD such as IR and fibrosis will become exacerbated.

The consequences of poor *in utero* growth and poor postnatal diets have been widely accepted to play critical independent roles in the later life development of CVDs.



Recent work is now beginning to unravel the complex interactions in CVD development when both these situations occur concurrently. In this current report, we used DCE-CT to report reductions in coronary blood flow at young adulthood associated with LBW. In support, molecular results also indicated evidence of cardiac hypertrophy, which likely contributes to the alterations in blood flow. These findings suggests that abnormal cardiac development processes at birth may arise from environmental pressures during pregnancy. This manifests in postnatal life, resulting in the development of key pre-clinical markers of CVDs. Additionally, the use of PET imaging also highlighted an early indication of altered cardiac insulin sensitivity, though it was only associated with WD consumption following weaning. Alterations in cardiac glucose uptake, or insulin sensitivity is also a strong early indicator of many CVDs, where by young adulthood, WD fed offspring, irrespective of birthweight, were significantly impacted. Despite the healthy, non-obese, glucose tolerant phenotype (K. Dunlop, per comms), these changes in the cardiovascular system exposes the underlying development of severe CVDs. Furthermore, since *in utero* predisposition and WD consumption share common consequences such as early indication of cardiac fibrosis and IR development, we believe that with time, the exacerbated effects of these two insults will become more apparent. In summary, this study used non-invasive, novel imaging techniques to detect specific early markers of CVDs, and highlights the need for additional long term studies on the combined effects of *in utero* and postnatal insult.

## 2.5 References

1. A Global Brief on Hypertension World Health Day 2013. (2013).
2. Kasper, D. *Harrison's Principles of Internal Medicine*. (McGraw-Hill, 2005).
3. Maron, B. J. *et al.* Contemporary definitions and classification of the cardiomyopathies: an American Heart Association Scientific Statement from the Council on Clinical Cardiology, Heart Failure and Transplantation Committee; Quality of Care and Outcomes Research and Functio. *Circulation* **113**, 1807–16 (2006).
4. Levy, D. & Garrison, R. Prognostic implications of echocardiographically determined left ventricular mass in the Framingham Heart Study. *N. Engl. J. Med.* **322**, 1561–1566 (1990).
5. Maron, B. J. *et al.* American College of Cardiology/European Society of Cardiology Clinical Expert Consensus Document on Hypertrophic Cardiomyopathy. *J. Am. Coll. Cardiol.* **42**, 1687–1713 (2003).
6. McFarlane, S. I., Banerji, M. & Sowers, J. R. Insulin resistance and cardiovascular disease. *J. Clin. Endocrinol. Metab.* **86**, 713–8 (2001).
7. Hooper, L. *et al.* Reduced or modified dietary fat for preventing cardiovascular disease. *Cochrane database Syst. Rev.* CD002137 (2011). doi:10.1002/14651858.CD002137.pub2
8. Howard, B. V. Sugar and Cardiovascular Disease: A Statement for Healthcare Professionals From the Committee on Nutrition of the Council on Nutrition, Physical Activity, and Metabolism of the American Heart Association. *Circulation* **106**, 523–527 (2002).

9. Fung, T. T., Willett, W. C., Stampfer, M. J., Manson, J. E. & Hu, F. B. Dietary patterns and the risk of coronary heart disease in women. *Arch. Intern. Med.* **161**, 1857–62 (2014).
10. Chess, D. J., Lei, B., Hoit, B. D., Azimzadeh, A. M. & Stanley, W. C. Effects of a high saturated fat diet on cardiac hypertrophy and dysfunction in response to pressure overload. *J. Card. Fail.* **14**, 82–8 (2008).
11. Barker, D. J. Intrauterine programming of adult disease. *Mol. Med. Today* **1**, 418–23 (1995).
12. Manning, F. Intrauterine growth retardation. *Fetal Med. Princ. Pract.* **317**, (1995).
13. Kingdom, J., Huppertz, B., Seaward, G. & Kaufmann, P. Development of the placental villous tree and its consequences for fetal growth. *Eur. J. Obstet. Gynecol. Reprod. Biol.* **92**, 35–43 (2000).
14. Anthony, R. V, Scheaffer, a N., Wright, C. D. & Regnault, T. R. H. Ruminant models of prenatal growth restriction. *Reprod. Suppl.* **61**, 183–94 (2003).
15. Saintonge, J. & Côté, R. Intrauterine growth retardation and diabetic pregnancy: two types of fetal malnutrition. *Am. J. Obstet. Gynecol.* **146**, 194–8 (1983).
16. Stettler, N., Zemel, B. S., Kumanyika, S. & Stallings, V. A. Infant Weight Gain and Childhood Overweight Status in a Multicenter, Cohort Study. *Pediatrics* **109**, 194–199 (2002).
17. Kuzawa, C. W. & Adair, L. S. Lipid profiles in adolescent Filipinos: relation to birth weight and maternal energy status during pregnancy. *Am J Clin Nutr* **77**, 960–966 (2003).
18. Thamotharan, M. *et al.* Transgenerational inheritance of the insulin-resistant phenotype in embryo-transferred intrauterine growth-restricted adult female rat offspring. *Am. J. Physiol. Endocrinol. Metab.* **292**, E1270–9 (2007).

19. Rueda-Clausen, C. F. *et al.* Hypoxia-induced intrauterine growth restriction increases the susceptibility of rats to high-fat diet-induced metabolic syndrome. *Diabetes* **60**, 507–16 (2011).
20. Kawada, N. *et al.* Hypertrophic cardiomyopathy: MR measurement of coronary blood flow and vasodilator flow reserve in patients and healthy subjects. *Radiology* **211**, 129–35 (1999).
21. Olivetto, I. *et al.* Relevance of coronary microvascular flow impairment to long-term remodeling and systolic dysfunction in hypertrophic cardiomyopathy. *J. Am. Coll. Cardiol.* **47**, 1043–8 (2006).
22. Nikolaidis, L. The development of myocardial insulin resistance in conscious dogs with advanced dilated cardiomyopathy. *Cardiovasc. Res.* **61**, 297–306 (2004).
23. Ouwens, D. M. *et al.* Cardiac dysfunction induced by high-fat diet is associated with altered myocardial insulin signalling in rats. *Diabetologia* **48**, 1229–37 (2005).
24. So, A. *et al.* Non-invasive assessment of functionally relevant coronary artery stenoses with quantitative CT perfusion: preliminary clinical experiences. *Eur. Radiol.* **22**, 39–50 (2012).
25. So, A. & Lee, T.-Y. Quantitative myocardial CT perfusion: a pictorial review and the current state of technology development. *J. Cardiovasc. Comput. Tomogr.* **5**, 467–81 (2011).
26. Sadato, N. *et al.* Non-invasive estimation of the net influx constant using the standardized uptake value for quantification of FDG uptake of tumours. *Eur. J. Nucl. Med. Mol. Imaging* **25**, 559–564 (1998).
27. Louvaris, Z. *et al.* Blood flow does not redistribute from respiratory to leg muscles during exercise breathing heliox or oxygen in COPD. *J. Appl. Physiol.* **117**, 267–76 (2014).

28. Briscoe, T. A. *et al.* Cardiovascular and renal disease in the adolescent guinea pig after chronic placental insufficiency. (2004). doi:10.1016/j.ajog.2004.01.050
29. Thompson, J. A., Sarr, O., Piorkowska, K., Gros, R. & Regnault, T. R. H. Low birth weight followed by postnatal over-nutrition in the guinea pig exposes a predominant player in the development of vascular dysfunction. *J. Physiol.* **592**, 5429–43 (2014).
30. Detmer, A., Gu, W. & Carter, A. M. The blood supply to the heart and brain in the growth retarded guinea pig fetus. *J. Dev. Physiol.* **15**, 153–60 (1991).
31. Kind, K. L. *et al.* Restricted fetal growth and the response to dietary cholesterol in the guinea pig. *Am. J. Physiol.* **277**, R1675–82 (1999).
32. Kind, K. L. *et al.* Effect of maternal feed restriction during pregnancy on glucose tolerance in the adult guinea pig. *Am. J. Physiol. Regul. Integr. Comp. Physiol.* **284**, R140–52 (2003).
33. Greulich, S. *et al.* Secretory products of guinea pig epicardial fat induce insulin resistance and impair primary adult rat cardiomyocyte function. *J. Cell. Mol. Med.* **15**, 2399–410 (2011).
34. Menendez-castro, C. *et al.* Early and Late Postnatal Myocardial and Vascular Changes in a Protein Restriction Rat Model of Intrauterine Growth Restriction. **6**, (2011).
35. Livak, K. J. & Schmittgen, T. D. Analysis of relative gene expression data using real-time quantitative PCR and the 2<sup>(-Delta Delta C(T))</sup> Method. *Methods* **25**, 402–8 (2001).
36. Helms, S. a. *et al.* Smaller cardiac cell size and reduced extra-cellular collagen might be beneficial for hearts of Ames dwarf mice. *Int. J. Biol. Sci.* **6**, 475–490 (2010).
37. Abel, E. D. *et al.* Cardiac hypertrophy with preserved contractile function after selective deletion of GLUT4 from the heart. *J. Clin. Invest.* **104**, 1703–14 (1999).

38. Ott, W. J. Sonographic diagnosis of fetal growth restriction. *Clin. Obstet. Gynecol.* **49**, 295–307 (2006).
39. Camici, P. *et al.* Coronary vasodilation is impaired in both hypertrophied and nonhypertrophied myocardium of patients with hypertrophic cardiomyopathy: a study with nitrogen-13 ammonia and positron emission tomography. *J. Am. Coll. Cardiol.* **17**, 879–86 (1991).
40. Jerosch-Herold, M. *et al.* Cardiac magnetic resonance imaging of myocardial contrast uptake and blood flow in patients affected with idiopathic or familial dilated cardiomyopathy. *Am. J. Physiol. Heart Circ. Physiol.* **295**, H1234–H1242 (2008).
41. Neglia, D. Prognostic Role of Myocardial Blood Flow Impairment in Idiopathic Left Ventricular Dysfunction. *Circulation* **105**, 186–193 (2002).
42. Rutter, M. K. Impact of Glucose Intolerance and Insulin Resistance on Cardiac Structure and Function: Sex-Related Differences in the Framingham Heart Study. *Circulation* **107**, 448–454 (2003).
43. Prior, J. O. *et al.* Coronary circulatory dysfunction in insulin resistance, impaired glucose tolerance, and type 2 diabetes mellitus. *Circulation* **111**, 2291–8 (2005).
44. Christopher, B. a *et al.* Myocardial insulin resistance induced by high fat feeding in heart failure is associated with preserved contractile function. *Am. J. Physiol. Heart Circ. Physiol.* **299**, H1917–27 (2010).
45. Sopontammarak, S. *et al.* Mitogen-activated protein kinases (p38 and c-Jun NH2-terminal kinase) are differentially regulated during cardiac volume and pressure overload hypertrophy. *Cell Biochem. Biophys.* **43**, 61–76 (2005).
46. Knöll, R., Hoshijima, M. & Chien, K. Cardiac mechanotransduction and implications for heart disease. *J. Mol. Med. (Berl)*. **81**, 750–6 (2003).
47. Gunasinghe, S. K., & Spinale, F. G. Myocardial basis for heart failure. In D. L. Mann (Ed.). *Role Card. Interstitium Hear. Fail.* 57–70 (2004).

48. McMullen, J. R. & Jennings, G. L. Differences between pathological and physiological cardiac hypertrophy: novel therapeutic strategies to treat heart failure. *Clin. Exp. Pharmacol. Physiol.* **34**, 255–62 (2007).
49. Tsou, P.-S., Haak, A. J., Khanna, D. & Neubig, R. R. Cellular mechanisms of tissue fibrosis. 8. Current and future drug targets in fibrosis: focus on Rho GTPase-regulated gene transcription. *Am. J. Physiol. Cell Physiol.* **307**, C2–13 (2014).
50. Park, S.-Y. *et al.* Unraveling the Temporal Pattern of Diet-Induced Insulin Resistance in Individual Organs and Cardiac Dysfunction in C57BL/6 Mice. *Diabetes* **54**, 3530–3540 (2005).
51. Prada, P. O. *et al.* Western diet modulates insulin signaling, c-Jun N-terminal kinase activity, and insulin receptor substrate-1ser307 phosphorylation in a tissue-specific fashion. *Endocrinology* **146**, 1576–87 (2005).
52. Fischer, Y. *et al.* Insulin-induced Recruitment of Glucose Transporter 4 (GLUT4) and GLUT1 in Isolated Rat Cardiac Myocytes: Evidence of the existence of different intracellular GLUT4 vesicle populations. *J. Biol. Chem.* **272**, 7085–7092 (1997).
53. Kitamura, T. *et al.* Requirement for Activation of the Serine-Threonine Kinase Akt (Protein Kinase B) in Insulin Stimulation of Protein Synthesis but Not of Glucose Transport. *Mol. Cell. Biol.* **18**, 3708–3717 (1998).
54. Lizcano, J. M. & Alessi, D. R. The insulin signalling pathway. *Curr. Biol.* **12**, R236–8 (2002).
55. Shao, J. Decreased Akt kinase activity and insulin resistance in C57BL/KsJ-Leprdb/db mice. *J. Endocrinol.* **167**, 107–115 (2000).
56. Jensen, C. B. *et al.* Altered PI3-kinase/Akt signalling in skeletal muscle of young men with low birth weight. *PLoS One* **3**, e3738 (2008).

57. Nagarajan, V. *et al.* Cardiac function and lipid distribution in rats fed a high-fat diet: in vivo magnetic resonance imaging and spectroscopy. *Am. J. Physiol. Heart Circ. Physiol.* **304**, H1495–504 (2013).
58. Engle, W. A. & Lemons, J. A. Composition of the fetal and maternal guinea pig throughout gestation. *Pediatr. Res.* **20**, 1156–60 (1986).
59. Jones, C. T. & Parer, J. T. The effect of alterations in placental blood flow on the growth of and nutrient supply to the fetal guinea-pig. *J. Physiol.* **343**, 525–537 (1983).
60. Heinonen, S., Taipale, P. & Saarikoski, S. Weights of placentae from small-for-gestational age infants revisited. *Placenta* **22**, 399–404 (2001).
61. Aviram, R., T, B. S. & Kidron, D. Placental aetiologies of foetal growth restriction: clinical and pathological differences. *Early Hum. Dev.* **86**, 59–63 (2010).
62. Turner, A. J. & Trudinger, B. J. A modification of the uterine artery restriction technique in the guinea pig fetus produces asymmetrical ultrasound growth. *Placenta* **30**, 236–40 (2009).
63. Wollmann, H. A. Intrauterine Growth Restriction: Definition and Etiology. *Horm. Res. Paediatr.* **49**, 1–6 (1998).
64. Forsen, T., Eriksson, J. G., Tuomilehto, J., Osmond, C. & Barker, D. J. P. Growth in utero and during childhood among women who develop coronary heart disease: longitudinal study. *BMJ* **319**, 1403–1407 (1999).
65. Crowther, N. J., Cameron, N., Trusler, J. & Gray, I. P. Association between poor glucose tolerance and rapid post natal weight gain in seven-year-old children. *Diabetologia* **41**, 1163–7 (1998).
66. Kaijser, M. *et al.* Perinatal risk factors for ischemic heart disease: disentangling the roles of birth weight and preterm birth. *Circulation* **117**, 405–10 (2008).



67. Ritter, O. & Neyses, L. The molecular basis of myocardial hypertrophy and heart failure. *Trends Mol. Med.* **9**, 313–321 (2003).
68. Morrison, J. L. *et al.* Restriction of placental function alters heart development in the sheep fetus. *Am. J. Physiol. Regul. Integr. Comp. Physiol.* **293**, R306–13 (2007).
69. Corstius, H. B. *et al.* Effect of intrauterine growth restriction on the number of cardiomyocytes in rat hearts. *Pediatr. Res.* **57**, 796–800 (2005).
70. Kiserud, T., Ebbing, C., Kessler, J. & Rasmussen, S. Fetal cardiac output, distribution to the placenta and impact of placental compromise. *Ultrasound Obstet. Gynecol.* **28**, 126–36 (2006).
71. Cooper, G. Cardiocyte adaptation to chronically altered load. *Annu. Rev. Physiol.* **49**, 501–518 (1987).
72. Baltabaeva, A. *et al.* Regional left ventricular deformation and geometry analysis provides insights in myocardial remodelling in mild to moderate hypertension. *Eur. J. Echocardiogr.* **9**, 501–8 (2008).
73. Crispi, F. *et al.* Fetal growth restriction results in remodeled and less efficient hearts in children. *Circulation* **121**, 2427–36 (2010).
74. Kitamura, T. *et al.* Requirement for Activation of the Serine-Threonine Kinase Akt (Protein Kinase B) in Insulin Stimulation of Protein Synthesis but Not of Glucose Transport. *Mol. Cell. Biol.* **18**, 3708–3717 (1998).
75. Vincent, E. E. *et al.* Akt phosphorylation on Thr308 but not on Ser473 correlates with Akt protein kinase activity in human non-small cell lung cancer. *Br. J. Cancer* **104**, 1755–61 (2011).
76. Guertin, D. A. *et al.* Ablation in mice of the mTORC components raptor, rictor, or mLST8 reveals that mTORC2 is required for signaling to Akt-FOXO and PKCalpha, but not S6K1. *Dev. Cell* **11**, 859–71 (2006).

77. Kondapaka, S. B., Zarnowski, M., Yver, D. R., Sausville, E. A. & Cushman, S. W. 7-hydroxystaurosporine (UCN-01) inhibition of Akt Thr308 but not Ser473 phosphorylation: a basis for decreased insulin-stimulated glucose transport. *Clin. Cancer Res.* **10**, 7192–8 (2004).
78. Molkenin, J. D. Calcineurin-NFAT signaling regulates the cardiac hypertrophic response in coordination with the MAPKs. *Cardiovasc. Res.* **63**, 467–75 (2004).
79. Kandasamy, A. D., Chow, A. K., Ali, M. A. M. & Schulz, R. Matrix metalloproteinase-2 and myocardial oxidative stress injury: beyond the matrix. *Cardiovasc. Res.* **85**, 413–23 (2010).
80. Akki, A. & Seymour, A.-M. L. Western diet impairs metabolic remodelling and contractile efficiency in cardiac hypertrophy. *Cardiovasc. Res.* **81**, 610–7 (2009).
81. Rueda-Clausen, C. F., Morton, J. S. & Davidge, S. T. Effects of hypoxia-induced intrauterine growth restriction on cardiopulmonary structure and function during adulthood. *Cardiovasc. Res.* **81**, 713–22 (2009).
82. Shulman, G. I. Cellular mechanisms of insulin resistance. *J. Clin. Invest.* **106**, 171–6 (2000).
83. Kahn, S. E., Hull, R. L. & Utzschneider, K. M. Mechanisms linking obesity to insulin resistance and type 2 diabetes. *Nature* **444**, 840–6 (2006).
84. Lassarre, C. *et al.* Serum insulin-like growth factors and insulin-like growth factor binding proteins in the human fetus. Relationships with growth in normal subjects and in subjects with intrauterine growth retardation. *Pediatr. Res.* **29**, 219–25 (1991).
85. Cianfarani, S., Germani, D. & Branca, F. Low birthweight and adult insulin resistance: the ‘catch-up growth’ hypothesis. *Arch. Dis. Child. - Fetal Neonatal Ed.* **81**, F71–F73 (1999).

## **Chapter 3**

- 3 The Impact of an Adverse Maternal Diet Prior to and During Pregnancy Upon Young Guinea Pigs Fed a Postnatal Western Diet on the Early Development of Cardiovascular Diseases.**

### 3.1 Introduction

Development of cardiovascular diseases (CVD) are typically associated with unhealthy lifestyle choices such as physical inactivity, smoking, and the consumption of Westernized Diets (WD)<sup>1,2</sup>. As the highest cause of mortality in the developed world, CVDs like cardiomyopathy are a major risk factor to our society. That is before taking into account the recent revelations in perinatal research, which highlights the contributions of adverse fetal programming on the development of chronic diseases in adulthood<sup>3</sup>. This concept of prenatal stress as origins of CVDs and its markers such as myocardial insulin resistance (IR), and left ventricular hypertrophy have been coined “fetal programming”<sup>4-6</sup>. Indeed, previous studies have demonstrated that maternal WD consumption during pregnancy was associated with a higher risk for developing growth restriction, LBW and later life chronic diseases in the offspring<sup>6-8</sup>. Similarly, our previous findings also demonstrated that postnatal WD feeding could result in disruptions in myocardial glucose uptake - a sign of IR, and deteriorating cardiac health. Conceivably, the consumption of a WD during pregnancy may also deny the developing fetus the necessary dietary and nutritional requirements, therefore providing another means of developing later life diseases. Compelling evidence have strongly advocated that ongoing consumption of unhealthy diets in pregnancy and in postnatal life, can further hasten or exacerbate the progression of chronic diseases in adult life<sup>5,6,9,10</sup>.

Studies have demonstrated that the onset of severe cardiovascular consequences such as cardiac dysfunction could result from *in utero* and postnatal dietary insults<sup>11-13</sup>. However, these end-point studies represents a mature disease state, and hence miss the

preclinical developmental markers which precedes them. For example, the development of cardiac dysfunction resulting from severe CVDs are often preceded by cardiac remodeling processes including hypertrophy, and fibrosis in the myocardium<sup>14,15</sup>. This onset of pathological hypertrophy occurs in conjunction with a reduction in capillary density, which is strongly associated with alterations in coronary blood circulation and cardiomyocyte hypoxia<sup>16</sup>. Furthermore, reductions in coronary flow reserve – the ratio of stress to basal coronary flow – which precedes the onset CVDs is an effective pre-clinical indicator of heart failure<sup>17–20</sup>. From a clinical perspective, techniques which can non-invasively visualize these pre-clinical parameters and predicate later life CVD development are highly important. An effective predictor of long-term atherosclerotic disease progression appears to be coronary endothelial and flow function<sup>18</sup>. However, traditional methods in measuring coronary flow often requires invasive catheterization<sup>21</sup>, while molecular studies in animals again only provides end point results. In the previous chapter, we have demonstrated the potential of non-invasive imaging in cardiovascular research, therefore we again proposed the use of Dynamic Contrast Enhanced Computed Tomography (DCE-CT) and Positron Emission Tomography (PET) as early detection methods of compromised coronary blood flow and cardiac glucose uptake respectively.

The purpose of this study was to determine whether the consequences of dietary insult, through all life exposure, and during pregnancy is translated to the next generation. Specifically, we aimed to investigate if these insults would result in the onset of preclinical markers of CVDs in the offspring by adulthood. We postulated that maternal WD consumption prior to and during pregnancy and lactation, combined with offspring

postnatal WD consumption would result in alterations in coronary blood flow, and cardiac glucose uptake, both early markers of CVDs, in adulthood.

## 3.2 Methods

### 3.2.1 *Animal Model*

This study utilized female Dunkin-Hartly guinea pigs (Charles River Laboratories, Wilmington, MA) which were fed *ad libitum* from weaning to either a control diet (CD) (TD:110240, Harlan Laboratories, Madison WI), or a Western Diet (WD) (TD:110239, Harlan Laboratories, Madison WI) (See Table 2.1). Guinea pigs were housed individually at 19°C and 30% humidity with 12 hour light-dark cycle. These female guinea pigs were allowed to breed with male guinea pigs that were fed *ad libitum* to guinea pig chow (LabDiet diet 5025: 27% protein, 13% fat, 60% carbohydrates). Sows delivered naturally, and birth weights of each pup were recorded. Subsequently, these pups were weaned at 15 days of age, and randomly assigned onto either a CD or WD, which formed the four treatment groups of Maternal CD/ Postnatal CD (MC/CD), Maternal CD/ Postnatal WD (MC/WD), Maternal WD/ Postnatal CD (MW/CD), and Maternal WD/ Postnatal WD (MW/WD). Pups were weighed twice a week, and feed intake determined daily out to study endpoint.

### 3.2.2 *Imaging*

Previously, a study had reported that alternations in glucose tolerance associated with *in utero* insults occurred at approximately 101 days in a guinea pig model<sup>22</sup>. Similarly,

we selected the 110 day as a representative time point at young adulthood to investigate cardiac health. Additionally, another study also reported onset of IR at 210 days following high fat diet introduction<sup>23</sup>. Therefore, a 210 day time point was also selected to investigate changes which may develop later in adulthood. At the chosen 110 and 210 days of postnatal life, guinea pigs underwent DCE-CT and PET]. Induction of anesthesia was performed in an air tight chamber, through which 4-5% isoflurane was administered at a rate of 2L/min. During both DCE-CT and PET scanning, anesthesia was maintained with a tight fitting nose cone with 2-3% isoflurane flowing at a rate of 1L/min

### 3.2.3 *Dynamic Contrast Enhanced Computed Tomography (DCE-CT)*

This study utilized a GE Healthcare multi-slice CT system (Discovery VCT, GE Healthcare). Guinea pigs were positioned in the center of the CT scanner. To measure baseline coronary flow levels, a two phase DCE-CT scan was conducted following an intravenous injection of 1ml/kg of iodinated contrast (Omnipaque 200mgI/mL) via a pedal vein catheter at 8 ml/min. In the first phase of the scan, images were acquired continuously every second for 14.6 seconds. This was immediately followed by the second phase, where images were acquired every 15 seconds for 200 seconds. For both phases, images were acquired at a tube voltage of 120 kV, current of 180 mA, and a rotation speed of one revolution per second. Ten minutes following baseline data acquisition, hyperaemic blood flow was also recorded by induced cardiac stress. Briefly, dipyridamole (DIP, 0.56mg/kg) was injected at 0.142 mg/kg of body weight/ minute over four minutes, and a two phase



DCE-CT scan, similar to the one at baseline was repeated three minutes after infusion of measurement of hyperaemic blood flow.

DCE-CT images were reconstructed at a 1.25mm slice thickness, and transferred to an image processing workstation (Advantage Windows 4.0; GE Healthcare, Waukesha, Wis). Using CT Perfusion 5 program (GE Healthcare, Waukesha, Wis), an arterial input curve of contrast medium concentration was generated with a region of interest (ROI) placed in the left ventricle chamber of a slice which showed maximum size of the chamber. Following which, another ROI was outlined around the contour of the heart in the first image of the dynamic series of the same slice. Subsequent images which did not conform to this heart outline were removed from the study as they were mis-registered with the first image from either breathing or cardiac motion of the animal. Blood flow maps of the chosen slice was generated with CT Perfusion 5 software (GE Healthcare, Waukesha, Wis). Myocardial blood flow was calculated as the mean pixel value in a ROI placed in the inferior wall of the left ventricle. This process was repeated for images acquired following dipyridamole injection, and coronary reserve was calculated as the ratio of DIP to basal coronary flow.

#### 3.2.4 *Positron Emission Tomography*

Guinea pigs were anaesthetized in an air tight box with 4-5% isoflurane at 2L/min, and injected with ~25kBq/kg (0.2-0.3mL) of [<sup>18</sup>F] - fluoro-deoxy-glucose ([<sup>18</sup>F] FDG) via the pedal vein. Animals were allowed to recover for 40 minutes in their cage behind a lead

brick shield. Animals were then anaesthetized again transferred onto micro-PET scanner (GE eXpore Vista DR, GE Healthcare, Waukesha, Wis), and maintained at the anaesthetized state with 2.5-3% isoflurane at 1L/min in a nose cone. Images of the heart region were acquired by a 20 minute emission. Following correction for scatter and random coincidences, images were reconstructed into sixty 0.78mm thick slices. The reconstructed images were analyzed using an in-house MATLAB program (MathWorkds Inc., MA, USA). Two ROIs were drawn in each slice in which the left ventricle was visible. One outlining the epicardial surface, and the other one the endocardial surface of the left ventricle. The difference in the total counts was divided by the difference in volume of the ROIs to arrive at the average count in the myocardium. This average was converted to activity (Bq) using a sensitivity calibration factor determined from routine quality assurance of the scanner. The image derived activities from all left ventricle slices were averaged together to calculate myocardial activity. Measurements of Standardized Uptake Value (SUV) was calculated as:

$$SUV = \frac{\textit{Myocardial Activity}}{\textit{Injected Activity/Body Weight}} \quad (1)$$

### 3.2.5 *Tissue Collection*

At approximately postnatal day 250, animals were fasted overnight, and sacrificed by CO<sub>2</sub> inhalation<sup>23</sup>. The heart was removed, trimmed of connective tissue, carefully

separated into left or right ventricle, weighed and snaps frozen in liquid nitrogen for RNA and protein analysis.

### 3.2.6 *Quantitative Real-Time PCR*

Frozen tissues were homogenized in Trizol® (Invitrogen Life Technologies Co., Burlington, ON) with mortar and pestle, and 200 µL of chloroform was added. The mixtures were centrifuged at 12,000g for 15 minutes at 4°C, and the separated aqueous phase was transferred to new RNase-free tube, and mixed with 500 µL of isopropyl alcohol. RNA precipitate were obtained by an additional centrifugation at 12,000g for 10 minutes at 4°C, and three washes with 75% ethanol at 7500g for 5 minutes. The resulting RNA pellet was reconstituted in RNAase free diethylpyrocarbonate water, and yield quantity and quality (A260/A280 ration) of RNA was determined with NanoDrop 2000 UV-Vis Spectrophotometer (Thermo Scientific, Waltham MA, US). To obtain complementary DNA, 4µg of RNA were reverse transcribed with Moloney Murine Leukemia Virus Reverse Transcriptase (Invitrogen Life Technologies Co., Burlington ON). Measurement of gene expressions were completed by Real-time Quantitative Polymerase Chain Reaction (qPCR) in a triplicate manner using a Bio-Rad CFX384 real time PCR detector (Bio-Rad Laboratories Mississauga, ON). QPCR reactions were performed with a denature temperature of 95°C, annealing temperature of 59.5°C and elongation temperature of 72°C for 39 cycles. The  $2^{-\Delta CT}$  method was used for analysis, with  $\beta$ -Actin as the housekeeping gene<sup>24</sup>. Primer and genes used are shown in Appendix A.

### 3.2.7 *Western Blot*

Flash frozen left ventricle tissues were individually pulverized and homogenized in RIPA lysis buffer (50 mM Tris-HCl, NP-40 1%, Na-deoxycholate 0.25%, 1mM EDTA, 150 mM NaCl, 50 mM NAF, 1mM NaV, 25 mM  $\beta$ -glycerophosphate, pH 7.4) with protease and phosphatase inhibitor. Homogenates were centrifuged at 10,000g for 15 minutes at 4°C. The resulting supernatant were isolated as protein preparations, and quantified with DC™ Protein Assay Kit (Bio-Rad Laboratories, Mississauga, ON). Using 6% Bis-Tris gels, 30  $\mu$ g of protein were separated by size, and then transferred on to nitrocellulose membranes. Each membrane was stained with Amido Black stain, and imaged with VersaDoc Imaging System (Bio-Rad Laboratories Mississauga, ON) as house-keeping. The membranes were then washed and blocked overnight with 5% bovine serum albumin at 4°C. Blots were then probed with AKT-1 (Cell Signaling® #4691, 1:1000), pAKT Serine 473 (Cell Signaling® #9271, 1:1000), pAKT Threonine 308 (Cell Signaling® #9275, 1:1000), and monoclonal horseradish peroxidase-conjugated  $\beta$ -actin (Sigma-Aldrich #A3854, 1:50000) diluted in 5% bovine serum albumin in Tris-buffered saline – Tween 20 (0.01%) for 1 hour at room temperature. After washing, a horseradish peroxidase conjugated goat anti-rabbit IgG (Cell Signaling® #7074, 1:1000) secondary antibody diluted in 5% bovine serum albumin in Tris-buffered saline – Tween 20 (0.01%) was used to incubate blots at room temperature for 1 hour. Immunoreactive bands were detected using Luminata Forte Western HRP Substrate chemi-luminescence (EMD Millipore, Darmstadt, Germany), and imaged with VersaDoc Imaging System (Bio-Rad Laboratories Mississauga, ON). Abundance of protein were calculated using densitometry

values (arbitrary units) determined with ImageLab software (Bio-Rad Laboratories, Mississauga, ON), and expressed relative to Amido Black Staining.

### 3.2.8 *Statistical Analysis*

Statistical Analysis was performed with SPSS software (SPSS v22.0, Chicago, IL, USA). A mixed model ANOVA analysis was used to determine significant differences ( $p < 0.05$ ) from age, maternal diet, and postnatal diet. If significant differences or interactions were determined, student t-tests were used to for post-hoc analysis of differences between groups.

### 3.3 Results

#### 3.3.1 *Maternal WD Did Not Result in LBW, or Rapid Catch-Up Growth*

We aimed to determine if the consequences of dietary insult, through all life exposure, and during pregnancy is translated to the next generation. Offspring from WD fed mothers did not demonstrate any reductions in birth weight, or weight/length ratio compared to those born from CD fed mothers (Figure 3.1.). Furthermore, offspring growth, caloric intake, and food efficiencies from weaning to postnatal day 50, and postnatal day 50 to 110 were not significantly different between the four groups (Figure 3.2). As a result, no initial signs of growth restriction, or the rapid postnatal catch-up growth was observed from maternal WD pregnancies when placed on a postnatal CD or WD.

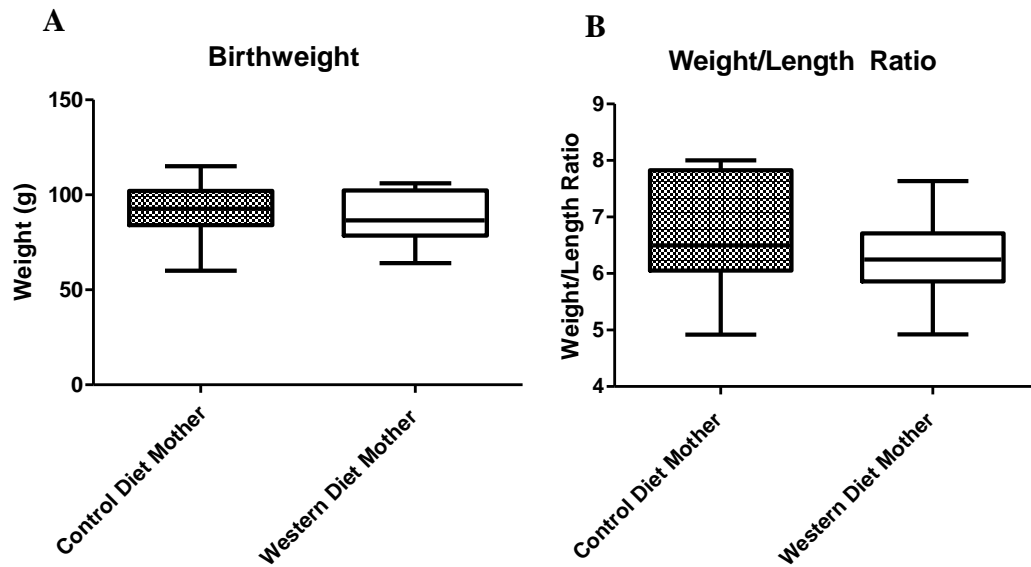


**Figure 3.1 Birth Characteristics** A) Birth weight and B) Weight/length of guinea pig pups. Pups were from either CD or WD fed mother bred with a chow fed control male. No significant changes in birth weight or weight/length ratio were observed due to maternal diet. N= 11 for offspring from CD mothers, and N=12 for offspring from WD fed mothers. Box represents Mean and SEM, while whiskers represents Max and Min values. Statistical significance was determined by student's t-test.

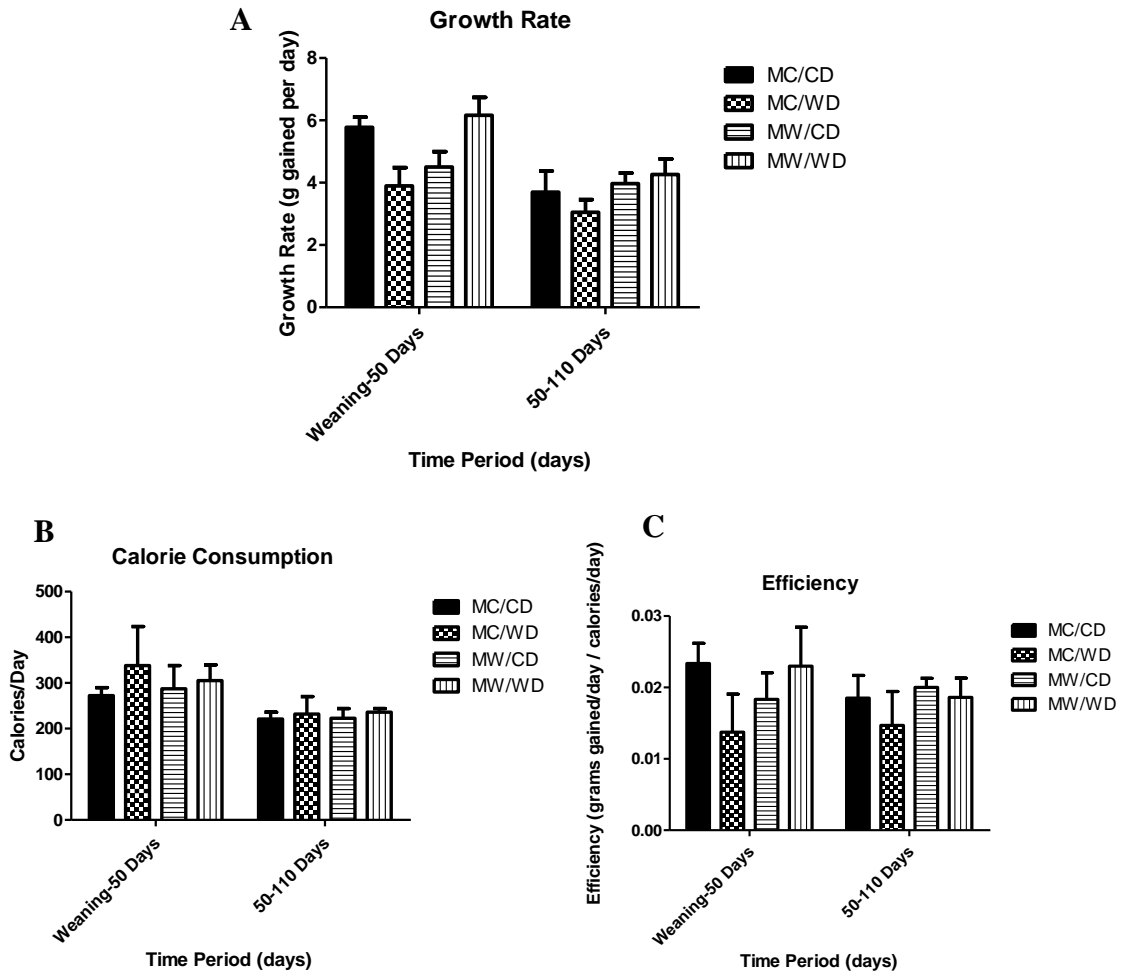


**Figure 3.2 Post-Weaning Growth Characteristics.** A) Growth rate, grams gained per day. B) Calories consumed per day. C) Food efficiency, gram gained per day/calories consumed per day from weaning to postnatal 50 days, and postnatal 50 days to 110 days was determined. All data sets are presented by mean  $\pm$  standard error, and no significant changes were observed between all four treatment groups. N=8 (MC/CD), 3 (MC/WD), 6 (MW/CD), and 4 (MW/WD). Statistical significance was determined by two-way ANOVA.



### 3.3.2 *Basal and Reserve Coronary Blood Flow Not Affected by Maternal or Postnatal WD Consumption*

Alterations in basal coronary blood flow have been reported to precede heart failure and increases in severity with the onset of cardiomyopathy<sup>19,20,25,26</sup>. Therefore, in this study, baseline coronary blood flow levels were assessed at postnatal 110 days, and 210 days by DCE-CT as a marker for CVD development. Coronary blood flow in the inferior wall of the left ventricle were compared between maternal diet, postnatal diet, and age factors. However, basal coronary blood flow appeared to be consistent across all treatment groups (Figure 3.3).

Reductions in coronary reserve are also strong indicators of cardiomyopathy, and systolic dysfunction, particularly in situations of low peripheral arterial resistance where basal coronary flow could appear normal<sup>17,25,27</sup>. However, despite a dipyridamole challenge, an average 69% coronary flow increase was observed across all four treatment groups (Figure 3.4). Thus, it appears that maternal diet, and postnatal diet do not result in changes in coronary reserve as determined by non-invasive imaging at the ages examined. Additionally, this study also investigated the mRNA expression of genes which may provide insight into possible fibrotic processes in the left ventricle. These included Collagen 1, 3, and matrix metalloproteinase-2 (MMP-2). Interestingly, the expression of these genes were also not altered as a result of diets in maternal or postnatal period. Collectively, these findings suggests that at the ages studied, both maternal and postnatal WD consumption did not result in disruptions in coronary circulation and indicators of pathological hypertrophy.

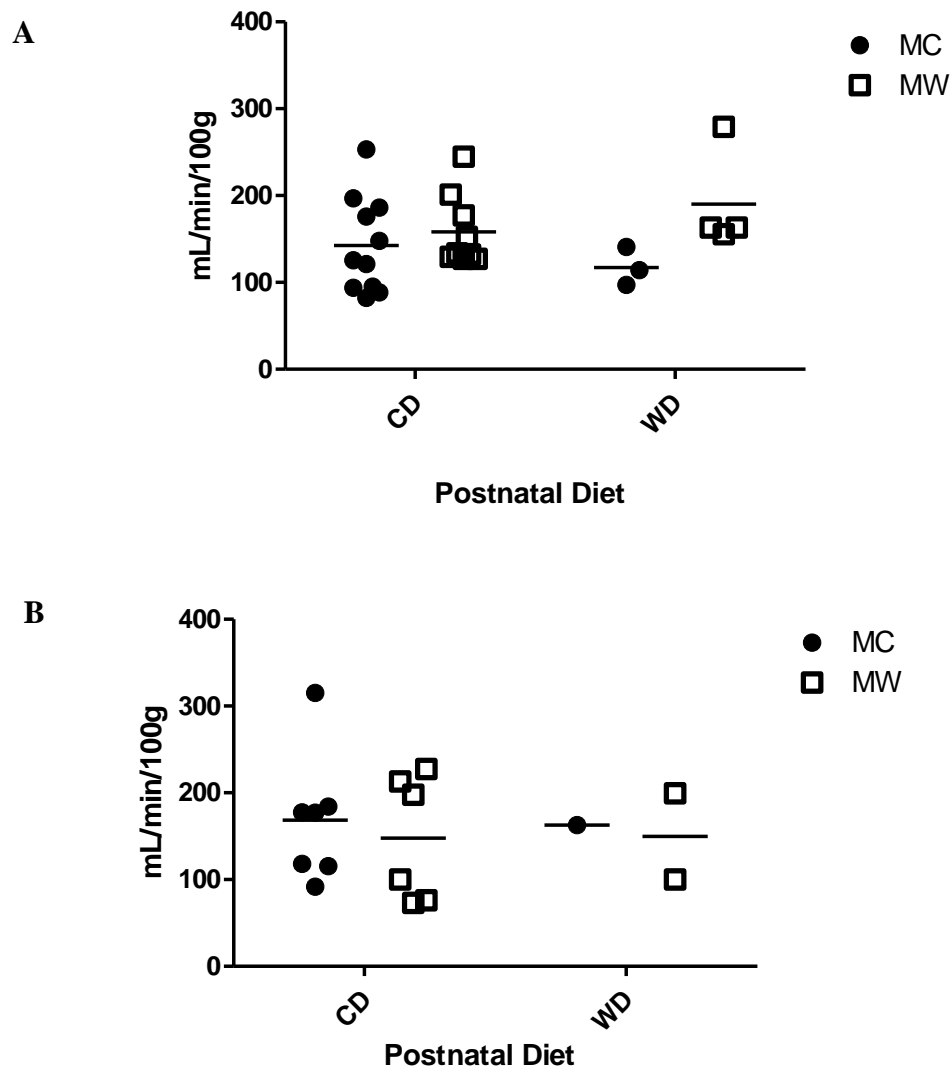


**Figure 3.3 Basal Coronary Blood Flow at 110 and 210 Days.** Basal blood flow in the inferior wall of left ventricle at **A**) 110 and **B**) 210 days of age were determined by CT Perfusion 5. No statistical differences were determined between groups. At 110 days N=11 (MC/CD), 3 (MC/WD), 9 (MW/CD), and 4 (MW/WD). At 210 days N=7 (MC/CD), 1 (MC/WD), 6 (MW/CD), and 2 (MW/WD). Statistical analyses were performed using a two-way ANOVA.

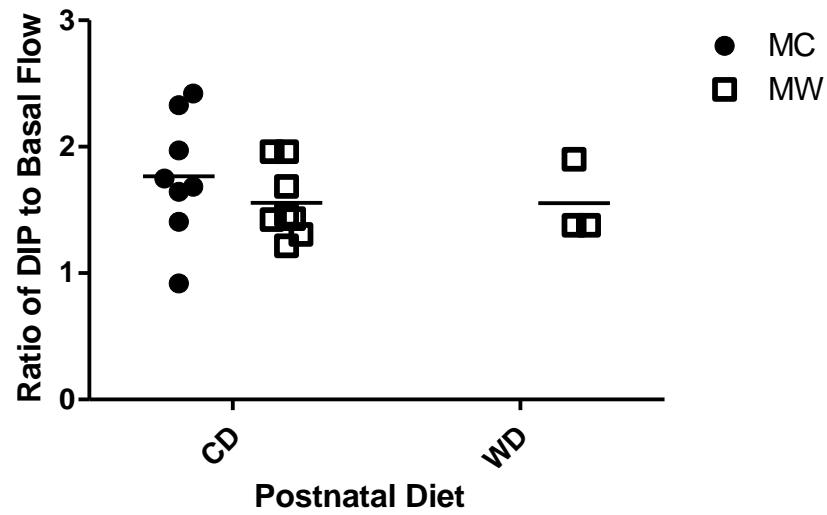


**Figure 3.4 Coronary Reserve.** Mean coronary blood flow was determined prior to after dipyridamole stress at 110 days scan. Coronary reserve was calculated as ratio of stress to basal coronary flow. No significant differences were observed between the treatment groups. N= 7 (MC/CD), 8 (MW/CD), and 3 (MW/WD). Statistical analyses were performed using a two-way ANOVA.

### 3.3.3 *Postnatal WD Consumption Resulting in Reduced Glucose Uptake*

To assess cardiac glucose uptake, as a proxy indicator for insulin sensitivity, PET was utilized. Previous studies have reported that during the developmental phase of CVDs, IR also develops, and is believed to be a protective mechanism against further cardiac injury<sup>28-30</sup>. Although an interaction between maternal diet and post-natal diet was observed, this was not statistically significant (Figure 3.5,  $p=0.056$ ). However, this trend suggested that maternal diet's effects were not consistent between the different postnatal diets. Specifically, a MC/WD mismatch resulted in a 30% decrease in glucose uptake compared to MC/CD group.

Underlying the changes in cardiac glucose uptake is insulin sensitivity. The insulin signaling pathway is primarily responsible for the insulin mediated uptake of glucose through glucose transporters in the heart, and is primarily regulated by series of phosphorylation steps<sup>31-33</sup>. Specifically, we investigated the protein expression of Protein Kinase B (AKT) Threonine 308, Serine 473, and Insulin Receptor Substrate 1 (IRS-1). The expression of AKT-1 T308 demonstrated a significant decrease as a result of postnatal feeding in both MC and MW groups (Figure 3.6). Associated markers of insulin signaling, IRS-1 and Ser473 AKT-1 were however, unaltered (Figure 3.7).

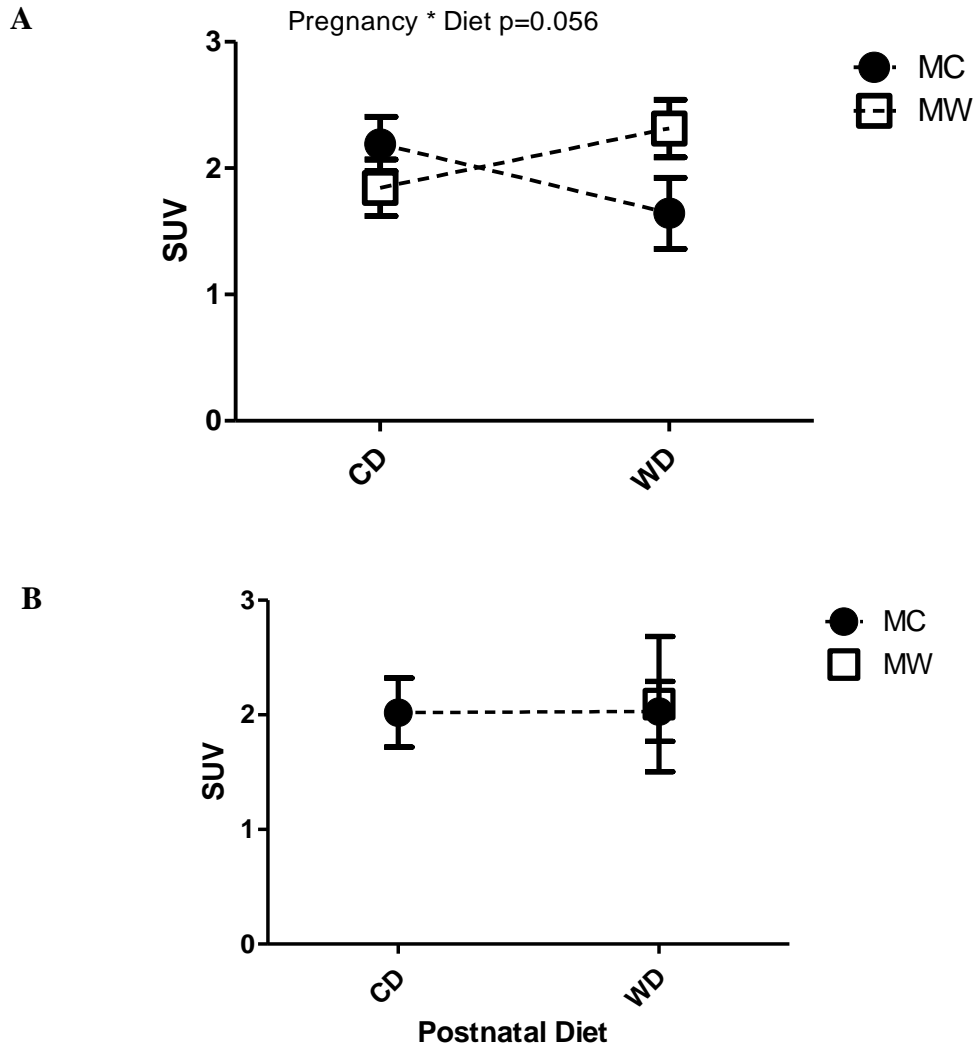


**Figure 3.5 Glucose Uptake Determined by PET.** Standard Uptake Value of the left ventricle acquired by PET at **A**) 110 and **B**) 210 days. Data presented as Mean  $\pm$  Standard Error. No statistical significance was observed between groups at both time point. At 110 days N= 11 (MC/CD), 3 (MC/WD), 6 (MW/CD), and 5 (MW/WD). At 210 days N= 8 (MC/CD), 3 (MC/WD), and 3 (MW/WD). Box represents Mean and SEM, while whiskers represents Max and Min values. Statistical significance was determined by a repeated measures two-way ANOVA. ANOVA table presented in Appendix I

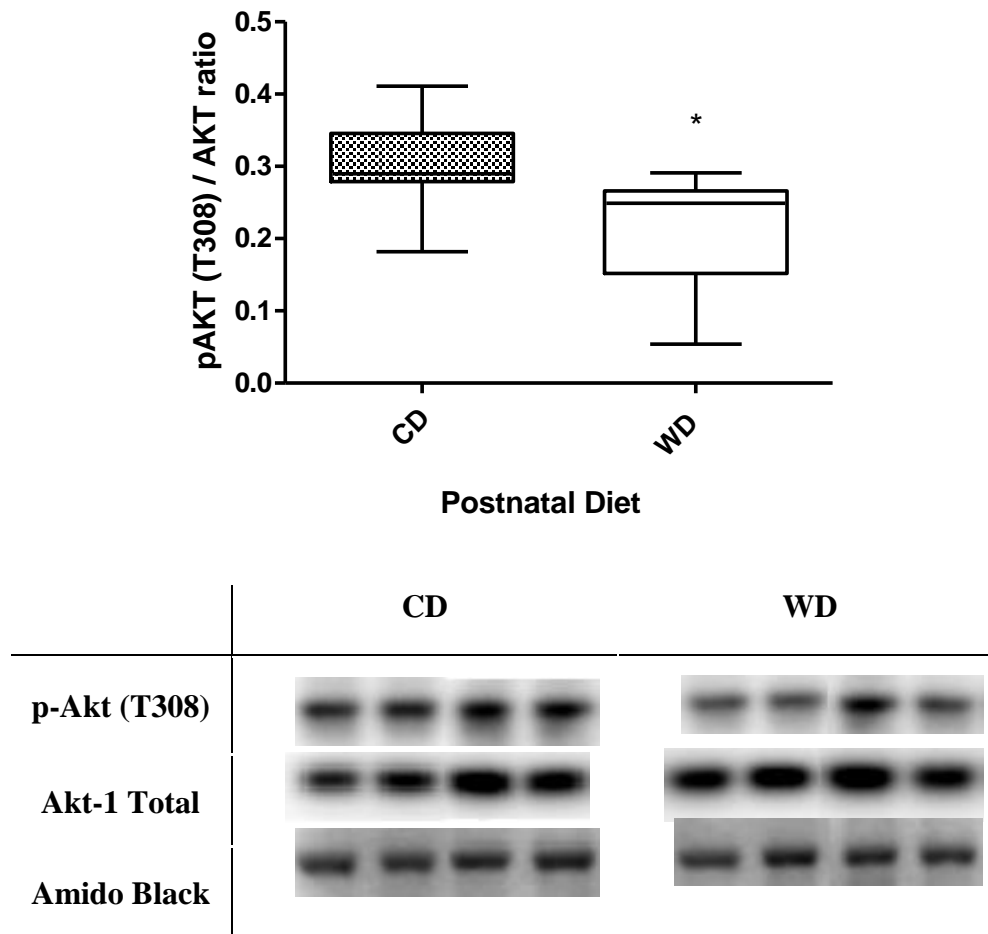


**Figure 3.6 Protein Expression of pAKT (T308) at Putdown.** Expression of pAKT (T308) relative to total AKT-1 protein in the left ventricle at 240 days of age. \* $p < 0.05$ .  $N=11$  for CD, and  $N=9$  for WD groups. Statistical significance was first determined by two-way ANOVA, and further analyzed by student's t-test. Box represents Mean and SEM, while whiskers represents Max and Min values. ANOVA table presented in Appendix J

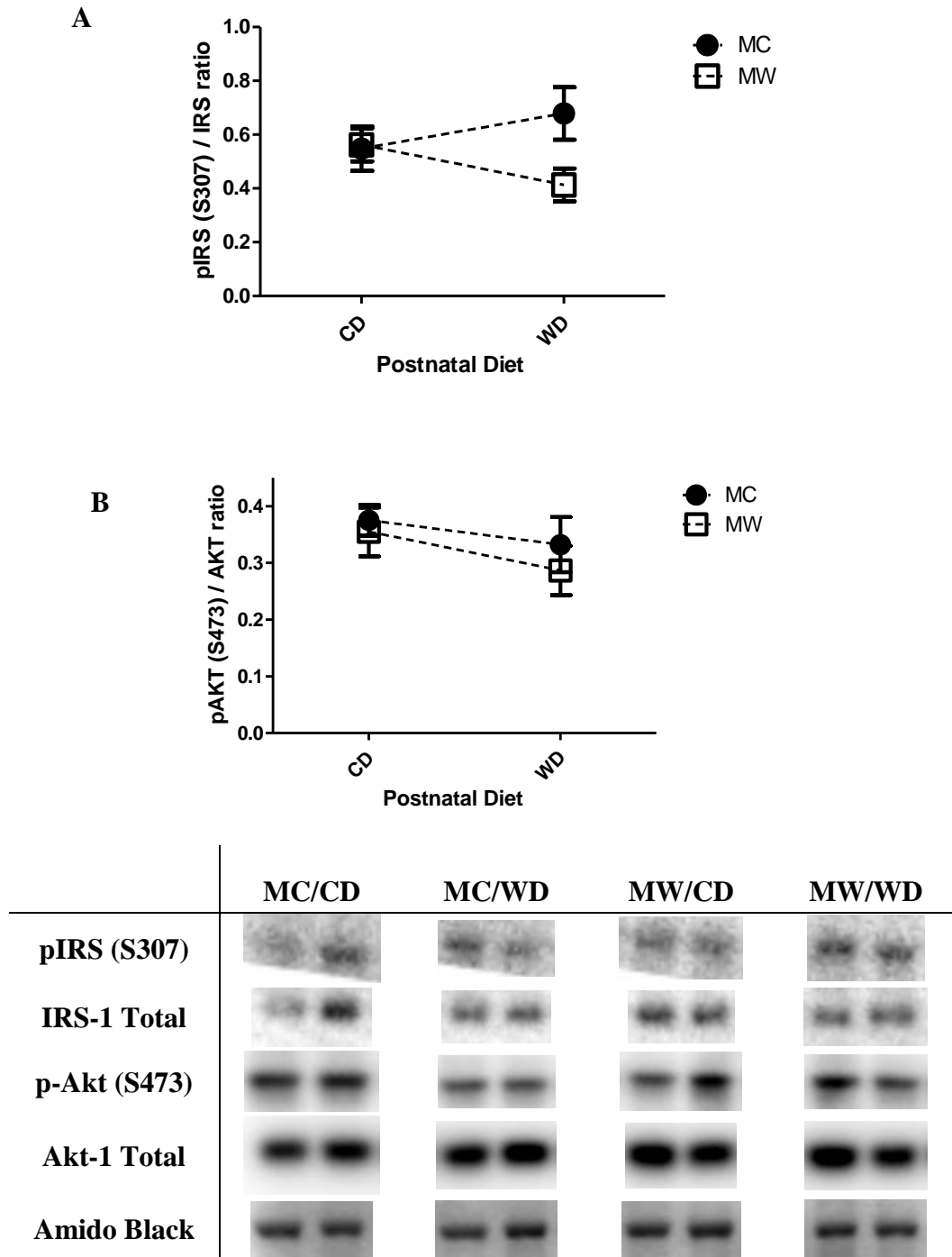


**Figure 3.7 Protein Expression of pIRS (S307) and pAKT (S473) at Putdown.** Protein expression of **A**) Serine 307 pIRS relative to total IRS protein, and **B**) Serine 473 pAKT relative to total AKT-1 protein expression. No significant differences were observed. N=7 (MC/CD), 4 (MC/WD), 4 (MW/CD), and 5 (MW/WD). Statistical significance was examined by two-way ANOVA.

### 3.4 Discussion

This current study explored the consequences of WD, particularly its influences *in utero*, and in postnatal life on the development of CVDs in offspring as they mature into adulthood. Interestingly, maternal WD consumption from weaning through maturation and pregnancy did not appear to aggravate cardiac function in the next generation, which are either control fed or further challenged with a postnatal WD. We believe that due to *in utero* adaptation to maternal diets, maternal WD may not have prominent or direct effects on offspring health at the age studied. Quite possibly, maternal obesity, or further postnatal diet challenge is necessary to fully elucidate the programming effects of a maternal WD<sup>34</sup>. However, we can speculate from related studies that given maternal WD's effects on other organ systems, and its long term predisposition for further postnatal insult, it can impact cardiovascular function later in adulthood.

In contrast to the Uterine Artery Ablation (UAA) model used in the previous chapter, a maternal WD introduces an abundance of carbohydrates, and saturated fatty acids. We have already determined that restriction in fetal nutrients is associated with LBW, and by late adulthood, left ventricular hypertrophy like symptoms. Other studies have also determined that LBW (induced by maternal hypoxia) and other extreme prenatal insults such as maternal obesity, resulting in large birth weight, and poor postnatal outcomes when challenged with an adverse postnatal high fat diet insult<sup>9,35,36</sup>. Consumption of WD in postnatal life is known to result in the development of chronic diseases such as CVD, even in individuals born of NBW<sup>37,38</sup>. Naturally, we are interested in whether



prolonged exposure to WD, particularly during *in utero* period, can accelerate or exacerbate these processes.

We observed that lifelong maternal WD feeding did not yield LBW pups. Studies in non-human primates reported that maternal consumption of a high fat diets increases the risks of placental inflammation, and stillbirth, and more importantly, it was also associated with a reduction in uterine artery blood flow<sup>39</sup>. This revelation is analogous to the UAA model, and we predicted that a lifelong a maternal WD would result in similar consequences, however that was not the case. Although high energy diet consumption and obesity during pregnancy are associated with IUGR<sup>40</sup>, fetal overgrowth and large-for-gestational age is not uncommon<sup>41,42</sup>. In support, studies have suggested that prenatal programming of IR, and birthweight alterations may be more associated with maternal adiposity than dietary fat<sup>34</sup>. However, in this study, despite chronic WD feeding in mothers, they were by no means overweight, which perhaps provides an explanation for the lack of the extreme birth weight phenotypes in the offspring. Furthermore, offspring of postnatal growth and food efficiencies were similar across the treatment groups, therefore a postnatal catch-up growth profile commonly associated with development of chronic diseases was not apparent. However, adverse prenatal environment can still possibly give rise to adult chronic diseases, such as obesity, IR, and cardiac dysfunction later in adulthood<sup>9,35,39,43,44</sup>. As a result, we are interested in the effects of postnatal WD consumption, and how they might play a role in the development of chronic diseases in the offspring, particularly in combination with chronic maternal WD insult.

In the build-up to many CVDs such as cardiomyopathy, disturbances in coronary circulation can occur, providing a useful predictor of cardiac dysfunction<sup>45,46</sup>. Utilizing

DCE-CT, baseline coronary flow in the left ventricle microvasculature at postnatal day 110 and 210 were measured. Interestingly, no alterations in coronary blood flow was observed between the groups. However, baseline coronary flow may not be a definitive indicator of coronary complications. This is particularly important, as basal coronary blood flow can still be maintained at normal levels by reducing distal arterial resistance, therefore masking the disturbances in coronary physiology<sup>27</sup>. However, when challenged, the ratio of stressed to basal blood flow, or the coronary reserve of compromised hearts is diminished<sup>27</sup>. Inducing stress through dipyridamole creates a discrepancy between the blood flow of stenosed and normal coronary arteries, which can provide further insight on the changes of left ventricular hemodynamics. Intriguingly, despite a dipyridamole challenge, coronary reserve was similar across all four treatment groups. This observation was akin with our previous findings, where postnatal WD feeding alone was not associated with coronary disruptions and markers of left ventricular hypertrophy. This study draws an additional revelation in that offspring of maternal WD feeding also did not display hemodynamic alterations in the left ventricle.

Maternal high-fat feeding have been strongly associated with the development metabolic diseases development in later life, with cardiac IR as a strong indicator<sup>9,22,47</sup>. Furthermore, in conjunction with a post-natal WD challenge, development of hypertension, and heart failure can be further exacerbated<sup>48</sup>. A previous study have reported cardiomyocyte glucose intolerance resulting from high-fat diet feeding<sup>23</sup> Therefore, early diagnosis of pre-clinical markers such as cardiac IR is important. The PET technology opens up the possibility of detecting changes in glucose uptake in the left ventricle and identifying at risk individuals in a non-invasively manner. In this chapter, no statistical

differences in left ventricular glucose uptake was found, yet a strong interaction between maternal diet and postnatal diet may be at play. Where, offspring of a CD fed mother displayed lower glucose uptake when given a postnatal WD compared to offspring born of WD fed mothers that were also fed the same postnatal WD. In comparison, this pattern was reversed with postnatal CD, where maternal CD offspring displayed higher glucose uptake compared to offspring from a WD fed mother. Furthermore, molecular analyses revealed that a postnatal WD alone was associated with a reduced protein expression of phosphorylated T308. Typically, the phosphorylation of T308 is an important step in the insulin signaling pathway, which ultimately translates to the translocation of glucose transporters to the membrane<sup>49</sup>. This is yet another piece of evidence which suggests that at adulthood, these offspring displayed reduced glucose uptake and associated IR in the heart as a result of WD consumption in postnatal life. This is also in alignment with our results in the LBW model, where changes in cardiac insulin sensitivity are largely determined by postnatal diet.

These changes in cardiac glucose uptake also highlights *in utero* programming at work, where the prenatal environment is largely influential on the offspring's adaptability to the postnatal environment. Specifically the mismatch between maternal and postnatal diet introduces susceptibilities in cardiac glucose uptake. The fetus is programmed to adapt its growth and developmental profiles during adverse uterine environments to ensure its survival in a similar postnatal environment. This hypothesis harkens back to the studies on Dutch hunger winter, and the Leningrad Siege, which clearly demonstrates how glucose tolerance and other metabolic diseases are associated with a mismatch of prenatal and postnatal environments<sup>50-52</sup>. In support, a study has reported that in response to maternal

high fat diet, offspring development of endothelial dysfunction in adulthood was prevented if offspring were raised on the same diet<sup>53</sup>. This however, is not to say that offspring born of a WD pregnancy should continue to indulge on the unhealthy diets, as ultimately it did not prevent the development of hypertension, and may pose a higher risk in the long term<sup>53</sup>. Additionally, this inferred that postnatal dietary factors might play a more influential role in the outcome of cardiac insulin sensitivity at the young adult age. It is possible that maternal dietary effects may not yet be discernable at the young ages studied. A non-human primate study reported that offspring of chronic maternal high-fat diet animals that underwent a diet reversal just prior to breeding retained normal acetylation of histone H3, where its alteration is commonly accompanied by nonalcoholic fatty liver diseases<sup>54</sup>. Maternal WD effects may not be prominent at first, and may require an additional insult, such as a postnatal WD, to be fully elucidated. Although studies on maternal diet reversal and CVD developments are lacking, we can speculate that the associated effects of a maternal WD requires long term exposure, and predisposes the offspring to further insult from a postnatal WD challenge<sup>5,10</sup>.

Although chronic maternal WD consumption did not yield the same hallmarks of hypertrophic cardiomyopathy observed in the LBW model. Previous studies have reported the susceptibility of a pregnancy marred by a high-fat diet to the development of chronic diseases such as CVDs. For example, offspring of chronic maternal high-fat feeding in rats displays increased body weight, and insulin insensitivity by adulthood<sup>6</sup>. Additionally, these changes appears to be highly heritable, where it has been observed to persist onwards to the second generation, and are believed to be a result of changes in epigenetics<sup>55</sup>. At the cardiovascular level, offspring of high-fat fed moms are also associated with endothelial

dysfunction, and are moderately exacerbated by a postnatal high-fat diet consumption<sup>56</sup>. Interestingly, endothelial function appears to improve when offspring are switched to a control diet, further supporting the notion that postnatal dietary patterns may be more detrimental to cardiac health<sup>56</sup>. Comparatively, in this current study, alterations in coronary circulation were not observed even in adulthood. A possible explanation is that the onset of CVDs may not occur until later in adulthood. In support, epidemiological studies in humans highlighted the increased prevalence of CVD development and fatalities in men were associated with high saturated fatty acid consumption. However, the onset of these fatal CVDs tend to be in middle age at approximately ~55 years old, where early age development is categorized as <70 years of age<sup>57-60</sup>. Therefore we must consider the possibility that the onset of these complications in the guinea pigs may be well into middle to late adulthood.

Although poor maternal diet may not appear to play a direct role on CVD development in offspring at the age studied, we speculate that the offspring's predisposition for further insult from postnatal diets is a major risk factor in long term cardiac health. Previous studies with chronic maternal high-fat feeding have demonstrated severe consequences in other organ systems by adulthood in the offspring. For instance, maternal high-fat diet exposure has been linked to development of non-alcoholic liver disease, beta cell dysfunction and obesity in offspring<sup>6,55,61,62</sup>. Although maternal WD consumption may not be a primary influence on later life cardiovascular outcome, the onset of obesity, diabetes and diseases of other organ systems may impact cardiac function overall, leading to the emergence of CVDs later in adulthood<sup>63,64</sup>. Furthermore, chronic exposure to WD in postnatal life is also associated with the development of similar complications such as IR

and obesity. We speculate that when combined with the aforementioned maternal WD effects, severe cardiovascular complications may arise with age. Therefore, the long term implications of a maternal WD on CVD development should be further investigated in future studies.

### 3.5 References

1. Hooper, L. *et al.* Reduced or modified dietary fat for preventing cardiovascular disease. *Cochrane database Syst. Rev.* CD002137 (2011). doi:10.1002/14651858.CD002137.pub2
2. Howard, B. V. Sugar and Cardiovascular Disease: A Statement for Healthcare Professionals From the Committee on Nutrition of the Council on Nutrition, Physical Activity, and Metabolism of the American Heart Association. *Circulation* **106**, 523–527 (2002).
3. *Noncommunicable Diseases. World Health Organization.* (2013).
4. Barker, D. J. Intrauterine programming of adult disease. *Mol. Med. Today* **1**, 418–23 (1995).
5. Parente, L. B., Aguila, M. B. & Mandarim-de-Lacerda, C. A. Deleterious effects of high-fat diet on perinatal and postweaning periods in adult rat offspring. *Clin. Nutr.* **27**, 623–34 (2008).
6. Srinivasan, M., Katewa, S. D., Palaniyappan, A., Pandya, J. D. & Patel, M. S. Maternal high-fat diet consumption results in fetal malprogramming predisposing to the onset of metabolic syndrome-like phenotype in adulthood. *Am. J. Physiol. Endocrinol. Metab.* **291**, E792–9 (2006).
7. Knudsen, V. K., Orozova-Bekkevold, I. M., Mikkelsen, T. B., Wolff, S. & Olsen, S. F. Major dietary patterns in pregnancy and fetal growth. *Eur. J. Clin. Nutr.* **62**, 463–70 (2008).
8. Elahi, M. M. *et al.* Long-term maternal high-fat feeding from weaning through pregnancy and lactation predisposes offspring to hypertension, raised plasma lipids and fatty liver in mice. *Br. J. Nutr.* **102**, 514–519 (2009).

9. Bayol, S. A., Farrington, S. J. & Stickland, N. C. A maternal 'junk food' diet in pregnancy and lactation promotes an exacerbated taste for 'junk food' and a greater propensity for obesity in rat offspring. *Br. J. Nutr.* **98**, 843–51 (2007).
10. Turdi, S. *et al.* Interaction between maternal and postnatal high fat diet leads to a greater risk of myocardial dysfunction in offspring via enhanced lipotoxicity, IRS-1 serine phosphorylation and mitochondrial defects. *J. Mol. Cell. Cardiol.* **55**, 117–29 (2013).
11. Rueda-Clausen, C. F., Morton, J. S. & Davidge, S. T. Effects of hypoxia-induced intrauterine growth restriction on cardiopulmonary structure and function during adulthood. *Cardiovasc. Res.* **81**, 713–22 (2009).
12. Bjarnegård, N., Morsing, E., Cinthio, M., Länne, T. & Brodzki, J. Cardiovascular function in adulthood following intrauterine growth restriction with abnormal fetal blood flow. *Ultrasound Obstet. Gynecol.* **41**, 177–84 (2013).
13. Akki, A. & Seymour, A.-M. L. Western diet impairs metabolic remodelling and contractile efficiency in cardiac hypertrophy. *Cardiovasc. Res.* **81**, 610–7 (2009).
14. Swynghedauw, B. Molecular Mechanisms of Myocardial Remodeling. *Physiol Rev* **79**, 215–262 (1999).
15. Stawowy, P. *et al.* Regulation of matrix metalloproteinase MT1-MMP/MMP-2 in cardiac fibroblasts by TGF-beta1 involves furin-convertase. *Cardiovasc. Res.* **63**, 87–97 (2004).
16. Sabbah, H. N., Sharov, V. G., Lesch, M. & Goldstein, S. Progression of heart failure: A role for interstitial fibrosis. *Mol. Cell. Biochem.* **147**, 29–34 (1995).
17. Olivotto, I. *et al.* Relevance of coronary microvascular flow impairment to long-term remodeling and systolic dysfunction in hypertrophic cardiomyopathy. *J. Am. Coll. Cardiol.* **47**, 1043–8 (2006).



18. Schachinger, V., Britten, M. B. & Zeiher, a. M. Prognostic Impact of Coronary Vasodilator Dysfunction on Adverse Long-Term Outcome of Coronary Heart Disease. *Circulation* **101**, 1899–1906 (2000).
19. Kawada, N. *et al.* Hypertrophic cardiomyopathy: MR measurement of coronary blood flow and vasodilator flow reserve in patients and healthy subjects. *Radiology* **211**, 129–35 (1999).
20. Neglia, D. Prognostic Role of Myocardial Blood Flow Impairment in Idiopathic Left Ventricular Dysfunction. *Circulation* **105**, 186–193 (2002).
21. Cannon, R. O. *et al.* Myocardial ischemia in patients with hypertrophic cardiomyopathy: contribution of inadequate vasodilator reserve and elevated left ventricular filling pressures. *Circulation* **71**, 234–43 (1985).
22. Kind, K. L. *et al.* Effect of maternal feed restriction during pregnancy on glucose tolerance in the adult guinea pig. *Am. J. Physiol. Regul. Integr. Comp. Physiol.* **284**, R140–52 (2003).
23. Greulich, S. *et al.* Secretory products of guinea pig epicardial fat induce insulin resistance and impair primary adult rat cardiomyocyte function. *J. Cell. Mol. Med.* **15**, 2399–410 (2011).
24. Livak, K. J. & Schmittgen, T. D. Analysis of relative gene expression data using real-time quantitative PCR and the 2(-Delta Delta C(T)) Method. *Methods* **25**, 402–8 (2001).
25. Camici, P. *et al.* Coronary vasodilation is impaired in both hypertrophied and nonhypertrophied myocardium of patients with hypertrophic cardiomyopathy: a study with nitrogen-13 ammonia and positron emission tomography. *J. Am. Coll. Cardiol.* **17**, 879–86 (1991).
26. Jerosch-Herold, M. *et al.* Cardiac magnetic resonance imaging of myocardial contrast uptake and blood flow in patients affected with idiopathic or familial dilated cardiomyopathy. *Am. J. Physiol. Heart Circ. Physiol.* **295**, H1234–H1242 (2008).

27. Leppo, J. A. Dipyridamole myocardial perfusion imaging. *J. Nucl. Med.* **35**, 730–3 (1994).
28. Rutter, M. K. Impact of Glucose Intolerance and Insulin Resistance on Cardiac Structure and Function: Sex-Related Differences in the Framingham Heart Study. *Circulation* **107**, 448–454 (2003).
29. Prior, J. O. *et al.* Coronary circulatory dysfunction in insulin resistance, impaired glucose tolerance, and type 2 diabetes mellitus. *Circulation* **111**, 2291–8 (2005).
30. Christopher, B. a *et al.* Myocardial insulin resistance induced by high fat feeding in heart failure is associated with preserved contractile function. *Am. J. Physiol. Heart Circ. Physiol.* **299**, H1917–27 (2010).
31. Fischer, Y. *et al.* Insulin-induced Recruitment of Glucose Transporter 4 (GLUT4) and GLUT1 in Isolated Rat Cardiac Myocytes: Evidence of the existence of different intracellular GLUT4 vesicle populations. *J. Biol. Chem.* **272**, 7085–7092 (1997).
32. Bell, G. I. *et al.* Molecular biology of mammalian glucose transporters. *Diabetes Care* **13**, 198–208 (1990).
33. Pessin, J. E. & Saltiel, A. R. Signaling pathways in insulin action: molecular targets of insulin resistance. *J. Clin. Invest.* **106**, 165–9 (2000).
34. White, C. L., Purpera, M. N. & Morrison, C. D. Maternal obesity is necessary for programming effect of high-fat diet on offspring. *Am. J. Physiol. Regul. Integr. Comp. Physiol.* **296**, R1464–72 (2009).
35. Tamashiro, K. L. K., Terrillion, C. E., Hyun, J., Koenig, J. I. & Moran, T. H. Prenatal stress or high-fat diet increases susceptibility to diet-induced obesity in rat offspring. *Diabetes* **58**, 1116–25 (2009).
36. Rich-Edwards, J. W. *et al.* Longitudinal study of birth weight and adult body mass index in predicting risk of coronary heart disease and stroke in women. *BMJ* **330**, 1115 (2005).

37. Hu, F. B. *et al.* Prospective study of major dietary patterns and risk of coronary heart disease in men. *Am J Clin Nutr* **72**, 912–921 (2000).
38. Chess, D. J., Lei, B., Hoit, B. D., Azimzadeh, A. M. & Stanley, W. C. Effects of a high saturated fat diet on cardiac hypertrophy and dysfunction in response to pressure overload. *J. Card. Fail.* **14**, 82–8 (2008).
39. Frias, A. E. *et al.* Maternal high-fat diet disturbs uteroplacental hemodynamics and increases the frequency of stillbirth in a nonhuman primate model of excess nutrition. *Endocrinology* **152**, 2456–64 (2011).
40. Perlow, J. H., Morgan, M. A., Montgomery, D., Towers, C. V & Porto, M. Perinatal outcome in pregnancy complicated by massive obesity. *Am. J. Obstet. Gynecol.* **167**, 958–62 (1992).
41. Sebire, N. J. *et al.* Maternal obesity and pregnancy outcome: a study of 287,213 pregnancies in London. *Int. J. Obes. Relat. Metab. Disord.* **25**, 1175–82 (2001).
42. Cnattingius, S., Bergström, R., Lipworth, L. & Kramer, M. S. Prepregnancy weight and the risk of adverse pregnancy outcomes. *N. Engl. J. Med.* **338**, 147–52 (1998).
43. Khan, I. Y. *et al.* A high-fat diet during rat pregnancy or suckling induces cardiovascular dysfunction in adult offspring. *Am. J. Physiol. Regul. Integr. Comp. Physiol.* **288**, R127–33 (2005).
44. Fang, X. *et al.* Hyperglycemia- and hyperinsulinemia-induced alteration of adiponectin receptor expression and adiponectin effects in L6 myoblasts. *J. Mol. Endocrinol.* **35**, 465–76 (2005).
45. Levy, D. & Garrison, R. Prognostic implications of echocardiographically determined left ventricular mass in the Framingham Heart Study. *N. Engl. J. Med.* **322**, 1561–1566 (1990).
46. Ritter, O. & Neyses, L. The molecular basis of myocardial hypertrophy and heart failure. *Trends Mol. Med.* **9**, 313–321 (2003).

47. Ouwens, D. M. *et al.* Cardiac dysfunction induced by high-fat diet is associated with altered myocardial insulin signalling in rats. *Diabetologia* **48**, 1229–37 (2005).
48. Fung, T. T., Willett, W. C., Stampfer, M. J., Manson, J. E. & Hu, F. B. Dietary patterns and the risk of coronary heart disease in women. *Arch. Intern. Med.* **161**, 1857–62 (2014).
49. Lizcano, J. M. & Alessi, D. R. The insulin signalling pathway. *Curr. Biol.* **12**, R236–8 (2002).
50. Stanner, S. A. *et al.* Does malnutrition in utero determine diabetes and coronary heart disease in adulthood? Results from the Leningrad siege study, a cross sectional study. *BMJ* **315**, 1342–1348 (1997).
51. Stein, Z. & Susser, M. The Dutch famine, 1944-1945, and the reproductive process. I. Effects on six indices at birth. *Pediatr. Res.* **9**, 70–6 (1975).
52. Ravelli, A. *et al.* Glucose tolerance in adults after prenatal exposure to famine. *Lancet* **351**, 173–177 (1998).
53. Khan, I., Dekou, V., Hanson, M., Poston, L. & Taylor, P. Predictive adaptive responses to maternal high-fat diet prevent endothelial dysfunction but not hypertension in adult rat offspring. *Circulation* **110**, 1097–102 (2004).
54. Suter, M. a. *et al.* A maternal high-fat diet modulates fetal SIRT1 histone and protein deacetylase activity in nonhuman primates. *FASEB J.* **26**, 5106–5114 (2012).
55. Dunn, G. A. & Bale, T. L. Maternal high-fat diet promotes body length increases and insulin insensitivity in second-generation mice. *Endocrinology* **150**, 4999–5009 (2009).
56. Fan, L. *et al.* Maternal high-fat diet impacts endothelial function in nonhuman primate offspring. *Int. J. Obes. (Lond)*. **37**, 254–62 (2013).

57. Ascherio, A. *et al.* Dietary fat and risk of coronary heart disease in men: cohort follow up study in the United States. *BMJ* **313**, 84–90 (1996).
58. Reddy, K. S. & Yusuf, S. Emerging Epidemic of Cardiovascular Disease in Developing Countries. *Circulation* **97**, 596–601 (1998).
59. Hu, F. B. *et al.* Prospective study of major dietary patterns and risk of coronary heart disease in men. *Am. J. Clin. Nutr.* **72**, 912–21 (2000).
60. De Oliveira Otto, M. C. *et al.* Dietary intake of saturated fat by food source and incident cardiovascular disease: the Multi-Ethnic Study of Atherosclerosis. *Am. J. Clin. Nutr.* **96**, 397–404 (2012).
61. McCurdy, C. E. *et al.* Maternal high-fat diet triggers lipotoxicity in the fetal livers of nonhuman primates. *J. Clin. Invest.* **119**, 323–35 (2009).
62. Han, J., Xu, J., Epstein, P. N. & Liu, Y. Q. Long-term effect of maternal obesity on pancreatic beta cells of offspring: reduced beta cell adaptation to high glucose and high-fat diet challenges in adult female mouse offspring. *Diabetologia* **48**, 1810–8 (2005).
63. Hubert, H. B., Feinleib, M., McNamara, P. M. & Castelli, W. P. Obesity as an independent risk factor for cardiovascular disease: a 26- year follow-up of participants in the Framingham Heart Study. *Circulation* **67**, 968–977 (1983).
64. Hamaguchi, M. Nonalcoholic fatty liver disease is a novel predictor of cardiovascular disease. *World J. Gastroenterol.* **13**, 1579 (2007).

## Chapter 4

### 4 Discussion

## 4.1 Summary

Since Forsdahl and Barker put forth the idea of Developmental Origins of Health and Disease, many have started to recognize the importance of *in utero* environments on the onset of adult diseases. This hypothesis, now further expanded, suggests that the development of chronic metabolic diseases in later life are the result of fetal programming mechanisms during critical periods of *in utero* environment<sup>1-3</sup>. In particular, a suboptimal *in utero* environment, resulting in Low Birth Weight (LBW), and an altered postnatal growth profile is strongly believed to increase the risk of developing chronic diseases such as Cardiovascular Diseases (CVDs) in later life<sup>1,4</sup>. These adverse *in utero* environments, can be a result of placental insufficiencies (PI), where the inability to provide the required oxygen and nutrient supply to the fetus induces a state of growth restriction. In contrast to a restrictive insult, adverse *in utero* environments can also arise from excessive maternal consumption of unhealthy diets such as a Western Diet (WD) through life and pregnancy. Alarmingly, recent evidence have also suggested that postnatal insults such as the consumption of WD can further exacerbate the abnormal growth patterns resulting from *in utero* insults<sup>5</sup>. Given the increasing prevalence of WD, its exposure to individuals of an adverse *in utero* environment may enhance the detrimental consequences of the growth restricted developmental profile. However, the mechanisms and relationships in the combination of prenatal and postnatal factors on the development of chronic diseases are still unknown.

Of the many non-communicable diseases associated with fetal programming, CVD distinguishes itself with the highest mortality rate. In 2008, approximately 17.3 million

people worldwide died from complications related to CVDs, and this number is expected to rise in the future<sup>6,7</sup>. Prior to the onset of severe functional phenotypes of CVDs, disease progression in the myocardium is often marked by cardiac IR, and pre-clinical markers such as hypertrophy, as well as alterations in coronary circulation<sup>8-12</sup>. It is likely that the development of CVDs may stem from the *in utero* period, and further hampered by unhealthy diet consumption. Given the severity of the consequences, such as systolic dysfunction, heart failure, and ultimately death, it is therefore crucial to investigate possible diagnostic techniques which could detect these early pre-clinical markers of CVDs.

In Chapter 2, we investigated the associated effects of low birth weight (LBW) resulting from a restrictive *in utero* environment and postnatal exposure to WD on the potential for CVD development in adulthood. We postulated that LBW, and WD consumption combined would result in the development of early pre-clinical markers of CVDs. Our findings demonstrated that LBW offspring displayed a rapid catch up growth profile shortly after birth. This accelerated growth trajectory has been implicated as an underlying factor in the manifestation of chronic diseases such as CVD<sup>13-15</sup>. Indeed, using Dynamic Contrast Enhanced Computed Tomography (DCE-CT), this study also highlighted that this accelerated growth in LBW animals was associated with a reduction in basal coronary blood flow at postnatal day 110. Moreover accompanying these alterations in coronary flow was histological evidence of pathological hypertrophy, including cardiomyocyte enlargement, and fibrosis. However these changes were not associated with the postnatal consumption of WD. In comparison, WD consumption was associated with reductions in left ventricular glucose uptake, as indicated by Positron Emission Tomography (PET). This was also supported by a decreased protein activation



of AKT-1, therefore possibly contributing to a state of cardiac IR. While *in utero* environment and WD consumption independently displayed different components of compromised cardiac health, their combination however, did not appear to result in an exacerbated effect at the ages studied.

In Chapter 3, we expanded our experimental focus on chronic maternal WD consumption as means of prenatal insult. Maternal WD consumption have been reported to trigger placental inflammation, and disruptions in placental hemodynamics, which is also associated with a higher frequency of stillbirths, and prenatal complications<sup>16,17</sup>. Furthermore, this unhealthy maternal dietary pattern is associated with the development of cardiovascular complications such as endothelial dysfunction, hypertension, and IR in the offspring<sup>18-20</sup>. Of additional concern is the possibility that the vulnerability induced by an *in utero* exposure to WD can be aggravated by a postnatal consumption of the same unhealthy WD<sup>18</sup>. However, detailed studies investigating their combined effects on CVDs are still lacking. In this chapter, we demonstrated that basal coronary flow and coronary reserve following a dipyridamole challenge were not significantly altered from either maternal or postnatal WD feeding. PET studies however indicated a strong trend which suggested that maternal WD may have differential effects on offspring cardiac glucose uptake depending on the type of postnatal diet consumed. Specifically, this highlights the effects of a mismatched *in utero* and postnatal environment, where reductions in cardiac glucose uptake appears to be more severe in maternal control diet to WD group than maternal WD to WD group. Although maternal WD's effects on cardiac health may not yet be discernable at the ages studied, this study further supported our observation in

Chapter 2, where postnatal WD consumption is linked to cardiac glucose uptake reductions, which are suggestive of IR.

In summary, these studies provide evidence for *in utero* programming of CVDs in adulthood. In particular, the growth restriction and LBW insult appear to have significant consequences in the early development of pathological hypertrophy. Moreover, both studies demonstrated the impact of postnatal WD consumption on the onset of markers of CVDs in early adulthood. Offspring of chronic maternal WD treatment appears to be free of the pre-clinical markers of CVDs at the ages studied. However, it is certainly possible that with age, a postnatal insult can unmask these *in utero* programmed risks as observed in reports of HFD, and IUGR interactive studies<sup>21</sup>. Lastly, although offspring appear healthy and non-obese while maintaining whole body glucose tolerance (K. Dunlop, per comms), important preclinical markers of CVDs such as disruptions in coronary flow and cardiac glucose uptake are present. A key significance of this study, is the applicability of imaging modalities, which effectively and non-invasively highlight these key developmental markers of CVD prior to the onset of a disease phenotype.

## 4.2 Speculations

Adverse *in utero* environments are known risks for the development of heart diseases, such as cardiomyopathy in later life<sup>4,22</sup>. This disease of the myocardium may have its origins *in utero* due to the unfavourable conditions during cardiovascular development. For example, a common cause of growth restriction and LBW is placental insufficiency, where the placenta fails to provide the required oxygen and nutritional needs of the fetus<sup>23</sup>. PI can also induce an increase in placental vascular bed resistance, as a result, fetal hearts must overcome this increased mechanical force for ejection, thereby creating pressure overload<sup>24,25</sup>. This complication predisposes the offspring to the development of hypertrophy, as concentric hypertrophy is induced by chronic increases in ventricular pressure<sup>26,27</sup>. Since this onset of pressure overload occurs in such an early stage during fetal development, it explains the early presence of left ventricular hypertrophy in LBW offspring. Moreover, *in utero* complications during fetal cardiac development can also hinder cardiac growth, resulting in a reduction in cardiomyocyte number at birth<sup>22</sup>. However, the heart is a post-mitotic organ, therefore postnatal growth is dependent on hypertrophy, or proliferation of non-myocytes<sup>22,28</sup>. This is further exacerbated by a postnatal catch-up growth profile that puts additional pressure for rapid cardiac growth. When the postnatal heart reaches its capacity for hypertrophic growth, further growth will occur through the deposition of extracellular matrix, therefore beginning the process of cardiac fibrosis<sup>29</sup>. This onset of pathological hypertrophy, characterized by fibrosis, can then lead to severe functional consequences such as cardiac dysfunction<sup>30</sup>. In our study the development of hypertrophy and fibrosis were also accompanied by reductions in basal

coronary flow. Interestingly, since hypoxia during *in utero* restriction is a stimulus for coronary vascularization, why is it that our study observed the opposite<sup>31</sup>? Other studies have supported our observation, where maternal restriction was not associated with any increases in coronary vascularization<sup>29</sup>. Perhaps this can be explained by an associated effect of hypertrophy and fibrosis, which is the reduction in coronary capillary density<sup>32</sup>. These mechanisms are likely what underlie the presence of pathological hypertrophy and reductions in coronary blood flow in the LBW offspring. However, these were not present in offspring from the chronic maternal WD model. Although a maternal WD insult may share similarities with a growth restriction insult, it can result in different outcomes including LBW and large birthweight<sup>18,33,34</sup>. Furthermore, its effects on postnatal health can easily be reversed<sup>35</sup>. This led us to believe that maternal WD's effects on offspring CVD development may be indirect. This is further supported by the fact that maternal WD offspring did not demonstrate signs of LBW, or the rapid catch-up growth profile that is usually associated with chronic diseases development in later life.

Similarly, the development of cardiac IR is another pre-clinical marker of many CVDs<sup>11,12</sup>. This state of IR, accompanied by a greater demand on fatty acid oxidation as a fuel source during high-fat feeding can be seen as a protective mechanism against cardiac dysfunction<sup>36</sup>. This state of IR can be attributed to the high levels of saturated fatty acids present in the WD. For example, high levels of saturated fatty acids have been known to increase the secretion of inflammatory cytokines which impair insulin sensitivity in skeletal muscle cells<sup>37,38</sup>. More importantly, saturated fatty acids can also reduce the activity of peroxisome proliferator-activated receptor gamma coactivator 1- alpha (PGC-1 $\alpha$ ), resulting in a reduction in oxidative phosphorylation and insulin-stimulated glucose

uptake<sup>39</sup>. Eventually, the onset of severe CVDs occurs when fatty acid oxidation is maladapted<sup>40-42</sup>. For example, studies have reported that the expression of peroxisome proliferator-activated receptor alpha (PPAR- $\alpha$ ) – an important activator of fatty oxidation - is reduced, while glucose metabolism was increased in rats with pathological hypertrophy<sup>42,43</sup>. The accumulation of saturated fatty acids, and its harmful by-products such as reactive oxygen species (ROS), diacylglycerols (DAG), and ceramide may result in the onset of fibrosis, and cardiac dysfunction<sup>44-47</sup>. Our present findings appeared consistent with these reports, where a postnatal WD depression in basal glucose uptake was observed. Additionally, early indication of fibrosis was also present in WD fed animals in chapter 2. This purported that the WD fed guinea pigs, with the reductions in glucose uptake, likely indicates an early stage of CVD development, with severe cardiovascular related consequences in later life.

### 4.3 Potential Limitations and Future Improvements

Given the ambitious scope, and detail of this study, there are certainly some limitations that must be addressed. Firstly, this study only chose to examine the pre-clinical parameters with non-invasively imaging at three different time points, 50, 110, and 210 days. These ages were strategically selected based on a previous study which demonstrate that the onset of IR, a key marker of metabolic disease development in guinea pigs occurred around 101 days<sup>48</sup>. However, they could not fully encompass the early developmental period in guinea pig adolescence, nor later in adulthood where CVDs typically occur. Future studies should introduce additional scanning time points to fully assess the progression of CVD development. In particular, future studies should also focus on the later life *in utero* induced multi-organ failure and its relation to CVD development to ascertain the developmental implications of *in utero* insults. Studies should also introduce molecular analysis immediately following scanning to further strengthen the findings of the non-invasive imaging techniques.

Secondly, non-invasive assessment of coronary blood flow using DCE-CT in a small animal model have many physical limitations. For example, the rapid heart rate, and breathing of guinea pigs introduces motion in the generation of blood flow maps. Although our study compensated for motion with the removal images where the heart shape was not consistent, this method was not perfect. A solution to this problem is to intubate the animals during the scanning procedure. However this would induce further stress to the animal. Future imaging studies should investigate techniques which can fully translate the use of clinical DCE-CT on small animal research. Despite this, the significance of DCE-CT for

the detection of preliminary clinical markers should not be ignored. Many of these limitations do not apply to human subjects – the intended subject of these imaging modalities– where it has been extensively been used for the study of coronary circulation<sup>49,50</sup>.

Another limitation in chapter 2 was that coronary flow was determined at a basal state, and therefore was not a definitive indicator of coronary complications. Basal coronary blood flow can be maintained at normal levels by reducing distal arterial resistance, therefore masking the disturbances in coronary physiology<sup>51</sup>. However, when under stress, the coronary reserve - the ratio of increase in coronary flow from stress to basal levels - of these compromised hearts are diminished<sup>51</sup>. Therefore, in future studies, coronary reserve of the LBW model must be examined similar to chapter 3. Moreover, we have speculated that the onset of hypertrophy and fibrosis underlies the reductions in coronary blood flow due to a reduction in capillary density<sup>32</sup>. Therefore, in addition to histological analysis on cardiomyocyte enlargement, and collagen deposition, future studies should also investigate ventricular capillary density. This could further strengthen and ascertain the relationship between *in utero* insult and coronary vascularization during CVD development.

Thirdly, the *in vivo* assessments of glucose uptake by PET were performed under basal conditions, as opposed to an insulin stimulated dynamic assessment. Similarly the final tissue collection for molecular analysis were also performed under fasted states in basal conditions. Measurement of glucose uptake under insulin stimulated situations could further strengthen our claim of changing insulin sensitivity, given this approach would demonstrate the implications of the disruptions in the insulin signaling pathway. Therefore

future [<sup>18</sup>F] FDG-PET studies should be conducted following insulin administration to determine the cardiovascular response to insulin. Previous studies which utilized a hyperinsulinemic clamp prior to [<sup>18</sup>F] FDG PET clearly demonstrated decreases in cardiac and skeletal glucose uptake that were associated with insulin resistance<sup>36,52,53</sup>. Similarly, tissue collection immediately following insulin injection would also allow us to investigate the changes in the insulin signaling pathway in response to insulin, and provide further support of an insulin resistant state.

Lastly, is the limitation in the characterization of a late stage severe CVD. In this study, we proposed that the pre-clinical markers such as coronary blood flow reductions, cardiac IR, and hypertrophy are precursors to a more severe phenotype of CVD. Indeed studies have demonstrated that these parameters have been used to effectively predict the onset of severe complications such as cardiac dysfunction, and death<sup>8,9,54-58</sup>. However, this study is limited in that a severe diseased phenotype was not characterized. Future studies should investigate an endpoint result from the prenatal and dietary insults, such as the onset of severe cardiac dysfunction. We propose the use of more traditional imaging systems such as echocardiography, where the measurement of ejection fraction is a useful tool in the characterization of deteriorating cardiac function<sup>59</sup>.



#### 4.4 Conclusions

This present study highlights the implications of an *in utero* insult, and a postnatal WD insult on the development of early preliminary clinical markers of CVD. Despite the healthy, non-obese, and glucose tolerant phenotype, we believe that the changes in the cardiovascular system exposes the underlying development of severe cardiovascular complications. Abnormal cardiac development processes may arise from prenatal insults, and the rapid catch-up growth profile. These inherent risks manifest themselves, and result in the onset of early development of pre-clinical markers of CVD such as hypertrophy, and coronary circulation alterations. Furthermore, our categorization of LBW based on the 25<sup>th</sup> percentile also inferred that there are potentially many at risk individuals outside of the clinically defined 10<sup>th</sup> percentile cutoff. This further supports the idea that offspring that have undergone a reprogramming event due to sub-optimal *in utero* conditions may not be fully reflected by the clinical birthweight cutoff at 10<sup>th</sup> percentile<sup>60,61</sup>. Interestingly, maternal WD did not appear to play a direct role in the development of CVDs. However, postnatal WD consumption resulted in alterations in cardiac glucose uptake, again indicative of eventual CVD development. Studies in our group, and other reports have demonstrated that *in utero* insults such as LBW, or a chronic maternal high-fat diet were associated with non-alcoholic liver disease, obesity, and dysfunctions in vascular function, and adipose development<sup>15,17,62–65</sup>. It is possible that these associated secondary effects of *in utero* insults such as LBW, or maternal WD consumption on other organ systems can eventually impact cardiac function, and lead to development of CVDs<sup>66,67</sup>. More importantly, chronic postnatal exposure to WD is also associated with similar

complications such as IR, and obesity, and can therefore enhance the deleterious effects of *in utero* insults. We propose that given the shared consequences of *in utero* and postnatal insults, the culmination of these complications would exacerbate and accelerate the development of CVDs in adulthood. Lastly this study also demonstrated the significance of non-invasive imaging on the early detection of markers of CVD development. The ability to identify at risk individuals before the onset of severe complications is important for the proposal of more effective treatment therapies. In summary the findings of this study not only highlighted the risks of *in utero* and postnatal insults on CVD development, but also opened new doors on the study of early diagnosis and intervention of the diseases which increasingly plague our society.

#### 4.5 References

1. Barker, D. Infant mortality, childhood nutrition, and ischaemic heart disease in England and Wales. *Lancet* **327**, 1077–1081 (1986).
2. Forsdahl, A. Are poor living conditions in childhood and adolescence an important risk factor for arteriosclerotic heart disease? *J. Epidemiol. Community Heal.* **31**, 91–95 (1977).
3. Hales, C. N. *et al.* Fetal and infant growth and impaired glucose tolerance at age 64. *BMJ* **303**, 1019–22 (1991).
4. Bjarnegård, N., Morsing, E., Cinthio, M., Länne, T. & Brodzki, J. Cardiovascular function in adulthood following intrauterine growth restriction with abnormal fetal blood flow. *Ultrasound Obstet. Gynecol.* **41**, 177–84 (2013).
5. Rueda-Clausen, C. F., Morton, J. S. & Davidge, S. T. Effects of hypoxia-induced intrauterine growth restriction on cardiopulmonary structure and function during adulthood. *Cardiovasc. Res.* **81**, 713–22 (2009).
6. A Global Brief on Hypertension World Health Day 2013. (2013).
7. *Noncommunicable Diseases. World Health Organization.* (2013).
8. Kawada, N. *et al.* Hypertrophic cardiomyopathy: MR measurement of coronary blood flow and vasodilator flow reserve in patients and healthy subjects. *Radiology* **211**, 129–35 (1999).
9. Olivotto, I. *et al.* Relevance of coronary microvascular flow impairment to long-term remodeling and systolic dysfunction in hypertrophic cardiomyopathy. *J. Am. Coll. Cardiol.* **47**, 1043–8 (2006).
10. Nikolaidis, L. The development of myocardial insulin resistance in conscious dogs with advanced dilated cardiomyopathy. *Cardiovasc. Res.* **61**, 297–306 (2004).

11. Ouwens, D. M. *et al.* Cardiac dysfunction induced by high-fat diet is associated with altered myocardial insulin signalling in rats. *Diabetologia* **48**, 1229–37 (2005).
12. McFarlane, S. I., Banerji, M. & Sowers, J. R. Insulin resistance and cardiovascular disease. *J. Clin. Endocrinol. Metab.* **86**, 713–8 (2001).
13. Crowther, N. J., Cameron, N., Trusler, J. & Gray, I. P. Association between poor glucose tolerance and rapid post natal weight gain in seven-year-old children. *Diabetologia* **41**, 1163–7 (1998).
14. Kaijser, M. *et al.* Perinatal risk factors for ischemic heart disease: disentangling the roles of birth weight and preterm birth. *Circulation* **117**, 405–10 (2008).
15. Thompson, J. A., Sarr, O., Piorkowska, K., Gros, R. & Regnault, T. R. H. Low birth weight followed by postnatal over-nutrition in the guinea pig exposes a predominant player in the development of vascular dysfunction. *J. Physiol.* **592**, 5429–43 (2014).
16. Frias, A. E. *et al.* Maternal high-fat diet disturbs uteroplacental hemodynamics and increases the frequency of stillbirth in a nonhuman primate model of excess nutrition. *Endocrinology* **152**, 2456–64 (2011).
17. McCurdy, C. E. *et al.* Maternal high-fat diet triggers lipotoxicity in the fetal livers of nonhuman primates. *J. Clin. Invest.* **119**, 323–35 (2009).
18. Tamashiro, K. L. K., Terrillion, C. E., Hyun, J., Koenig, J. I. & Moran, T. H. Prenatal stress or high-fat diet increases susceptibility to diet-induced obesity in rat offspring. *Diabetes* **58**, 1116–25 (2009).
19. Koukkou, E., Ghosh, P., Lowy, C. & Poston, L. Offspring of Normal and Diabetic Rats Fed Saturated Fat in Pregnancy Demonstrate Vascular Dysfunction. *Circulation* **98**, 2899–2904 (1998).
20. Turdi, S. *et al.* Interaction between maternal and postnatal high fat diet leads to a greater risk of myocardial dysfunction in offspring via enhanced lipotoxicity, IRS-

- 1 serine phosphorylation and mitochondrial defects. *J. Mol. Cell. Cardiol.* **55**, 117–29 (2013).
21. Rueda-Clausen, C. F. *et al.* Hypoxia-induced intrauterine growth restriction increases the susceptibility of rats to high-fat diet-induced metabolic syndrome. *Diabetes* **60**, 507–16 (2011).
  22. Morrison, J. L. *et al.* Restriction of placental function alters heart development in the sheep fetus. *Am. J. Physiol. Regul. Integr. Comp. Physiol.* **293**, R306–13 (2007).
  23. Salafia, C. M., Pezzullo, J. C., Ghidini, A., Lopèz-Zeno, J. A. & Whittington, S. S. Clinical correlations of patterns of placental pathology in preterm pre-eclampsia. *Placenta* **19**, 67–72 (1998).
  24. Kiserud, T., Ebbing, C., Kessler, J. & Rasmussen, S. Fetal cardiac output, distribution to the placenta and impact of placental compromise. *Ultrasound Obstet. Gynecol.* **28**, 126–36 (2006).
  25. Cooper, G. Cardiocyte adaptation to chronically altered load. *Annu. Rev. Physiol.* **49**, 501–518 (1987).
  26. Grossman, W., Jones, D. & McLaurin, L. P. Wall stress and patterns of hypertrophy in the human left ventricle. *J. Clin. Invest.* **56**, 56–64 (1975).
  27. Pluim, B. M., Zwinderman, A. H., van der Laarse, A. & van der Wall, E. E. The Athlete's Heart: A Meta-Analysis of Cardiac Structure and Function. *Circulation* **101**, 336–344 (2000).
  28. Corstius, H. B. *et al.* Effect of intrauterine growth restriction on the number of cardiomyocytes in rat hearts. *Pediatr. Res.* **57**, 796–800 (2005).
  29. Lim, K., Zimanyi, M. A. & Black, M. J. Effect of maternal protein restriction in rats on cardiac fibrosis and capillarization in adulthood. *Pediatr. Res.* **60**, 83–7 (2006).

30. Capasso, J. M., Palackal, T., Olivetti, G. & Anversa, P. Severe myocardial dysfunction induced by ventricular remodeling in aging rat hearts. *Am. J. Physiol.* **259**, H1086–96 (1990).
31. Schultz, A. *et al.* Interindividual Heterogeneity in the Hypoxic Regulation of VEGF: Significance for the Development of the Coronary Artery Collateral Circulation. *Circulation* **100**, 547–552 (1999).
32. Gunasinghe, S. K., & Spinale, F. G. Myocardial basis for heart failure. In D. L. Mann (Ed.). *Role Card. Interstitium Hear. Fail.* 57–70 (2004).
33. Bayol, S. A., Farrington, S. J. & Stickland, N. C. A maternal ‘junk food’ diet in pregnancy and lactation promotes an exacerbated taste for ‘junk food’ and a greater propensity for obesity in rat offspring. *Br. J. Nutr.* **98**, 843–51 (2007).
34. Rich-Edwards, J. W. *et al.* Longitudinal study of birth weight and adult body mass index in predicting risk of coronary heart disease and stroke in women. *BMJ* **330**, 1115 (2005).
35. Suter, M. a. *et al.* A maternal high-fat diet modulates fetal SIRT1 histone and protein deacetylase activity in nonhuman primates. *FASEB J.* **26**, 5106–5114 (2012).
36. Christopher, B. a *et al.* Myocardial insulin resistance induced by high fat feeding in heart failure is associated with preserved contractile function. *Am. J. Physiol. Heart Circ. Physiol.* **299**, H1917–27 (2010).
37. Jové, M., Planavila, A., Laguna, J. C. & Vázquez-Carrera, M. Palmitate-induced interleukin 6 production is mediated by protein kinase C and nuclear-factor kappaB activation and leads to glucose transporter 4 down-regulation in skeletal muscle cells. *Endocrinology* **146**, 3087–95 (2005).
38. Jové, M. *et al.* Palmitate induces tumor necrosis factor-alpha expression in C2C12 skeletal muscle cells by a mechanism involving protein kinase C and nuclear factor-kappaB activation. *Endocrinology* **147**, 552–61 (2006).

39. Handschin, C. & Spiegelman, B. M. Peroxisome proliferator-activated receptor gamma coactivator 1 coactivators, energy homeostasis, and metabolism. *Endocr. Rev.* **27**, 728–35 (2006).
40. Molkenin, J. D. Calcineurin-NFAT signaling regulates the cardiac hypertrophic response in coordination with the MAPKs. *Cardiovasc. Res.* **63**, 467–75 (2004).
41. Kandasamy, A. D., Chow, A. K., Ali, M. A. M. & Schulz, R. Matrix metalloproteinase-2 and myocardial oxidative stress injury: beyond the matrix. *Cardiovasc. Res.* **85**, 413–23 (2010).
42. Wilson, C. R., Tran, M. K., Salazar, K. L., Young, M. E. & Taegtmeyer, H. Western diet, but not high fat diet, causes derangements of fatty acid metabolism and contractile dysfunction in the heart of Wistar rats. *Biochem. J.* **406**, 457–67 (2007).
43. Akki, A. & Seymour, A.-M. L. Western diet impairs metabolic remodelling and contractile efficiency in cardiac hypertrophy. *Cardiovasc. Res.* **81**, 610–7 (2009).
44. Yu, C. *et al.* Mechanism by which fatty acids inhibit insulin activation of insulin receptor substrate-1 (IRS-1)-associated phosphatidylinositol 3-kinase activity in muscle. *J. Biol. Chem.* **277**, 50230–6 (2002).
45. Suematsu, N. Oxidative Stress Mediates Tumor Necrosis Factor-alpha-Induced Mitochondrial DNA Damage and Dysfunction in Cardiac Myocytes. *Circulation* **107**, 1418–1423 (2003).
46. Touyz, R. M. & Schiffrin, E. L. Reactive oxygen species in vascular biology: implications in hypertension. *Histochem. Cell Biol.* **122**, 339–52 (2004).
47. Abel, E. D., Litwin, S. E. & Sweeney, G. Cardiac remodeling in obesity. *Physiol. Rev.* **88**, 389–419 (2008).
48. Kind, K. L. *et al.* Effect of maternal feed restriction during pregnancy on glucose tolerance in the adult guinea pig. *Am. J. Physiol. Regul. Integr. Comp. Physiol.* **284**, R140–52 (2003).

49. So, A. *et al.* Non-invasive assessment of functionally relevant coronary artery stenoses with quantitative CT perfusion: preliminary clinical experiences. *Eur. Radiol.* **22**, 39–50 (2012).
50. So, A. & Lee, T.-Y. Quantitative myocardial CT perfusion: a pictorial review and the current state of technology development. *J. Cardiovasc. Comput. Tomogr.* **5**, 467–81 (2011).
51. Leppo, J. A. Dipyridamole myocardial perfusion imaging. *J. Nucl. Med.* **35**, 730–3 (1994).
52. Paternostro, G. *et al.* Cardiac and skeletal muscle insulin resistance in patients with coronary heart disease. A study with positron emission tomography. *J. Clin. Invest.* **98**, 2094–9 (1996).
53. Hoh, C. K. Clinical use of FDG PET. *Nucl. Med. Biol.* **34**, 737–42 (2007).
54. Camici, P. *et al.* Coronary vasodilation is impaired in both hypertrophied and nonhypertrophied myocardium of patients with hypertrophic cardiomyopathy: a study with nitrogen-13 ammonia and positron emission tomography. *J. Am. Coll. Cardiol.* **17**, 879–86 (1991).
55. Neglia, D. Prognostic Role of Myocardial Blood Flow Impairment in Idiopathic Left Ventricular Dysfunction. *Circulation* **105**, 186–193 (2002).
56. Allard, F. *et al.* Contribution of oxidative metabolism to ATP production in hypertrophied and glycolysis hearts. *Am. J. Physiol.* **267**, H742–H750 (1994).
57. Christe, M. E. & Rodgers, R. L. Altered glucose and fatty acid oxidation in hearts of the spontaneously hypertensive rat. *J. Mol. Cell. Cardiol.* **26**, 1371–5 (1994).
58. Dávila-Román, V. G. *et al.* Altered myocardial fatty acid and glucose metabolism in idiopathic dilated cardiomyopathy. *J. Am. Coll. Cardiol.* **40**, 271–277 (2002).



59. Vasan, R. S. *et al.* Congestive heart failure in subjects with normal versus reduced left ventricular ejection fraction. *J. Am. Coll. Cardiol.* **33**, 1948–1955 (1999).
60. Kuzawa, C. W. & Adair, L. S. Lipid profiles in adolescent Filipinos: relation to birth weight and maternal energy status during pregnancy. *Am J Clin Nutr* **77**, 960–966 (2003).
61. Thamocharan, M. *et al.* Transgenerational inheritance of the insulin-resistant phenotype in embryo-transferred intrauterine growth-restricted adult female rat offspring. *Am. J. Physiol. Endocrinol. Metab.* **292**, E1270–9 (2007).
62. Srinivasan, M., Katewa, S. D., Palaniyappan, A., Pandya, J. D. & Patel, M. S. Maternal high-fat diet consumption results in fetal malprogramming predisposing to the onset of metabolic syndrome-like phenotype in adulthood. *Am. J. Physiol. Endocrinol. Metab.* **291**, E792–9 (2006).
63. Dunn, G. A. & Bale, T. L. Maternal high-fat diet promotes body length increases and insulin insensitivity in second-generation mice. *Endocrinology* **150**, 4999–5009 (2009).
64. Han, J., Xu, J., Epstein, P. N. & Liu, Y. Q. Long-term effect of maternal obesity on pancreatic beta cells of offspring: reduced beta cell adaptation to high glucose and high-fat diet challenges in adult female mouse offspring. *Diabetologia* **48**, 1810–8 (2005).
65. Sarr, O., Thompson, J. A., Zhao, L., Lee, T.-Y. & Regnault, T. R. H. Low birth weight male guinea pig offspring display increased visceral adiposity in early adulthood. *PLoS One* **9**, e98433 (2014).
66. Hubert, H. B., Feinleib, M., McNamara, P. M. & Castelli, W. P. Obesity as an independent risk factor for cardiovascular disease: a 26- year follow-up of participants in the Framingham Heart Study. *Circulation* **67**, 968–977 (1983).
67. Hamaguchi, M. Nonalcoholic fatty liver disease is a novel predictor of cardiovascular disease. *World J. Gastroenterol.* **13**, 1579 (2007).

## Appendices

**Appendix A.** Primer sequences of selected target genes utilized in real-time PCR.

<b>Gene</b>	<b>Accession Number</b>	<b>F</b>	<b>R</b>
<b><math>\alpha</math>SMA</b>	ENSCPOT00000010480	AGCAAGAGAGGTATCCTGAC	CGCAGCTCATTGTAGAAAGT
<b>Collagen 1</b>	XM_003466865.1	AACGGAGACACCTGGAAACC	TTGACTAGGTCCAGGGCTGA
<b>Collagen 3</b>	XM_003478706.1	TGCTACTTTGAACCGCTTTT	TTCATCAACTTCCTGGGTCT
<b>MMP-2</b>	XM_003477541.1	CAGGGCACCTCCTACAACAG	CCTTCTGAGTCCACCGAC

## Appendix B. Ethics Approval



\*This is the Original Approval for this protocol\*

\*A Full Protocol submission will be required in 06.30.2014\*

Your Animal Use Protocol form entitled:

In Utero Origins of Adult Insulin Resistance

Funding Agency CIHR - Grant #R3826A09

has been approved by the University Council on Animal Care. This approval is valid from 06.03.2010 to 06.30.2011.

The protocol number for this project is 2010-229.

This number must be indicated when ordering animals for this project.

Animals for other projects may not be ordered under this number.

If no number appears please contact this office when grant approval is received.

If the application for funding is not successful and you wish to proceed with the project, request that an internal scientific peer review be performed by the Animal Use Subcommittee office.

Purchases of animals other than through this system must be cleared through the ACVS office. Health certificates will be required.

### ANIMALS APPROVED FOR 4 Years

Species	Strain	Other Detail	Pain Level	Animal # Total for 4 Years
Guinea Pig	Hartley	Pregnant ~25 Days on Arrival	C	556

The holder of this Animal Use Protocol is responsible to ensure that all associated safety components (biosafety, radiation safety, general laboratory safety) comply with institutional safety standards and have received all necessary approvals. Please consult directly with your institutional safety officers.

**Appendix C. ANOVA Table for Figure 2.3 Basal Coronary Blood Flow Determined by DCE-CT.**

**Tests of Between-Subjects Effects**

Dependent Variable: Blood Flow

Source	Type III Sum of Squares	df	Mean Square	F	Sig.	Partial Eta Squared
Corrected Model	85632.376 <sup>a</sup>	15	5708.825	1.064	.403	.166
Intercept	3200825.235	1	3200825.235	596.304	.000	.882
Sex	2059.209	1	2059.209	.384	.537	.005
BirthType	1331.536	1	1331.536	.248	.620	.003
Diet	3436.354	1	3436.354	.640	.426	.008
Age	1162.622	1	1162.622	.217	.643	.003
Sex * BirthType	408.484	1	408.484	.076	.783	.001
Sex * Diet	2191.975	1	2191.975	.408	.525	.005
Sex * Age	3066.114	1	3066.114	.571	.452	.007
BirthType * Diet	16410.451	1	16410.451	3.057	.084	.037
BirthType * Age	22302.282	1	22302.282	4.155	.045	.049
Diet * Age	2220.977	1	2220.977	.414	.522	.005
Sex * BirthType * Diet	4188.972	1	4188.972	.780	.380	.010
Sex * BirthType * Age	474.092	1	474.092	.088	.767	.001
Sex * Diet * Age	5259.104	1	5259.104	.980	.325	.012
BirthType * Diet * Age	11771.423	1	11771.423	2.193	.143	.027
Sex * BirthType * Diet *	1536.422	1	1536.422	.286	.594	.004
Age						
Error	429421.793	80	5367.772			
Total	4043459.083	96				
Corrected Total	515054.169	95				

a. R Squared = .166 (Adjusted R Squared = .010)

### Appendix D. ANOVA Table for Figure 2.4 Cardiac Glucose Uptake by PET

#### Tests of Between-Subjects Effects

Dependent Variable: SUV

Source	Type III Sum of Squares	df	Mean Square	F	Sig.	Partial Eta Squared
Corrected Model	17.612 <sup>a</sup>	15	1.174	1.996	.024	.254
Intercept	353.522	1	353.522	600.876	.000	.872
Sex	.235	1	.235	.399	.529	.005
BirthType	.330	1	.330	.560	.456	.006
Diet	6.940	1	6.940	11.796	.001	.118
Age	.557	1	.557	.947	.333	.011
Sex * BirthType	.245	1	.245	.416	.520	.005
Sex * Diet	.249	1	.249	.423	.517	.005
Sex * Age	1.314	1	1.314	2.233	.139	.025
BirthType * Diet	.991	1	.991	1.684	.198	.019
BirthType * Age	.127	1	.127	.215	.644	.002
Diet * Age	1.607	1	1.607	2.731	.102	.030
Sex * BirthType * Diet	.878	1	.878	1.493	.225	.017
Sex * BirthType * Age	.230	1	.230	.391	.533	.004
Sex * Diet * Age	.365	1	.365	.621	.433	.007
BirthType * Diet * Age	1.966	1	1.966	3.341	.071	.037
Sex * BirthType * Diet * Age	.930	1	.930	1.581	.212	.018
Error	51.774	88	.588			
Total	507.525	104				
Corrected Total	69.387	103				

a. R Squared = .254 (Adjusted R Squared = .127)

### Appendix E. ANOVA Table for Figure 2.5 Cross-Sectional Area of Cardiomyocytes

#### Tests of Between-Subjects Effects

Dependent Variable: Surface Area of Cardiomyocytes

Source	Type III Sum of Squares	df	Mean Square	F	Sig.	Partial Eta Squared
Corrected Model	50224.931 <sup>a</sup>	7	7174.990	3.027	.026	.527
Intercept	2051230.300	1	2051230.300	865.426	.000	.979
Sex	4532.849	1	4532.849	1.912	.183	.091
BW	15683.581	1	15683.581	6.617	.019	.258
Diet	919.696	1	919.696	.388	.541	.020
Sex * BW	7925.713	1	7925.713	3.344	.083	.150
Sex * Diet	7416.964	1	7416.964	3.129	.093	.141
BW * Diet	1486.110	1	1486.110	.627	.438	.032
Sex * BW * Diet	3533.122	1	3533.122	1.491	.237	.073
Error	45033.740	19	2370.197			
Total	2661565.249	27				
Corrected Total	95258.671	26				

a. R Squared = .527 (Adjusted R Squared = .353)

### Appendix F. ANOVA Table for Figure 2.6 Collagen Content in the Left Ventricle

#### Tests of Between-Subjects Effects

Dependent Variable: Fibrosis, Collagen percentage

Source	Type III Sum of Squares	df	Mean Square	F	Sig.	Partial Eta Squared
Corrected Model	34.094 <sup>a</sup>	7	4.871	3.232	.021	.557
Intercept	141.860	1	141.860	94.126	.000	.839
Sex	1.695	1	1.695	1.124	.303	.059
BW	11.946	1	11.946	7.927	.011	.306
Diet	.848	1	.848	.563	.463	.030
Sex * BW	.020	1	.020	.014	.909	.001
Sex * Diet	7.469	1	7.469	4.956	.039	.216
BW * Diet	7.542	1	7.542	5.004	.038	.218
Sex * BW * Diet	19.298	1	19.298	12.805	.002	.416
Error	27.128	18	1.507			
Total	202.192	26				
Corrected Total	61.222	25				

a. R Squared = .557 (Adjusted R Squared = .385)



### Appendix G. ANOVA Table for Figure 2.7 Type 1 Collagen mRNA Expression

#### Tests of Between-Subjects Effects

Dependent Variable: Collagen Type 1 mRNA

Source	Type III Sum of Squares	df	Mean Square	F	Sig.	Partial Eta Squared
Corrected Model	.128 <sup>a</sup>	7	.018	3.020	.022	.490
Intercept	.681	1	.681	112.110	.000	.836
Sex	.069	1	.069	11.408	.003	.341
BW	.018	1	.018	3.041	.095	.121
Diet	.023	1	.023	3.774	.065	.146
Sex * BW	.031	1	.031	5.147	.033	.190
Sex * Diet	.001	1	.001	.178	.677	.008
BW * Diet	.005	1	.005	.784	.386	.034
Sex * BW * Diet	3.715E-5	1	3.715E-5	.006	.938	.000
Error	.134	22	.006			
Total	.934	30				
Corrected Total	.262	29				

a. R Squared = .490 (Adjusted R Squared = .328)

**Appendix H. ANOVA Table for Figure 2.8 AKT Expression in the Left Ventricle at Putdown.**

**Tests of Between-Subjects Effects**

Dependent Variable: Ratio of pAKT (T308)

Source	Type III Sum of Squares	df	Mean Square	F	Sig.	Partial Eta Squared
Corrected Model	.009 <sup>a</sup>	7	.001	2.580	.032	.368
Intercept	.195	1	.195	408.745	.000	.930
Sex	.003	1	.003	6.875	.013	.182
BW	.001	1	.001	2.745	.108	.081
Diet	.002	1	.002	5.060	.032	.140
Sex * BW	.000	1	.000	.303	.586	.010
Sex * Diet	.000	1	.000	.452	.506	.014
BW * Diet	.001	1	.001	1.784	.191	.054
Sex * BW * Diet	.001	1	.001	1.757	.195	.054
Error	.015	31	.000			
Total	.216	39				
Corrected Total	.023	38				

a. R Squared = .368 (Adjusted R Squared = .225)

### Appendix I. ANOVA Table for Figure 3.5 A. Glucose Uptake Determined by PET

#### Tests of Between-Subjects Effects

Dependent Variable: SUV

Source	Type III Sum of Squares	df	Mean Square	F	Sig.	Partial Eta Squared
Corrected Model	2.581 <sup>a</sup>	3	.860	1.654	.207	.191
Intercept	66.294	1	66.294	127.425	.000	.859
Pregnancy	.782	1	.782	1.503	.234	.067
Diet	.532	1	.532	1.022	.324	.046
Pregnancy * Diet	2.129	1	2.129	4.092	.056	.163
Error	10.925	21	.520			
Total	107.195	25				
Corrected Total	13.507	24				

a. R Squared = .191 (Adjusted R Squared = .076)

**Appendix J. ANOVA Table for Figure 3.6 Protein Expression of pAKT (T308) at Putdown.**

**Tests of Between-Subjects Effects**

Dependent Variable: Ratio pAKT (T308)

Source	Type III Sum of Squares	df	Mean Square	F	Sig.	Partial Eta Squared
Corrected Model	.055 <sup>a</sup>	3	.018	3.548	.038	.400
Intercept	1.282	1	1.282	249.749	.000	.940
Pregnancy	.010	1	.010	1.964	.180	.109
Diet	.035	1	.035	6.761	.019	.297
Pregnancy * Diet	.003	1	.003	.601	.449	.036
Error	.082	16	.005			
Total	1.530	20				
Corrected Total	.137	19				

a. R Squared = .400 (Adjusted R Squared = .287)

## Curriculum Vitae

**Name:** Jacky Chiu

**Post-secondary  
Education and  
Degrees:** University of Western Ontario  
London, Ontario, Canada  
2007-2011 BMSc

The University of Western Ontario  
London, Ontario, Canada  
2013-2015 MSc

### Honours and Awards:

Canadian Institute of Health and Research Travel Award	2014
Children's Health Research Institute Travel Award	2013
Ontario Graduate Scholarship (Queen Elizabeth II Graduate Scholarship in Science and Technology)	2013-2014
Obstetrics and Gynecology (London Ontario, Canada) Graduate Scholarship	2012-2014
Western Graduate Research Scholarship	2012-2014

### Related Work Experience:

Teaching Assistant.	2012 – 2014
- Fetal Physiology 4700B. Western University	
Thesis in Physiology and Pharmacology	2012 – 2014
- Studying effects of ginseng's immune-modulating effects on placenta	
Research Student, Department of Physiology and Pharmacology.	2009 – 2010
- Investigated Peroxisome Proliferator-Activated Receptor and Resveratrol on changes in activators of muscle oxidative metabolism	
- Explored the alterations in lung development following diaphragmatic hernia in sheep	

**Publications:**

Regnault, T. R., Zhao, L., **Chiu, J. S.**, Gottheil, S. K., Foran, A., & Yee, S. P. (2010). Peroxisome Proliferator-Activated Receptor- $\beta/\delta$ , $-\gamma$  Agonists and Resveratrol Modulate Hypoxia Induced Changes in Nuclear Receptor Activators of Muscle Oxidative Metabolism. *PPAR research*, 2010.

Emmert-Coughlin H.M.A, Martin K.K., **Chiu J.S.**, Zhao L., Scott L.A., Regnault T.R.H., and Bütter A. WNT Signaling Pathway in an Ovine Model of Congenital Diaphragmatic Hernia is down regulated. Submitted to *Frontiers in Surgery, Pediatric Surgery*. August 2014.

**Extracurricular Activities:**

Volunteer Friendly Visitor, Children's Aid Society of London	2008 – 2014
Phys/Pharm Intramural Soccer	2012 – 2014
Captain, Phys/Pharm Intramural Indoor Volleyball	2013
Richmond Hill Soccer League	2013
Volunteer, YMCA of Western Ontario	2009 – 2012
Volunteer, Western University March Break Open House	2010
Volunteer, Boys' and Girls' Club of London	2009 – 2010
Volunteer, TD Summer Reading Club	2010
Volunteer, United Christian's Hospital of Hong Kong	2008
Executive, Hong Kong Connexion Club of University of Western Ontario	2008-2009
Volunteer, UNICEF of Western Ontario	2008-2009
Chartered Member, St John Ambulance of York East	2003-2008